

UC Berkeley

UC Berkeley Electronic Theses and Dissertations

Title

The Role of Flavins During Infection and Immunity to *Listeria monocytogenes*

Permalink

<https://escholarship.org/uc/item/8nz0z9g6>

Author

Rivera-Lugo, Rafael

Publication Date

2022

Peer reviewed|Thesis/dissertation

The Role of Flavins During Infection and Immunity to *Listeria monocytogenes*

By

Rafael J. Rivera-Lugo

A dissertation submitted in partial satisfaction of the

requirements for the degree of

Doctor of Philosophy

in

Molecular and Cell Biology

in the

Graduate Division

of the

University of California, Berkeley

Committee in charge:

Professor Daniel A. Portnoy, Chair

Professor Ellen Robey

Professor Sarah Stanley

Professor Jeffery S. Cox

Fall 2022

Abstract

The Role of Flavins During Infection and Immunity to *Listeria monocytogenes*

by

Rafael J. Rivera-Lugo

Doctor of Philosophy in Molecular and Cell Biology

University of California, Berkeley

Professor Daniel A. Portnoy, Chair

Intracellular pathogens account for a significant majority of infectious disease cases and deaths worldwide. These pathogens enter host cells to hide from the extracellular immune defenses and establish this environment as their replicative niche. Intracellular pathogens have evolved to acquire nutrients from the host cell and use the cell's machinery to avoid innate immune responses, grow, and disseminate. In the Portnoy lab, we study the pathogenesis of, and host responses to, the model intracellular pathogen *Listeria monocytogenes*. *L. monocytogenes* live freely in the soil and decaying plant matter but can become an intracellular pathogen upon ingesting contaminated food. *L. monocytogenes* affects immunocompromised individuals, including the elderly and pregnant women, where it can infect the placenta and cause miscarriages. *L. monocytogenes* has relatively few growth requirements and can synthesize most of its nutrients, which allows it to reside in diverse environments. However, unlike most bacteria, *L. monocytogenes* cannot synthesize riboflavin (vitamin B₂). Not much was known about flavin metabolism in *L. monocytogenes*, the requirements during infection, or why *L. monocytogenes* are in the minority of bacteria that lack the capacity to synthesize riboflavin *de novo*. My dissertation aimed to describe flavin metabolism and transport in *L. monocytogenes* and examine the implications of riboflavin requirement during infection. More broadly, my work explored how intracellular pathogens that cannot produce riboflavin acquire flavins from host cells and why they might have evolved to lack the riboflavin biosynthetic pathway.

The riboflavin-derived molecules, flavin mononucleotide (FMN) and flavin adenine dinucleotide (FAD), are essential redox-active cofactors used by all forms of life to perform a myriad of redox reactions, including energy production and catabolism of amino acids. Since *L. monocytogenes* does not synthesize riboflavin *de novo*, it must acquire this flavin from the environment. I discovered that *L. monocytogenes* encodes a flavin transporter (RibU) that is essential exclusively during infection and allows the pathogen to scavenge FMN and FAD, and not riboflavin as previously suggested, directly from the host cytosol. This research was the first report of a pathogen importing FMN and FAD from the host to sustain its intracellular growth. Interestingly, obligate intracellular pathogens in the *Rickettsia* and *Cryptosporidium* genera do not produce riboflavin but also lack the enzymes that convert riboflavin to FMN and FAD. I

hypothesize that like *L. monocytogenes*, these obligate intracellular pathogens import FMN and FAD directly from the host to satisfy their flavin requirements. I also found that *L. monocytogenes* encodes an energy-coupling factor (ECF) transporter that exports FAD and is distributed across the Firmicutes phylum. This ECF exporter is required for the flavinylation of extracytosolic proteins and is essential for extracellular electron transfer, which confers *L. monocytogenes* a growth advantage in the host's gastrointestinal tract. Importantly, this is the first example of an ECF transporter capable of exporting substrates, as all other characterized ECF complexes are importers.

It is evident that flavins play essential roles in *L. monocytogenes* physiology and pathogenesis and this led us to question why *L. monocytogenes* lost the capacity to synthesize riboflavin. We speculated that *L. monocytogenes* evolved to avoid recognition by mucosal-associated invariant T (MAIT) cells. MAIT cells are innate-like T cells that recognize host cells infected with pathogens that synthesize riboflavin (riboflavin precursors act as MAIT cell activating ligands). Upon encountering host cells that display the riboflavin precursor, MAIT cells kill the infected cells and activate other immune cells by secreting cytokines. To test the hypothesis that *L. monocytogenes* is avoiding MAIT cells by lacking the capacity to produce riboflavin, I engineered *L. monocytogenes* to produce riboflavin *de novo*. We observed that riboflavin-producing *L. monocytogenes* was highly attenuated in mice and mediated the expansion and activation of MAIT cells. Thus, riboflavin biosynthesis is detrimental to *L. monocytogenes* pathogenesis and could explain why this pathogen lacks riboflavin biosynthetic genes. The conclusions of my thesis suggest that flavins are essential for *L. monocytogenes* physiology and pathogenesis but that they lost the capacity to synthesize riboflavin, and instead evolved to import FMN and FAD cofactors from the cytosol of infected cells to avoid activation of MAIT cells.

Table of Contents

DEDICATION.....	III
ACKNOWLEDGEMENTS	IV
CHAPTER 1: INTRODUCTION.....	1
1.1 FLAVINS AND THEIR IMPORTANCE IN BIOLOGY	2
1.2 RIBOFLAVIN BIOSYNTHESIS AND FLAVIN TRANSPORT	2
1.3 <i>LISTERIA MONOCYTOGENES</i> : A MODEL INTRACELLULAR PATHOGEN THAT LACKS THE RIBOFLAVIN BIOSYNTHETIC GENES	4
1.4 MUCOSAL-ASSOCIATED INVARIANT T CELLS RECOGNIZE A PATHOGEN-ASSOCIATED MOLECULAR PATTERN DERIVED FROM RIBOFLAVIN BIOSYNTHESIS.....	9
CHAPTER 2: RIBU IS AN ESSENTIAL DETERMINANT OF <i>LISTERIA</i> PATHOGENESIS THAT MEDIATES ACQUISITION OF FMN AND FAD DURING INTRACELLULAR GROWTH.....	12
2.1 SUMMARY OF RESULTS	13
2.2 INTRODUCTION.....	13
2.3 RESULTS	14
2.3.1 <i>RibU is dispensable for growth in nutrient-rich media but is required for virulence in mice.</i>	14
2.3.2 <i>L. monocytogenes uses RibU to grow in macrophages</i>	16
2.3.3 <i>L. monocytogenes uses RibU to scavenge FMN and FAD from the cytosol of host cells</i>	19
2.3.4 <i>The $\Delta ribC\Delta ribF$ mutant cannot grow in blood, gallbladders, or the gastrointestinal tract</i>	21
2.4 DISCUSSION	23
2.5 MATERIALS AND METHODS	24
2.6 SUPPLEMENTARY MATERIALS	28
CHAPTER 3: DISTINCT ENERGY-COUPPLING FACTOR TRANSPORTER SUBUNITS ENABLE FLAVIN ACQUISITION AND EXTRACYTOSOLIC TRAFFICKING FOR EXTRACELLULAR ELECTRON TRANSFER IN <i>LISTERIA MONOCYTOGENES</i>	29
3.1 SUMMARY OF RESULTS	30
3.2 INTRODUCTION.....	30
3.3 RESULTS	32
3.3.1 <i>RibU is dispensable for PplA flavinylation when flavin auxotrophy is relieved</i>	32
3.3.2 <i>FmnA and EetB are required for PplA flavinylation in the absence of exogenous FAD</i>	33
3.3.3 <i>EetB is an FAD-binding protein that resembles characterized ECF-S subunits</i>	34
3.3.4 <i>ECF ATPases are required for PplA flavinylation in the absence of exogenous FAD</i>	35
3.3.5 <i>Structural models illuminate ECF transporters with distinct subunit compositions</i>	36
3.3.6 <i>EcfT and FmnA ECF-T subunits are functionally redundant in flavin import</i>	37
3.3.7 <i>Gene colocalization suggests a conserved role for EetB in ApbE-associated flavin trafficking</i>	37
3.4 DISCUSSION	39
3.5 MATERIALS AND METHODS	40
3.6 SUPPLEMENTAL FIGURES.....	44
CHAPTER 4: MAIT CELL AVOIDANCE IS A DETERMINANT OF <i>LISTERIA MONOCYTOGENES</i> PATHOGENESIS	45
4.1 SUMMARY OF RESULTS	46
4.2 INTRODUCTION.....	46
4.3 RESULTS	48
4.3.1 <i>L. monocytogenes expressing ribDEAHT produce riboflavin and have no detectable virulence defects in host cells</i>	48
4.3.2 <i>Riboflavin-producing L. monocytogenes are attenuated in mice</i>	50
4.3.3 <i>MAIT cells accumulate in response to riboflavin-producing L. monocytogenes infection and lead to their attenuation in vivo</i>	51

4.3.4 <i>High-dose infection with riboflavin-producing L. monocytogenes strains in an ActA-minus background leads to substantial and sustained accumulation of MAIT cells in infected tissues</i>	52
4.3.5 <i>Perforin is required for MAIT cells to restrict riboflavin-producing L. monocytogenes in mice</i>	55
4.4 DISCUSSION	56
4.5 MATERIALS AND METHODS	59
CHAPTER 5: CONCLUSIONS AND FUTURE DIRECTIONS	61
CONCLUSIONS	62
FUTURE DIRECTIONS	63
CHAPTER 6: REFERENCES	66

Dedication

I dedicate this work to my mother, Ladin, who sacrificed her professional career, raised my brothers and me single-handedly, and gave us everything we needed to be contributing members of society. I love you mom, even though I do not say it enough!

Le dedico este trabajo a mi madre, Ladin, quien sacrificó su carrera profesional, nos crió a mis hermanos y a mi siendo madre soltera y nos dió todo lo necesario para ser miembros contribuyentes de la sociedad. ¡Te amo mami, aunque no lo diga lo suficiente!

Acknowledgements

I want to thank my family: Mami (Ladin), Goy, Gerardo, Papi (Aciselo), Maria, Grandpa (Jose), and Grandma (Edith), for your support and well wishes. I would like to give a special thanks to my mom, Ladin, who always made sure I was doing well and worried too much every time she called me during weekends and I was stuck in the lab. Thank you for encouraging me since I was a kid to pursue my dreams and always follow through with whatever I proposed to do. Thank you for working hard to give us the best life we could afford.

Thank you so much, Dan, for accepting me into your lab and believing in me when I said I wanted to study bacterial pathogenesis. Wowwww!! What an amazing time I've had here. To start, I never saw myself doing metabolism, especially vitamins. While in college, I thought that vitamin metabolism, specifically, was the most boring thing anyone could study, since so much was known already. But, with your guidance and infectious enthusiasm for pathogenesis, we were able to discover some pretty cool stuff. Have you noticed how, interestingly, bacterial metabolism and its relationship with pathogenesis is what everyone is talking about these days?! Although we can't (probably) take credit for this, we did contribute to this exciting field. I really enjoyed having long conversations where we discussed everything from my results, ideas, and future experiments, to politics, the state of the country, and our fragile democracy. I felt very comfortable sharing my thoughts and "debating" about a diverse range of topics, even the ones that we didn't agree on, and appreciate how respectful you were when we disagreed. I also appreciate those times when you reached out after the hurricanes and earthquakes in Puerto Rico, and how you asked about my family and offered to help. I will really miss going to your office, most of the time unannounced, to discuss results and science, and then quickly pivot to whatever important event was happening in the country. I never thought I was going to be able to connect with you like I feel I did, and for that, I am so glad. You are by far, the mentor I wanted to have in grad school so thank you. Thank you for teaching me the ways of bacterial pathogenesis. I hope to keep up the good work and spread the enthusiasm you have for *Listeria* and the bacterial pathogenesis field in general.

I would like to thank all my previous and current mentors, starting with Edu Suarez, Julie Dutil, Vern Carruthers, Scott Barolo, Andrea Ramos, Audrey Knowlton, Laurent Coscoy, Trever Greene, Ellen Robey, Sarah Stanley, Jeff Cox, Guillaume Golovkine, Sam Light, Dan Portnoy, and all others that have made an impact on my personal and scientific journey. I am the scientist I am today because you gave me a chance and taught me what you knew, and I could do. Thank you for supporting me through the years. I promise to pass on what you have taught me.

Thank you, past and current lab members of the Portnoy lab, for your input during lab meetings and for being great lab mates. Neil, Sam, Freddy, Alex, Ying, Helia, Chen, Gabe, Eric, Brittney, Bret, John, Victoria, Mariya, Bere, Andrea, Ted, Leslie, and Preethi. My time here has been very pleasant, and full of fun, and you all played a big role in that.

I would like to thank Mariya and Jesse who have always gladly extended me a hand in the lab, many times without me asking first, and were there helping me until the very, very end. Thank you!

I would also like to thank Sam. Thank you for teaching me the ways in the Portnoy lab. You were very patient with me, especially in the beginning when I used to go to you after having “breakthroughs” or freshly baked “ideas”, some that definitely needed more baking. Thanks for revising my fellowship applications and sharing ideas. You are a great mentor and I appreciate how you have always encouraged me. Thanks for teaching me how to ask the right questions. I hope to keep in touch regularly!

Thank you to my mentees: Han, Frank, and Eugene. You significantly contributed to your projects and that’s all I could have asked from you. I am so happy I got to witness your evolution from being newbies to knowing your way around cutting steps while cloning or doing minipreps, which takes a lot of confidence to do (for real). Han, thank you for being my first mentee and having a lot of patience. Frank, I still remember how you used to dance solo, to no music, in the middle of the lab, while doing experiments. Please don’t change and keep up the good work. Eugene, thank you for all the time and effort you put into your projects. As you know, we spent many days working in the lab 15+ hours doing growth curves. These experiments would’ve been significantly more difficult (if not impossible) if I had to do them by myself. I am glad you decided to join the lab when you did and work with me. I didn’t only get to be your mentor in lab, but also your friend outside school. Thank you for taking me in and for the good times we’ve spent with mutual friends. Like you have heard me say before, you will be a great medical doctor, but you have the skills to be an amazing scientist, so never stop doing research.

To my original “IMP” cohort: Michael, Justin, Nathalie, Valerie, and Huntly. We made it! Thank you for the times we got together to chat and de-stress. Justin, I will miss seeing you at conferences and hanging out. Michael, my friend, thank you for always making me laugh and for your help during our first years here. I wish you the best and hope to keep in touch from time to time.

I would like to give a special thanks to Valerie who has been there always and has made my experience at Berkeley so much better. We spent many nights studying together as undergrads and many weekends in the lab as grad students. It wasn’t easy but we made it. I am so grateful for spending all these years by your side. You helped me when I needed it the most. You have been there during my moments of joy, after getting fellowships as well as the frustrating times when my experiments were not working. I will never forget that. Thank you for sharing each one of those moments with me. Thank you for your help during the dissertation stage of the PhD, for your constant encouragement, and for your patience. I would also like to acknowledge our beautiful kittie, Seattle Marie Rivera Vargas. I am so glad we went to the shelter and decided to adopt her because she has made our time here so much better. And of course, for introducing me to BTS. Their music and videos have brought a lot of happiness to us both during the most stressful times. Thanks again Valerie and Seattle for all your love and support!

Chapter 1: Introduction

1.1 Flavins and their importance in biology

Flavins are water-soluble, organic compounds essential for all forms of life. These yellow-colored molecules perform key roles in many biological systems, acting mainly as electron carriers. The basic structure of flavins is composed of an isoalloxazine ring system and a ribityl side chain (1). The ability of flavins to carry electrons is conferred by the isoalloxazine ring, which can accept one or two electrons during oxidation-reduction (redox) reactions (2–4). The main role of the ribityl side chains of flavins is to stabilize the flavin-protein interaction, although they have also been implicated in catalysis in redox reactions and regulation of protein binding to membranes (5, 6). Riboflavin, or vitamin B₂, is the biologically available flavin that serves as the building block for the cofactors flavin mononucleotide (FMN) and flavin adenine dinucleotide (FAD) (4). FMN and FAD are biologically active essential cofactors for a myriad of redox reactions in the cell. It is estimated that approximately 1-3% of genes in the prokaryotic and eukaryotic genomes encode proteins that bind FMN and FAD cofactors (7). These cofactors play essential roles in aerobic and anaerobic respiration systems (8–12), metabolism of amino acids and nucleotides (13–17), synthesis of other vitamins (17–20), and generation and neutralization of reactive oxygen species (21–24), among other redox-dependent processes (1).

The mechanisms by which riboflavin is converted to FMN and FAD are shared by most organisms, and it involves the phosphorylation of riboflavin to FMN and adenynylation of FMN to produce FAD (4). In eukaryotes, the enzyme riboflavin kinase (EC 2.7.1.26) catalyzes the phosphorylation of riboflavin to synthesize FMN, while FAD synthase (EC 2.7.7.2) adenynyates FMN to yield FAD (25). Most prokaryotes encode a bifunctional enzyme with riboflavin kinase (EC 2.7.1.26) and FAD synthase (EC 2.7.7.2) activity, while a minority of bacteria encode an additional monofunctional FAD synthase (EC 2.7.7.2) enzyme (26).

1.2 Riboflavin biosynthesis and flavin transport

Plants, fungi, most bacteria and archaea synthesize riboflavin *de novo* via similar, although not identical, biochemical reactions (26). The pathways leading to the synthesis of riboflavin in plants and bacteria are highly similar (**Fig. 1.1**). Moreover, most plant and bacterial riboflavin biosynthesis enzymes have significant sequence homology (27, 28), suggesting that the riboflavin biosynthesis genes might have been transferred to the genome of the common ancestor of plants from a cyanobacterial endosymbiont (28). In bacteria, the riboflavin biosynthesis genes can be found either as a single operon or spread around the genome. The riboflavin biosynthesis pathways in fungi and archaea are more closely related to each other than the pathways found in plants and bacteria (26).

Animals and some bacterial and archaeal species lack the riboflavin biosynthesis pathway and rely on uptake from their diets or environments (29). Mammals encode three riboflavin transporters which have different sub-cellular and tissue-specific expression profiles (30). In

these animals, dietary and microbially derived riboflavin is absorbed through the small intestine while the excess is excreted into the urine (31).

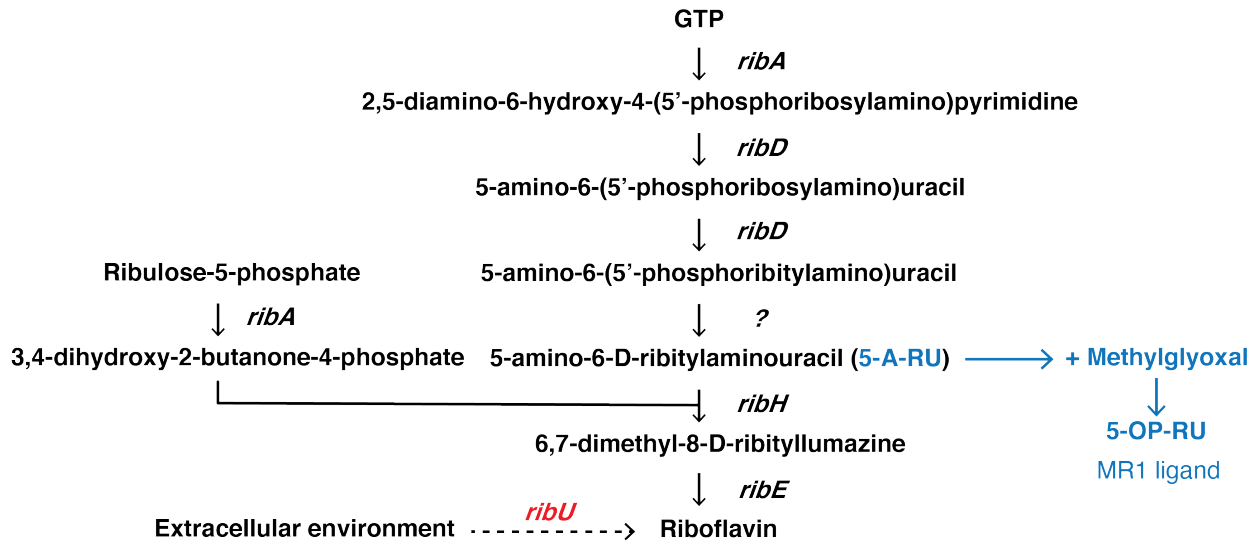


Figure 1.1 Riboflavin biosynthetic pathway and generation of 5-OP-RU. Biosynthesis of riboflavin begins from a molecule of GTP and ribulose-5-phosphate and through a series of enzymatic reactions generate riboflavin. 5-amino-6-D-ribitylamouracil (5-A-RU) is an intermediate of riboflavin biosynthesis that becomes a pathogen-associated molecular pattern (5-OP-RU) when it spontaneously condenses with methylglyoxal. Many bacteria possess riboflavin transporter systems like RibU to import riboflavin.

There are multiple flavin transporter systems widespread across bacteria (29), the majority of which are riboflavin importers and, interestingly, are present in bacteria that possess the riboflavin biosynthetic pathway (32). These transporters include ImpX, RfnT, RfuABCD, RibM, RibN, RibU, RibXYZ, and RibZ which have different binding affinities for riboflavin (29, 33). These flavin importers have a relatively high affinity for riboflavin and a lower affinity for FMN and FAD (29, 33, 34). In fact, only a handful are predicted to transport FMN or FAD (29). Interestingly, there have only been two flavin exporters described, the bacterial FAD exporter (Bfe) in *Shewanella oneidensis* and YeeO in *Escherichia coli*, both belonging to the multidrug and toxic compound extrusion systems (35, 36). However, it has been well documented that many bacterial species are capable of secreting flavins, and thus it is likely that other unidentified flavin exporter systems exist (29).

The role that flavins play in microbial metabolism has been well documented. However, the link between flavins and pathogenesis has only recently become the focus of investigation due to the discovery that intermediates of riboflavin biosynthesis can induce immune responses by a subset of T cells called mucosal-associated invariant T (MAIT) cells (37, 38). To study flavin transport, metabolism, and requirements during pathogenesis, we used the riboflavin auxotrophic, model intracellular pathogen *Listeria monocytogenes*. Our findings will be described in Chapters 2-4.

1.3 *Listeria monocytogenes*: a model intracellular pathogen that lacks the riboflavin biosynthetic genes

L. monocytogenes is a Gram-positive, facultative intracellular pathogen that can infect many animals including humans. *L. monocytogenes* is a foodborne pathogen that is ubiquitous in the environment, but transitions to an intracellular pathogen upon ingestion of *Listeria*-contaminated food (39). *L. monocytogenes* affects immunocompromised individuals, including the elderly and pregnant women, where it can infect the placenta and cause miscarriages (40). The intracellular *L. monocytogenes* life cycle begins when *L. monocytogenes* invades the host cell intestinal epithelia through receptor-mediated internalization or phagocytosis by professional phagocytes. Upon internalization, *L. monocytogenes* are found in phagosomal compartments where they are starved of nutrients and fail to grow (41). However, within minutes, they perforate the phagosomes using the cholesterol-dependent pore-forming cytolysin Listeriolysin O (LLO) and escape into the cytosol of host cells (42). Once *L. monocytogenes* is in the nutrient-rich cytosol, a switch in the transcription profile occurs mediated by the master regulator of virulence genes PrfA (43). PrfA is a transcription factor that controls the expression of key virulence genes including LLO and the actin assembly-inducing protein ActA. In the cytosol, *L. monocytogenes* replicates and use actin-based motility, driven by ActA, to spread from cell to cell without being exposed to the extracellular environment (44). In the newly infected cell, *L. monocytogenes* is found in a double membrane (remnants from the previously infected cell and new host cell) and again uses LLO to escape, allowing the intracellular *L. monocytogenes* life cycle to repeat.

For decades, *L. monocytogenes* has been used as a model of intracellular pathogens to study host innate and adaptive immune responses, bacterial pathogenesis, cell biology of infection, as well as bacterial metabolism and physiology (45–49). A few of the reasons why *L. monocytogenes* are a great model pathogen are because they are highly amenable to genetic manipulation, have a fast generation time, and have relatively few growth requirements, one of which is riboflavin (50, 51). Since *L. monocytogenes* is a riboflavin auxotroph and has no known mechanism to store flavins, it requires the constant transport of riboflavin for its growth, physiology, and pathogenesis. To acquire riboflavin, *L. monocytogenes* encodes the energy-coupling factor (ECF) II transporter complex RibU (52).

The RibU complex is composed of four different proteins: two homologous ATP-binding cassette ATPase subunits EcfA and EcfA', the transmembrane coupling subunit EcfT, and the membrane-embedded substrate binding subunit RibU (53) (**Fig. 1.2**). In the substrate unbound state, RibU is dissociated from EcfT, EcfA, and EcfA', which form a module that can be shared with other substrate-binding subunits (53–55) (**Fig. 1.2**). Once RibU binds riboflavin, its affinity for the EcfT-EcfA-EcfA' module increases (**Fig. 1.2**). The EcfA and EcfA' ATPases use the energy released from ATP hydrolysis to cause a conformational change that results in RibU “toppling” and releasing the riboflavin molecule into the cytoplasm, dissociating from the module, and adopting an extracellular facing conformation available for substrate binding (54) (**Fig. 1.2**).

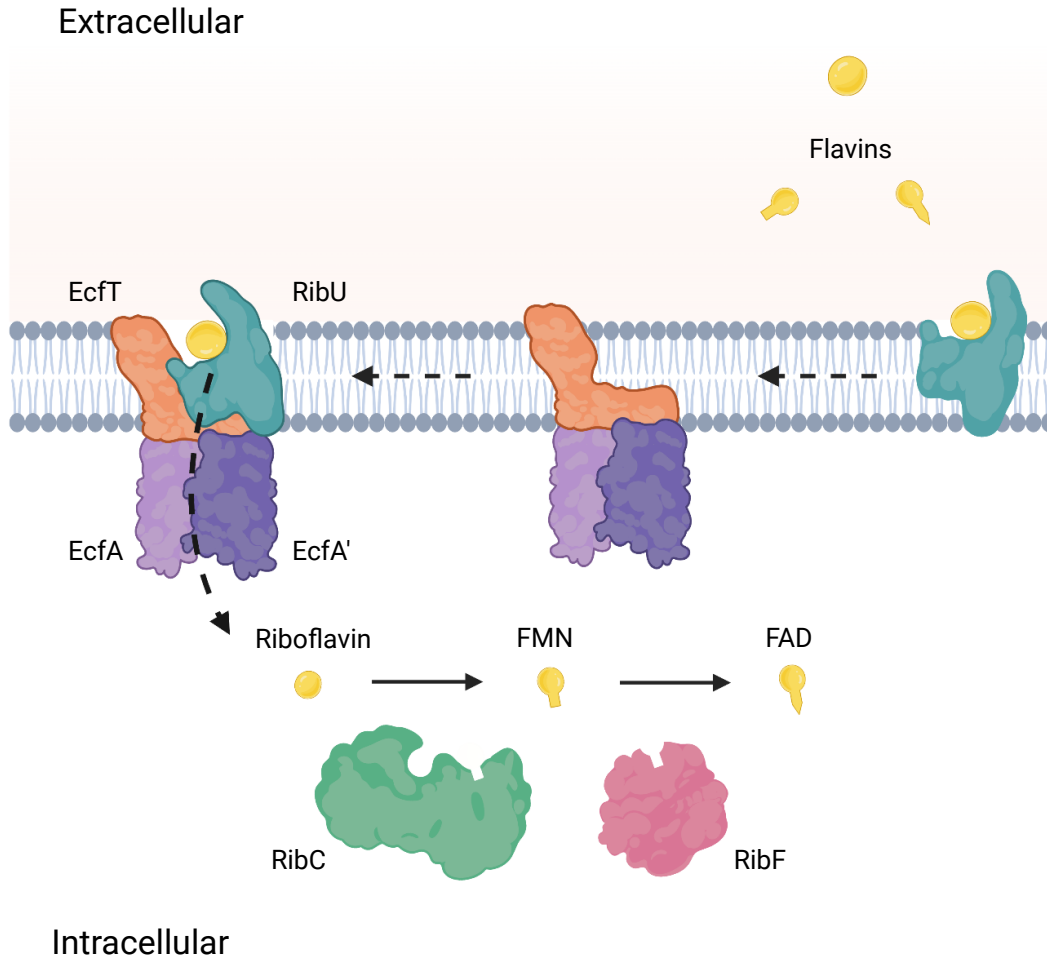


Figure 1.2 Riboflavin import, mediated by the ECF II transporter RibU, and metabolism in *L. monocytogenes*. *L. monocytogenes* encodes the energy-coupling factor (ECF) transporter RibU which is composed of four subunits: RibU, the substrate binding subunit; EcfT, the transmembrane coupling subunit; and EcfA and EcfA', two ATPase subunits. RibU binds and transports riboflavin, as well as FMN and FAD (this study). The RibU subunit is dissociated in the membrane in its flavin unbound form and upon capturing a flavin molecule it interacts with the transport module (EcfT:EcfA:EcfA') to import flavins across the membrane using energy from ATP hydrolysis (54). Upon riboflavin import, the bifunctional enzyme RibC catalyzes the phosphorylation of riboflavin to generate FMN and the conversion of FMN to FAD by attaching an adenosine monophosphate molecule (adenylylation) to FMN. The enzyme RibF can also adenylylate FMN to synthesize FAD (51, 56).

Like most bacteria, *L. monocytogenes* encode the bifunctional riboflavin kinase/FAD synthase (RibC) and the monofunctional enzyme FAD synthase (RibF). Both RibC and RibF convert the imported riboflavin into FMN and FAD (56) (**Fig. 1.2**). RibU, RibC, and RibF are the only known proteins that control flavin metabolism in *L. monocytogenes*. Even though the enzymes involved in flavin metabolism have been identified, an important question regarding *L.*

monocytogenes pathogenesis remained unanswered: How does *L. monocytogenes* satisfy their flavin requirements intracellularly, where riboflavin is limited? We answered this question in Chapter 2. Furthermore, other examples of intracellular pathogens that do not synthesize riboflavin and lack FMN and FAD synthases exist, namely members of the *Rickettsia* and *Cryptosporidium* genera (57, 58). Thus, elucidating how *L. monocytogenes* acquires flavins from the host might give us insight into how these other pathogens fulfill their flavin requirements.

The protein database UniProt predicts that *L. monocytogenes* encodes more than 44 flavin-binding proteins, some of which are essential (**Fig. 1.3**) (59). Several of these *L. monocytogenes* flavoproteins are involved in a novel flavin-based extracellular electron transfer (EET) mechanism found widespread in Gram-positive bacteria (9, 60). EET is the process by which electrons are transferred from the cytosol to a distinct electron transport chain and, ultimately, to extracellular electron acceptors like ferric iron, fumarate, and flavins (9, 60, 61). The EET genes in *L. monocytogenes* are mostly found in a previously uncharacterized 8.5-kilobase, eight-gene locus containing a distinct NADH dehydrogenase, proteins involved in quinone synthesis, a lipoprotein with flavin-binding domains, another lipoprotein with FMN transferase activity, and other proteins of unknown function (9). The EET locus encodes a novel type II NADH dehydrogenase that catalyzes the transfer of electrons from NADH to a discrete quinone pool in the membrane, distinct from the quinone pool involved in the aerobic electron transport chain. The quinone derivatives are synthesized by the EET proteins DmkA and DmkB and are hypothesized to segregate the electrons from EET and aerobic respiration. The electrons in the quinone pool were hypothesized to be relayed to the integral membrane proteins EetA and EetB, followed by transfer to the two covalently bound flavins in PplA. PplA is post-translationally flavinylated by the extracellular ApbE-like protein FmnB, a lipoprotein containing FMN transferase activity. The flavinylation of PplA requires extracellular FAD that is exported from the bacteria or can be added exogenously. It was hypothesized that RibU and the EET protein FmnA formed a FAD exporter complex capable of delivering FAD to extracellular FmnB (9). Finally, the last step in the EET pathway is the transfer of electrons from the covalently bound flavin groups in PplA to extracellular electron acceptors. EET activity in *L. monocytogenes* is particularly important during anaerobic growth conditions and provides a growth advantage in the gastrointestinal lumen of animals (9). The study describing the EET pathway in *L. monocytogenes* revealed the role of components important in electron transfer to extracellular acceptors (9). However, one key aspect that was proposed but not explored was the function of the putative FAD exporter complex. The data suggested RibU and FmnA might be involved in exporting FAD, but this was not proven. Moreover, other proteins might be required for flavin export. Elucidating this flavin export system in *L. monocytogenes* will likely have implications beyond this bacterium as bioinformatic analyses have revealed that approximately 50% of sequenced bacterial genomes are predicted to contain extracellularly flavinylated proteins that are linked to ApbE function (62). Thus, homologs of this putative flavin exporter might be present in other bacterial species. Furthermore, the extracytosolic flavinylated systems have been associated with a wide array of redox-dependent processes that play critical roles in microbial metabolisms (62). In Chapter 3, our work to characterize the FAD exporter complex and its prevalence in other bacterial species will be described.

It is clear that riboflavin is essential for all organisms. That begs the question, why do some organisms, especially intracellular pathogens, lack the capacity to synthesize riboflavin? One possible explanation is that these pathogens reside in flavin-rich environments and can import flavins, and thus are not obligated to synthesize riboflavin *de novo*. It is also possible that some of these intracellular pathogens have been evolutionarily pressured to discard the riboflavin biosynthetic pathway to avoid host responses, like the activation of mucosal-associated invariant T (MAIT) cells in mammals which recognize intermediates of riboflavin biosynthesis (37).

Number	lmo number	Common gene name	Protein Name	Predicted function	Cofactor
1	<i>lmo0227</i>	<i>lmo0227</i>	Hypothetical protein; tRNA-dihydrouridine synthase	Catalyzes the synthesis of 5,6-dihydrouridine (D), a modified base found in the D-loop of most tRNA	FMN
2	<i>lmo0295</i>	<i>lmo0295</i>	Hypothetical protein; Nitroreductase family	Energy production. FMN-containing NADPH-linked nitro/flavin reductase	FMN
3	<i>lmo0334</i>	<i>lmo0334</i>	Uncharacterized protein	Flavodoxin domain-containing protein	?
4	<i>lmo0355</i>	<i>frdA</i>	Fumarate reductase	Fumarate reductase activity. Involved in EET	FMN
5	<i>lmo0481</i>	<i>lmo0481</i>	Hypothetical protein	Oleate hydratase activity. Involved in fatty acid metabolism	FAD
6	<i>lmo0489</i>	<i>lmo0489</i>	Hypothetical protein; NADH:flavin oxidoreductase	Oxidoreductase activity	FMN
7	<i>lmo0588</i>	<i>lmo0588</i>	Uncharacterized protein; Deoxyribodipyrimidine photolyase	Predicted to be involved in replication, recombination, and repair	FAD
8	<i>lmo0611</i>	<i>acpD (azoR1)</i>	Azoreductase. FMN-dependent NADH:quinone oxidoreductase 1	Catalyzes the reductive cleavage of azo bond in aromatic azo compounds to the corresponding amines. Requires NADH. FMN-dependent NADH:quinone oxidoreductase 1	FMN
9	<i>lmo0728</i>	<i>ribF</i>	FAD synthase	Catalyzes the adeninylation of FMN to form FAD	N/A
10	<i>lmo0745</i>	<i>lmo0745</i>	Uncharacterized protein; Putative secreted flavoprotein	Flavodoxin domain-containing protein	?
11	<i>lmo0786</i>	<i>azoR2</i>	ACP phosphodiesterase	Quinone reductase that provides resistance to thiol-specific stress caused by electrophilic quinones. Catalyzes the reductive cleavage of the azo bond in aromatic azo compounds to the corresponding amines. FMN-dependent NADH:quinone oxidoreductase 2	FMN
12	<i>lmo0799</i>	<i>lmo0799</i>	Hypothetical protein; Blue-light photoreceptor	Exhibits the same spectroscopical features and blue-light induced photochemistry as plants phototropins, with the reversible formation of a blue-shifted photoproduct, assigned to an FMN-cysteine thiol adduct. Positive regulator in the activation of the general stress transcription factor sigma-B	FMN
13	<i>lmo0884</i>	<i>lmo0884</i>	Coproporphyrinogen III oxidase	Involved in coproporphyrin-dependent heme b biosynthesis. Catalyzes the oxidation of coproporphyrinogen III to coproporphyrin III.	FAD
14	<i>lmo0906</i>	<i>lmo0906</i>	Glutathione disulfide reductase	Catalyzes the reduction of glutathione disulfide to 2 glutathione; maintains high levels of reduced glutathione in the cytosol; involved in redox regulation and oxidative defense	FAD
15	<i>lmo0936</i>	<i>lmo0936</i>	Uncharacterized protein; Nitroflavin reductase	Oxygen-insensitive NADPH nitroreductase	?
16	<i>lmo1055</i>	<i>pdhD</i>	Dihydropyruvate dehydrogenase	E3 component of pyruvate complex; catalyzes the oxidation of dihydropyruvate to pyruvate	FAD
17	<i>lmo1276</i>	<i>gid (trmFO)</i>	Methylenetetrahydrofolate--tRNA-(uracil-5-)-methyltransferase	Catalyzes the folate-dependent formation of 5-methyl-uridine at position 54 (M-5-U54) in all tRNAs	FAD
18	<i>lmo1293</i>	<i>glpD</i>	Glycerol-3-phosphate dehydrogenase	Glycerone phosphate from sn-glycerol 3-phosphate (aerobic route)	FAD
19	<i>lmo1329</i>	<i>ribC</i>	Bifunctional riboflavin kinase/ FAD synthase	Catalyzes the phosphorylation of riboflavin to FMN followed by the adeninylation of FMN to FAD	N/A
20	<i>lmo1371</i>	<i>lmo1371</i>	Dihydropyruvate dehydrogenase	E3 component of the branched-chain alpha-keto acid dehydrogenase complex; catalyzes the oxidation of dihydropyruvate to pyruvate	FAD
21	<i>lmo1383</i>	<i>idi2</i>	Isopentenyl pyrophosphate isomerase	Involved in the biosynthesis of isoprenoids. Catalyzes the 1,3-allylic rearrangement of the homoallylic substrate isopentenyl (IPP) to its allylic isomer, dimethylallyl diphosphate (DMAPP)	FMN
22	<i>lmo1420</i>	<i>murB</i>	UDP-N-acetylenolpyruvoylglucosamine reductase	Catalyzes the reduction of UDP-N-acetylglucosamine enolpyruvate to form UDP-N-acetylmuramate in peptidoglycan biosynthesis	FAD
23	<i>lmo1433</i>	<i>lmo1433</i>	Hypothetical protein; Glutathione reductase	Catalyzes the reduction of glutathione disulfide to 2 glutathione	FAD
24	<i>lmo1678</i>	<i>lmo1678</i>	Bifunctional homocysteine S-methyltransferase/5,10-methylenetetrahydrofolate reductase	Amino acid transport and metabolism	FAD
25	<i>lmo1710</i>	<i>lmo1710</i>	Hypothetical protein; Flavodoxin	Low-potential electron donor to a number of redox enzymes	FMN
26	<i>lmo1734</i>	<i>lmo1734</i>	Hypothetical protein; Glutamate synthase large subunit	Biosynthesis of glutamate	FMN
27	<i>lmo1789</i>	<i>lmo1789</i>	Uncharacterized Protein; Flavodoxin-like protein	NAD(P)H dehydrogenase (quinone) activity	FAD
28	<i>lmo1825</i>	<i>lmo1825</i>	Pantothenate metabolism flavoprotein	Bifunctional protein that catalyzes two steps in the biosynthesis of coenzyme A	FMN
29	<i>lmo1833</i>	<i>pyrD</i>	Dihydroorotate dehydrogenase	Catalyzes the conversion of dihydroorotate to orotate in the pyrimidine biosynthesis pathway, using FMN as an essential cofactor; subclass 1B is a heterotetramer consisting of two PyrDB subunits	FMN
30	<i>lmo1834</i>	<i>pyrDII</i>	Dihydroorotate dehydrogenase electron transfer subunit	Responsible for channeling the electrons from the oxidation of dihydroorotate from the FMN redox center in the PyrD type B subunit to the ultimate electron acceptor NAD+	FAD
31	<i>lmo1928</i>	<i>aroF</i>	Chorismate synthase	Catalyzes the formation of chorismate from 5-O-(1-carboxyvinyl)-3-phosphoshikimate in aromatic amino acid biosynthesis	FMN
32	<i>lmo1961</i>	<i>lmo1961</i>	Hypothetical protein; Oxidoreductase	Predicted oxidoreductase activity	FAD
33	<i>lmo2023</i>	<i>nadB</i>	L-aspartate oxidase	Catalyzes the oxidation of L-aspartate to iminoaspartate, the first step in the de novo biosynthesis of NAD+	FAD
34	<i>lmo2111</i>	<i>lmo2111</i>	Hypothetical; Nitroreductase	Hypothetical oxidoreductase activity	FMN
35	<i>lmo2153</i>	<i>nrdI</i>	Flavodoxin	An electron-transfer protein that binds one FMN molecule	FMN
36	<i>lmo2343</i>	<i>lmo2343</i>	Hypothetical protein; Nitrotriacetate monooxygenase	Monooxygenase and oxidoreductase activity, acting on paired donors, with incorporation or reduction of molecular oxygen	FMN
37	<i>lmo2351</i>	<i>lmo2351</i>	FMN reductase	FMN reductase activity	FMN
38	<i>lmo2390</i>	<i>lmo2390</i>	Hypothetical protein; Thioredoxin reductase	Thioredoxin reductase activity	FAD
39	<i>lmo2471</i>	<i>namA</i>	NADPH dehydrogenase	Catalyzes the reduction of the double bond of an array of alpha, beta-unsaturated aldehydes and ketones. It also reduces the nitro group of nitroester and nitroaromatic compounds. It could have a role in detoxification processes.	FMN
40	<i>lmo2478</i>	<i>trxB</i>	Thioredoxin reductase	Thioredoxin-disulfide reductase activity	FAD
41	<i>lmo2636</i>	<i>fmnB</i>	FAD:protein FMN transferase	Flavin transferase that catalyzes the transfer of the FMN moiety of FAD to a hydroxyl group of a threonine residue in a target flavoprotein	FAD
42	<i>lmo2637</i>	<i>pplA</i>	Lipoprotein precursor of the pPplA pheromone	Precursor of pPplA pheromone which enhances L. monocytogenes escape from phagosomes. Involved in EET by relaying electrons through its two covalently bound flavin groups to extracellular acceptors	FMN
43	<i>lmo2738</i>	<i>lmo2738</i>	Hypothetical protein; Hemolysin	Predicted integral component of membrane. Protein with oxidoreductase activity. Magnesium and cobalt exporter	FAD
44	<i>lmo2810</i>	<i>gidA (mnmG)</i>	tRNA uridine 5-carboxymethylaminomethyl modification enzyme	NAD-binding protein involved in the addition of a carboxymethylaminomethyl (cmnm) group at the wobble position (U34) of certain tRNAs, forming tRNA-cmnm5s2U34	FAD

Figure 1.3 Predicted flavoproteins encoded by *L. monocytogenes*. Data was compiled from the protein databases Uniprot, Biocyc.org, and Kyoto Encyclopedia of Genes and Genomes (KEGG) (59).

1.4 Mucosal-associated invariant T cells recognize a pathogen-associated molecular pattern derived from riboflavin biosynthesis

Mucosal-associated invariant T (MAIT) cells are an innate-like T cell subset that recognizes intermediates of riboflavin biosynthesis during infection (37, 63). In humans, MAIT cells represent one of the most abundant T cell populations and can reach up to 10% and 40% of T cells in the blood and the liver, respectively (64–66). Furthermore, human MAIT cells have an invariant T cell receptor- α (TCR- α) chain that is homologous to TCR- α chains in other mammalian species like mice and cattle, indicating a high degree of evolutionary conservation (67, 68). MAIT cells display rapid and potent antimicrobial responses to a wide range of microorganisms and have been associated with inflammatory diseases and cancer (66, 69–72). Due to their abundance in humans, evolutionary conservation, unique antigenic specificity, and implication in an array of infectious and non-infectious diseases, MAIT cells have been brought to the fore of immunological studies in recent years.

MAIT cells were first discovered in 1993 when Porcelli and colleagues identified CD4-CD8 double-negative (DN) $\alpha\beta$ T cells expressing the invariant TCR- α chain TRAV1-2/TRAJ33 in multiple human peripheral blood samples (73). They hypothesized that expression of this specific TCR by DN T cells suggests these T cells might recognize a limited range of antigens and use non-polymorphic antigen-presenting molecules (73). Indeed, two years later, another study paved the way for the eventual characterization of MAIT cells with the discovery of the monomorphic major histocompatibility complex (MHC) class I-like molecule, MHC-related protein 1 (MR1) (74), now known to be the antigen-presenting molecule for MAIT cells. In a seminal 2003 study, MAIT cells were found to be MR1-restricted, enriched in the gut lamina propria (hence the name “mucosal-associated invariant T cells”), and absent in germ-free mice (75). These observations led the researchers to hypothesize that MR1 might present non-peptide-derived microbial products necessary for the accumulation of MAIT cells, which were corroborated in another seminal study a decade later (37).

Despite these discoveries and initial characterization that spurred further research into MAIT cells for the next decade, efforts on elucidating the antigen specificity of MAIT cells were largely unsuccessful, hindering further advances in understanding MAIT cell biology. One of the reasons why MAIT cells were difficult to study was the lack of suitable animal models. For example, in laboratory mice, MAIT cells are rare and only account for 0.6% of all T cells in the liver, as compared with 40% in humans (63). Another reason was the lack of tools, like MR1 tetramers, to easily identify MAIT cells in samples since the MR1 ligand was still unidentified. It was not until 2010 that the field made significant headway in the discovery of MAIT cell ligands— two groups independently discovered that MAIT cells respond to a wide range of microbes, including a multitude of bacteria and yeast (66, 69). Interestingly, they also observed that MAIT cells failed to respond to bacteria like *Enterococcus faecalis*, *Streptococcus pyogenes*, and five different viruses, suggesting that although MAIT cells can detect a broad range of microbially-derived antigens, they are unable to sense and respond to all microbes (64, 66, 69). The ensuing groundbreaking study by Kjer-Nielsen *et al.* in 2012 made sense of these provocative discoveries. They revealed that MR1 binds ribityllumazines and pyrimidine-based

intermediates of riboflavin and other B vitamins, respectively (37). This study shed light on the critical importance of the riboflavin biosynthetic pathway and made the correlation that microbes that encoded components of the pathway activate MAIT cells, whereas the bacterial species that lacked the genes necessary for the *de novo* synthesis of riboflavin did not (37, 76). Further genetic experiments confirmed that the otherwise potent response of MAIT cells to *Lactococcus lactis* and *Escherichia coli* is eliminated following the deletion of their riboflavin biosynthetic genes (76, 77). These studies determined that one of the most potent MAIT cell activating ligands covalently bound and presented by MR1 was the 5-(2-oxopropylideneamino)-6-D-ribitylamino-uracil (5-OP-RU), a very unstable riboflavin metabolite derivative formed through the non-enzymatic condensation between the riboflavin precursor 5-amino-6-(D-ribitylamino)uracil (5-A-RU) and methylglyoxal, a byproduct of metabolism (**Fig. 1.1**) (76, 78, 79). Since mammals lack the riboflavin biosynthetic pathway, which is present in most bacteria, and thus are incapable of generating 5-A-RU, this intermediate metabolite fits the profile of a pathogen-associated molecular pattern that hosts have evolved to recognize as an indicator of an active infection.

MR1 Presentation and MAIT Cell Function

MR1 is constitutively expressed by all nucleated cells and remains in an unfolded ligand-receptive state stabilized by chaperones in the endoplasmic reticulum (ER) (80–82). During infection with riboflavin-producing microorganisms, 5-OP-RU enters the ER, by an unknown mechanism, and reacts with Lysine 43 in the MR1 binding groove to form a Schiff base (79, 80). This reaction causes a conformational change that leads to the stabilization of the antigen-MR1 complex (76, 83). The complex then exits the ER, traffics through the Golgi, and is finally presented at the plasma membrane for MAIT cell recognition (80, 81, 84). Upon recognition of MR1:5-OP-RU complexes and costimulatory ligands, MAIT cells activate, proliferate, and exhibit rapid effector function responses including production of proinflammatory cytokines (like interferon- γ (IFN- γ), tumor necrosis factor- α (TNF- α), and interleukin-17 (IL-17)), and secretion of cytotoxic effectors (like granzyme B and perforin) (85–90). More recently, it has been appreciated that during some viral infections MAIT cells can become activated through MR1/TCR-independent signaling, although the mechanisms that lead to MAIT cell activation and their effector responses in this context have not been well-characterized (91). MR1/TCR-independent activation of MAIT cells by viruses is mediated by a combination of proinflammatory cytokines like IL-7, IL-12, IL-15, IL-18, IL-23, and type-I IFNs (91–93). MR1/TCR-independently activated MAIT cells produce proinflammatory cytokines and cytotoxic effectors that act on infected/bystander cells to restrict viral replication and dissemination (92, 94)

MAIT cells can respond to a broad range of pathogens including yeast, bacteria, and viruses (95), but the most potent effector responses are against riboflavin-producing intracellular bacteria (87, 88). For example, Meierovics and colleagues used the riboflavin-producing facultative intracellular pathogen *Francisella tularensis* to show that mice depleted of CD4⁺ and CD8⁺ conventional $\alpha\beta$ T cells, which had normal number of MAIT cells, survived pulmonary infection (96). In contrast, mice lacking both $\alpha\beta$ T cells and MAIT cells succumbed to *F. tularensis* infection. These results demonstrated that MAIT cells respond and generate an

effective immune response, which includes bridging the innate and adaptive immune systems, that is sufficient to protect mice from *F. tularensis* lethal challenge (96). Furthermore, another group studying the riboflavin-producing facultative intracellular pathogen *Legionella longbeachae* showed that in severely immunodeficient mice lacking T, B, and natural killer cells (RAG2^{-/-}γC^{-/-}), adoptively transferred MAIT cells were sufficient to protect mice from a lethal *L. longbeachae* challenge (97). They also showed that production of IFN-γ by MAIT cells, was required for control of *L. longbeachae* infection. These studies revealed the critical role played by MAIT cells in antimicrobial defense, specifically against riboflavin-producing intracellular bacteria, and highlighted their immunological relevance. However, the roles played by MAIT cells during infection with other riboflavin-producing intracellular pathogens are far from being completely elucidated. For example, even though MAIT cells get activated and respond to *Mycobacterium tuberculosis* (*Mtb*), a slow-growing riboflavin prototrophic bacterium and a leading cause of death worldwide, there is no clear consensus on their contribution to restriction of *Mtb* growth (98). During the first stages of *Mtb* infection in humans and mice, MAIT cells get depleted from the blood and are retained in the sites of infection, primarily the lungs, where they proliferate (99, 100). However, while earlier studies showed a modest contribution of MAIT cells to *Mtb* resistance, recent studies suggest that during the first stages of the infection, MAIT cells do not provide restriction of the pathogen and might actually be detrimental to adaptive responses since they might be responsible for delayed CD4⁺ T cell priming and responses (100–102). Interestingly, MAIT cell stimulation during the chronic stage of the infection leads to MAIT cell proliferation and production of IL-17A which correlated with reduced bacterial burden (100). These observations provide proof that even though MAIT cells were discovered almost thirty years ago, more tools and model systems are needed to understand MAIT cell biology and their responses to intracellular pathogens during acute and chronic infections. Likewise, more research should be devoted to understanding if pathogens have developed strategies to avoid MAIT cell recognition and restriction. As mentioned above, *L. monocytogenes* is an intracellular pathogen that, unlike most bacteria, lacks the riboflavin biosynthetic genes but relies significantly on flavins for growth, physiology, metabolism, and pathogenesis. Thus, it is tempting to speculate that *L. monocytogenes* might have lost the capacity to synthesize riboflavin *de novo* and was evolutionarily pressured to import flavins to avoid MAIT cell responses. In Chapter 3, I will address my progress toward researching this exciting evolutionary question.

Chapter 2: RibU is an essential determinant of *Listeria* pathogenesis that mediates acquisition of FMN and FAD during intracellular growth

2.1 Summary of Results

Flavin mononucleotide (FMN) and flavin adenine dinucleotide (FAD) are essential riboflavin-derived cofactors involved in a myriad of redox reactions across all forms of life. Nevertheless, the basis of flavin acquisition strategies by riboflavin auxotrophic pathogens remains poorly defined. In this study, we examined how the facultative intracellular pathogen *Listeria monocytogenes*, a riboflavin auxotroph, acquires flavins during infection. A *L. monocytogenes* mutant lacking the putative riboflavin transporter (RibU) was completely avirulent in mice but had no detectable growth defect in nutrient-rich media. However, unlike wild type, the RibU mutant was unable to grow in defined media supplemented with FMN or FAD or replicate in macrophages starved for riboflavin. Consistent with RibU functioning to scavenge FMN and FAD inside host cells, a mutant unable to convert riboflavin to FMN or FAD retained virulence and grew in cultured macrophages and in spleens and livers of infected mice. However, this FMN and FAD-requiring strain was unable to grow in the gallbladder or intestines, where *L. monocytogenes* normally grows extracellularly, suggesting that these sites do not contain sufficient flavin cofactors to promote replication. Thus, by deleting genes required to synthesize FMN and FAD we converted *L. monocytogenes* from a facultative to an obligate intracellular pathogen. Collectively, these data indicate that *L. monocytogenes* requires riboflavin to grow extracellularly *in vivo* but scavenges FMN and FAD to grow in host cells.

2.2 Introduction

Riboflavin (vitamin B₂) is a water-soluble vitamin essential to all organisms and the precursor of the biologically active flavin cofactors FMN and FAD (**Fig. 2.1a**), which are necessary for a diverse array of oxidation-reduction reactions (1, 4, 103). While plants, fungi, and most bacteria and archaea synthesize riboflavin, some bacteria and all mammals lack the genes to make this vitamin *de novo* (26, 104, 105). Many organisms encode transporters that allow them to obtain riboflavin from the environment (29, 32, 104, 105). Several bacterial and all eukaryotic intracellular pathogens require an exogenous source of riboflavin (57, 106, 107) and, interestingly, some also lack the enzymes that catalyze the conversion of riboflavin to FMN and FAD (57, 58). How these riboflavin auxotrophic intracellular pathogens fulfill their flavin requirement in host cells is poorly understood. Most of these intracellular pathogens encode annotated riboflavin transporters. Interestingly, however, riboflavin is scarce in host cells while FMN and FAD are abundant (108–110). To better understand flavin acquisition and requirements for pathogenesis, here we focused on the riboflavin auxotrophic bacterium *Listeria monocytogenes*.

L. monocytogenes is a Gram-positive bacterium that lives as both an environmental saprophyte and as a facultative intracellular pathogen of mammals including humans (39). Once *L. monocytogenes* enters a cell, it escapes from a phagosome and gains access to the cytosol where it acquires nutrients and rapidly divides (41). Although *L. monocytogenes* has few growth requirements (50), it lacks the riboflavin biosynthetic genes. To obtain this vitamin, *L. monocytogenes* encodes an energy-coupling factor (ECF) transporter, RibU, that is annotated as

a riboflavin transporter (51, 52). RibU is the substrate binding subunit of an ECF transporter, which is also composed of two ATPases and a transmembrane subunit that together form a complex for riboflavin import (54) (**Fig. 1.2**). RibU from *L. monocytogenes* binds riboflavin (54) and rescues the growth of a riboflavin auxotrophic *Bacillus subtilis* strain (51). Additionally, *L. monocytogenes* encodes the enzymes RibC and RibF, which are involved in the biosynthesis of FMN and FAD (51, 56). RibC is a bifunctional enzyme that catalyzes the phosphorylation of riboflavin to FMN and the adenylation of FMN to form FAD. RibF also converts FMN to FAD by adenylation. RibU, RibC, and RibF are the only proteins known to control flavin metabolism in *L. monocytogenes* (**Fig. 1.2**)

Recently, there has been renewed interest in flavin metabolism in the context of pathogenesis stemming from the discovery that intermediates of riboflavin biosynthesis activate innate-like mucosal-associated invariant T (MAIT) cells (37). In addition, we recently discovered that flavins are implicated in distinct extracytosolic redox activities in thousands of bacterial species (62). These bacterial redox systems allow bacteria to transfer electrons from the cytosol to various electron acceptors. We previously described that *L. monocytogenes* possesses a novel, but conserved, flavin-based extracellular electron transfer (EET) system that allows bacteria to respire anaerobically using various electron acceptors such as iron and fumarate (9, 60). Among the *L. monocytogenes* transposon mutants that lacked EET were mutations in genes encoding the riboflavin transporter, an extracellular flavin transferase, and an FMNylated surface protein (9). Surprisingly, mutants in *ribU* lacked EET activity, yet were able to grow in nutrient-rich media. In this study, we aimed to characterize how *L. monocytogenes* acquires flavins and their role during infection. We discovered that RibU was essential for intracellular growth and that its function is to transport FMN and FAD from the host cell cytosol. This is the first report of an intracellular pathogen importing FMN and FAD *in vivo*.

2.3 Results

2.3.1 RibU is dispensable for growth in nutrient-rich media but is required for virulence in mice.

We previously isolated a mutant with a transposon insertion in the *ribU* gene, the sole annotated riboflavin transporter in *L. monocytogenes* (9). Since flavins are necessary for a myriad of essential processes, we were surprised that the only annotated riboflavin transporter still was not an essential gene. To confirm that RibU was not essential for growth, and possibly assess flavin acquisition and requirements during pathogenesis, we generated a *L. monocytogenes* strain with an in-frame deletion in *ribU* ($\Delta ribU$). Like the transposon mutant, the $\Delta ribU$ strain had no detectable growth defect in nutrient-rich media compared to wild-type *L. monocytogenes* (**Fig. 2.1b**). In contrast, the $\Delta ribU$ strain had a 5-log virulence defect in the spleens of mice compared to wild-type *L. monocytogenes* (**Fig. 2.1c**), and no colony-forming units (CFUs) could be recovered from the livers of infected mice (**Fig. 2.1d**). Complementation of the $\Delta ribU$ mutant with a *ribU* gene with its endogenous promoter ($\Delta ribU + ribU$) fully restored virulence *in vivo* (**Fig. 2.1c,d**).

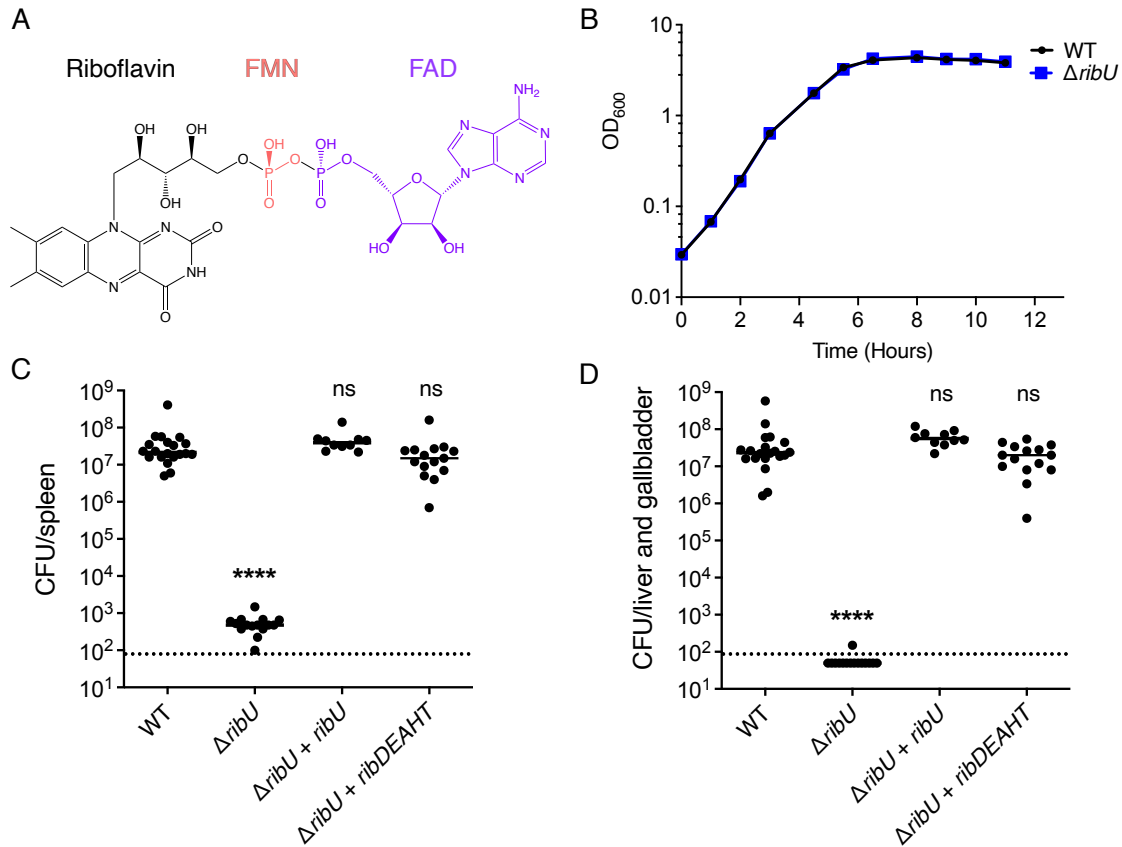


Figure 2.1 RibU is essential for virulence but dispensable for growth in nutrient-rich media. (A) Structures of riboflavin (black), FMN (red), and FAD (purple). Riboflavin is phosphorylated by riboflavin kinases to produce FMN. FAD synthetases adenylylate FMN to generate FAD. (B) Broth growth curve of *L.* strains grown in nutrient-rich media. OD₆₀₀ was used to determine cell density. The means and standard deviations of three independent experiments are shown. Note: both the wild-type and $\Delta ribU$ mutant growth curves are superimposable. (C-D) Bacterial burdens in CD-1 mice infected intravenously with 1×10^5 CFUs of indicated *L. monocytogenes* strains. 48 h post-infection, the spleens (C) and livers (D) were harvested, homogenized, and plated to determine the colony-forming units (CFUs) per organ. The data show the combination of at least two independent experiments, WT and $\Delta ribU$ ($n=20$ mice), $\Delta ribU + ribDEAHT$ ($n=15$ mice), and $\Delta ribU + ribU$ ($n=10$ mice). The black lines represent the median CFUs for each strain. The dashed line represents the limit of detection. Statistical significance of logarithmically transformed CFU values was determined using one-way ANOVA and Dunnett's post-test using wild type as the control. ****, $P < 0.0001$; ns, not significant $P > 0.05$.

To determine if the virulence defect of the $\Delta ribU$ strain was caused by riboflavin starvation *in vivo*, we engineered the $\Delta ribU$ mutant to synthesize riboflavin by inserting the riboflavin operon *ribDEAHT* from the closely related Gram-positive bacterium *B. subtilis* (111) onto the *L. monocytogenes* chromosome. This strain grew in colorless chemically defined synthetic media without riboflavin supplementation and turned the media yellow, the natural color of flavins (**Fig. 2.2**). Expression of the *ribDEAHT* operon rescued the $\Delta ribU$ strain's virulence to wild-type

L. monocytogenes levels in the spleens and livers of mice (**Fig. 2.1c,d**). Based on these observations we concluded that RibU is essential for *L. monocytogenes* pathogenesis and that its function relates to flavin acquisition since *de novo* riboflavin production in the RibU-minus strain completely bypassed RibU's essentiality *in vivo*.

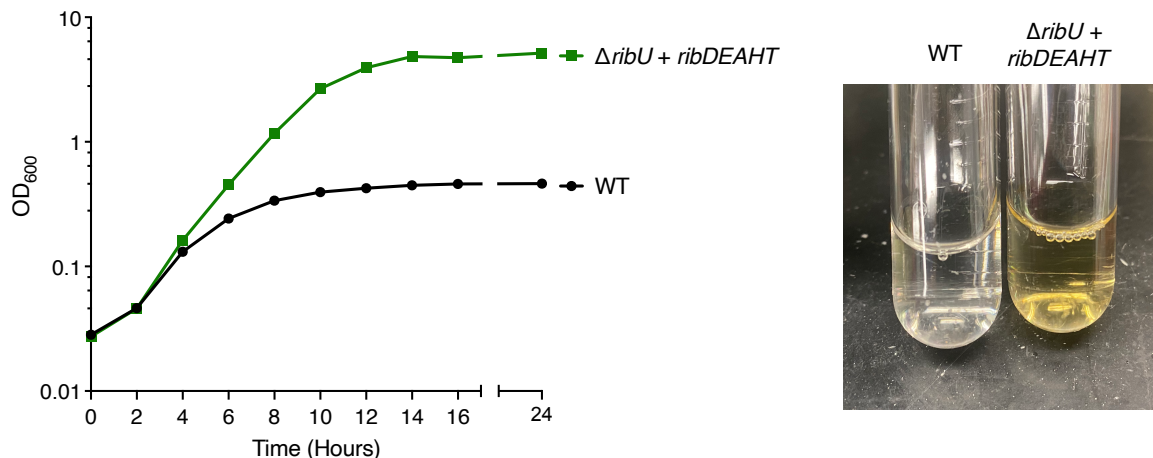


Figure 2.2. The $\Delta ribU$ strain producing riboflavin grows in chemically defined media lacking flavins. Broth growth curve of *L. monocytogenes* strains grown in chemically defined media lacking flavins. OD₆₀₀ was used to determine cell density. The data show the means and standard deviations of three independent experiments. In chemically defined media lacking flavins, wild-type *L. monocytogenes* grows until it depletes its flavin pool. In contrast, the $\Delta ribU + ribDEAHT$ strain grows to higher densities. The picture shows the media supernatant of wild-type (left) and the $\Delta ribU + ribDEAHT$ strain (right) after 24 h of growth at 37 °C shaking. The change in color from colorless to bright yellow, the natural color of flavins, suggests the $\Delta ribU + ribDEAHT$ strain is producing riboflavin and allowing it to grow in media lacking flavins.

2.3.2 *L. monocytogenes* uses RibU to grow in macrophages

To study why RibU was essential for growth of *L. monocytogenes* in mice, we performed infections *in vitro* using bone marrow-derived macrophages (BMMs). At 2 h post-infection, the $\Delta ribU$ mutant had a small but significant growth advantage over wild-type *L. monocytogenes* (**Fig. 2.3a**), which was associated with an increase in phagosomal escape (**Fig. 2.4a**). However, during exponential growth (2-5 h post-infection), the $\Delta ribU$ mutant had an apparent defect in replication rate and showed a loss in CFUs during the late stages of infection (5-8 h post-infection) (**Fig. 2.3a**). Complementation of the $\Delta ribU$ strain with the *ribU* gene or the *ribDEAHT* operon completely restored the growth defects in BMMs (**Fig. 2.4b**).

To test if the $\Delta ribU$ strain has an inherent intracellular virulence defect not related to riboflavin, BMMs were incubated with excess riboflavin (10 μ M) prior to infection to increase the concentration of intracellular riboflavin. In this condition of riboflavin excess, the $\Delta ribU$ mutant replicated to wild type levels (**Fig. 2.3b**). To assess if the growth of the $\Delta ribU$ strain observed during the exponential growth phase in BMMs (**Fig. 2.3a**) is due to residual flavins from the

medium, we infected riboflavin-deficient BMMs with riboflavin-starved bacteria. In this experiment, the $\Delta ribU$ mutant and wild-type *L. monocytogenes* strains were incubated in chemically defined synthetic media lacking flavins for 16-18 h prior to infection. The BMM cell culture media was replaced with media lacking riboflavin and the macrophages were incubated for 3 h prior to infection with the riboflavin-starved bacteria. We observed that riboflavin-starved wild-type *L. monocytogenes* were able to grow in riboflavin-deficient BMMs. However, the riboflavin-starved $\Delta ribU$ mutant was unable to replicate in riboflavin-depleted BMMs (**Fig. 2.3c**). The riboflavin-starved $\Delta ribU$ mutant was able to grow in riboflavin-deficient BMMs supplemented with 1 μ M riboflavin just prior to infection (**Fig. 2.4c**).

To further characterize the growth dynamics of the $\Delta ribU$ mutant, we focused on the late stage of infection and the loss of CFUs observed between 5 and 8 h post-infection. We hypothesized that the loss of CFUs was due to the inability of the $\Delta ribU$ mutant to obtain riboflavin from the cytosol of host cells and that riboflavin starvation led to bacterial and/or host cell death. Dying host cells allow access of gentamicin from the media into the cytoplasm where it kills the bacteria. To test if infection with the $\Delta ribU$ strain led to host cell death, we performed a lactate dehydrogenase (LDH) release assay. The results demonstrated that $\Delta ribU$ caused a significant increase in host cell death (**Fig. 2.3d**). Based on previous studies (112), we hypothesized that the $\Delta ribU$ strain was lysing in the macrophage cytosol and releasing DNA that activated the DNA-dependent AIM2 inflammasome, resulting in pyroptotic cell death. To test if $\Delta ribU$ was triggering AIM2-dependent pyroptosis, we performed LDH release assays using AIM2 knockout (KO) BMMs and observed that the $\Delta ribU$ mutant did not lead to LDH release (**Fig. 2.3e**). As a control, *L. monocytogenes* secreting flagellin (WT + *L.p.flaA*), which activates the NLRC4 inflammasome (113), still mediated cell death in infected AIM2 KO BMMs (**Fig. 2.3e**). Since the $\Delta ribU$ mutant did not lead to cell death in AIM2 KO BMMs, we hypothesized that the loss of CFUs in the $\Delta ribU$ mutant during the later stages of infection in wild-type BMMs should be rescued in AIM2 KO BMMs. Indeed, there was no loss of CFUs of the $\Delta ribU$ mutant at 8 h post-infection (**Fig. 2.3f**). These data suggested that the RibU-minus strain lysed to some extent *in vivo* and activated AIM2-dependent pyroptosis, which negatively impacted the virulence of the strain.

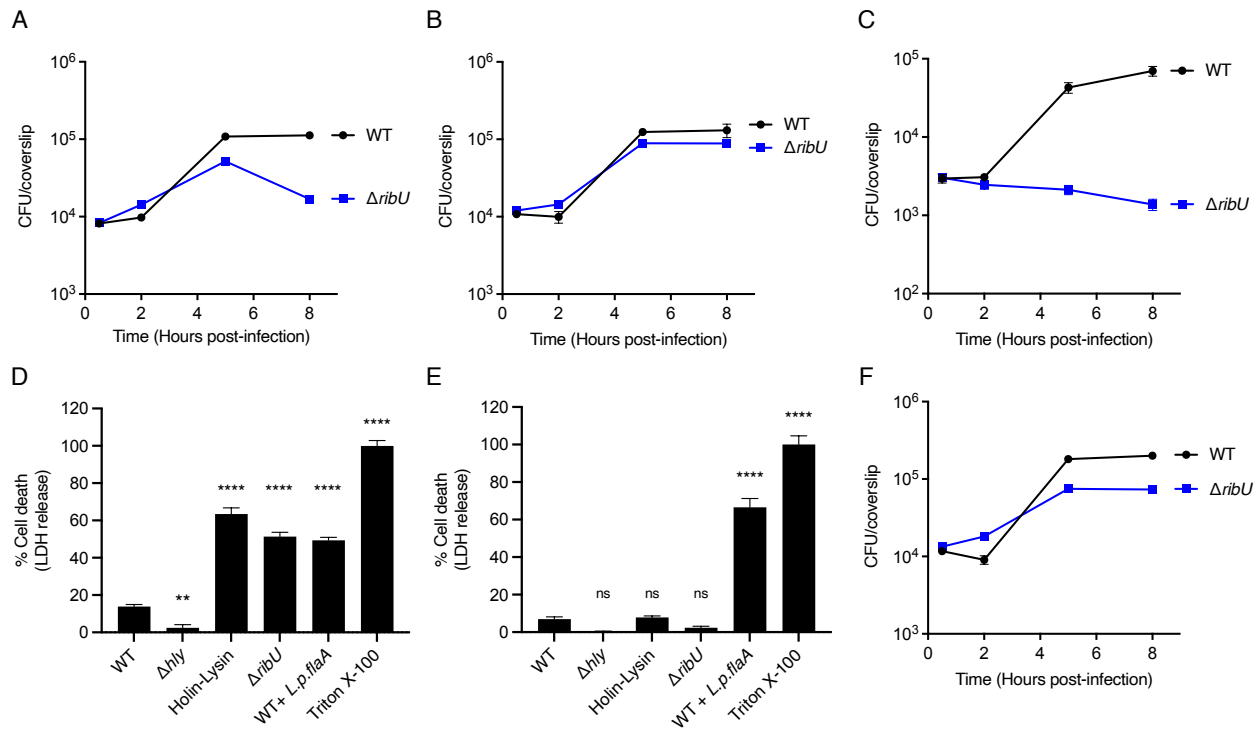


Figure 2.3 *L. monocytogenes* requires RibU to grow in riboflavin-starved macrophages. (A-C and F) Intracellular growth curves of *L. monocytogenes* strains in murine bone marrow-derived macrophages (BMMs). BMMs were infected at a multiplicity of infection (MOI) of 0.1 and CFUs were enumerated at the indicated times. (A) Intracellular growth curve of indicated *L. monocytogenes* strains in wild-type BMMs. The data show the means and standard errors of the mean of four independent experiments. (B) Intracellular growth curve of indicated *L. monocytogenes* strains in wild-type BMMs incubated with cell culture media containing excess (10 μ M) riboflavin during infection. The means and standard errors of the mean of three independent experiments are shown. (C) Intracellular growth curve of indicated flavin starved *L. monocytogenes* strains in riboflavin-deficient wild-type BMMs. The data represent the means and standard errors of the mean of three independent experiments. (D-E) Cell death of wild-type (D) or AIM2 KO (E) BMMs infected with specified *L. monocytogenes* strains. Lactate dehydrogenase (LDH) released to the cell culture media was used as an indicator of cell death. LDH release values were normalized to 1% Triton-X treated cells which represent 100% lysis. BMMs were infected at an MOI of 4. The data show the means and standard errors of the mean of three technical replicates from at least two (D) and four (E) independent experiments. Statistical significance was determined using one-way ANOVA and Dunnett's post-test using wild type as the control. ****, $P < 0.0001$; **, $P < 0.01$; ns, not significant $P > 0.05$. (F) Intracellular growth curve of indicated *L. monocytogenes* strains in AIM2 KO BMMs. The means and standard errors of the mean of five independent experiments are shown. WT + *L.p.flaA*, wild-type *L. monocytogenes* expressing *Legionella pneumophila* flagellin A under the control of the *actA* promoter (113). Holin-Lysin, wild-type *L. monocytogenes* expressing the bacteriophage proteins Holin and Lysin under the control of the *actA* promoter, which lead to lysis of the bacteria in the cytosol of the host cell (112).

2.3.3 *L. monocytogenes* uses RibU to scavenge FMN and FAD from the cytosol of host cells

Our observation that riboflavin-starved wild-type *L. monocytogenes* grew in riboflavin-deprived macrophages led us to question how *L. monocytogenes* fulfills its flavin requirements under these conditions. Interestingly, we did not observe any difference in the ability of wild-type *L. monocytogenes* to replicate intracellularly in the absence of riboflavin. The doubling time of riboflavin-starved wild-type *L. monocytogenes* in riboflavin-deficient BMMs was very similar to the doubling time of wild-type *L. monocytogenes* growing in BMMs with riboflavin, 48.6 and 51.5 minutes, respectively (**Fig. 2.4d**). Based on these results, and the fact that mammalian cells rapidly convert riboflavin to FMN and FAD upon import (108, 114), we hypothesized that wild-type *L. monocytogenes* imports FMN and/or FAD intracellularly to grow using RibU for their transport. To test if *L. monocytogenes* can import FMN and FAD to support growth, we used chemically defined synthetic media supplemented with riboflavin, FMN, or FAD as the sole flavin and found that wild-type *L. monocytogenes* grew in media containing each of the three flavins (**Fig. 2.5a**). By contrast, the $\Delta ribU$ strain did not replicate in chemically defined media with FMN or FAD (**Fig. 2.5b**) and had only a slight defect in growth in media containing riboflavin. These results suggested that RibU is responsible for growth on FMN and FAD and that riboflavin can enter cells using RibU and/or another, yet to be identified, riboflavin transporter.

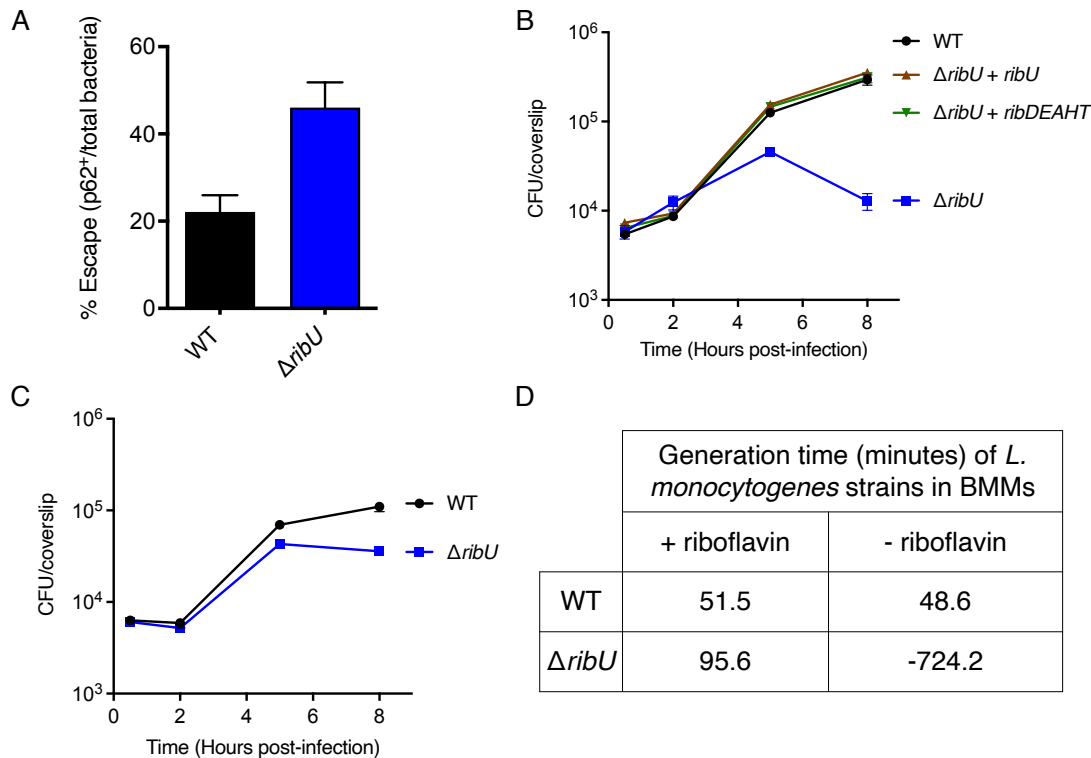


Fig. 2.4 Growth dynamics of the $\Delta ribU$ mutant in BMMs. (A) Percentage of bacteria that colocalized with the autophagy receptor p62 in infected BMMs. In BMMs treated with

cytochalasin D, bacteria that escape phagosomes are tagged with p62. Percent phagosomal escape is calculated by counting the number of p62⁺ bacteria of total bacteria. The data show the means and standard errors of the mean of two independent experiments. (B-C) Intracellular growth curves of *L. monocytogenes* strains in BMMs. BMMs were infected at an MOI of 0.1 and CFUs were enumerated at the indicated times. (B) Intracellular growth curve of indicated *L. monocytogenes* strains in wild-type BMMs. The data show the means and standard errors of the mean of two independent experiments. (C) Intracellular growth curve of indicated flavin-starved *L. monocytogenes* strains in riboflavin-deprived wild-type BMMs (for 3 h) supplemented with 1 μ M riboflavin just prior to infection. The data represent the means and standard errors of the mean of three independent experiments. (D) Generation time of intracellularly growing bacteria in riboflavin-sufficient and -deprived BMMs between 2 to 5 h. Negative values indicate that the number of recoverable bacteria was decreasing over time.

To test the hypothesis that *L. monocytogenes* utilizes RibU to scavenge FMN and FAD from the cytosol of host cells, we sought to generate an *L. monocytogenes* FMN and FAD auxotroph by constructing strains lacking *ribC*, *ribF*, or both (Δ *ribC* Δ *ribF*), enzymes responsible for converting riboflavin to FMN and FAD. Since FMN and FAD are essential cofactors, construction of this strain was performed in nutrient-rich media containing excess FMN and FAD to circumvent synthetic lethality. As predicted, the Δ *ribC* Δ *ribF* mutant was unable to replicate in chemically defined media with riboflavin as the sole flavin source (Fig. 2.5c).

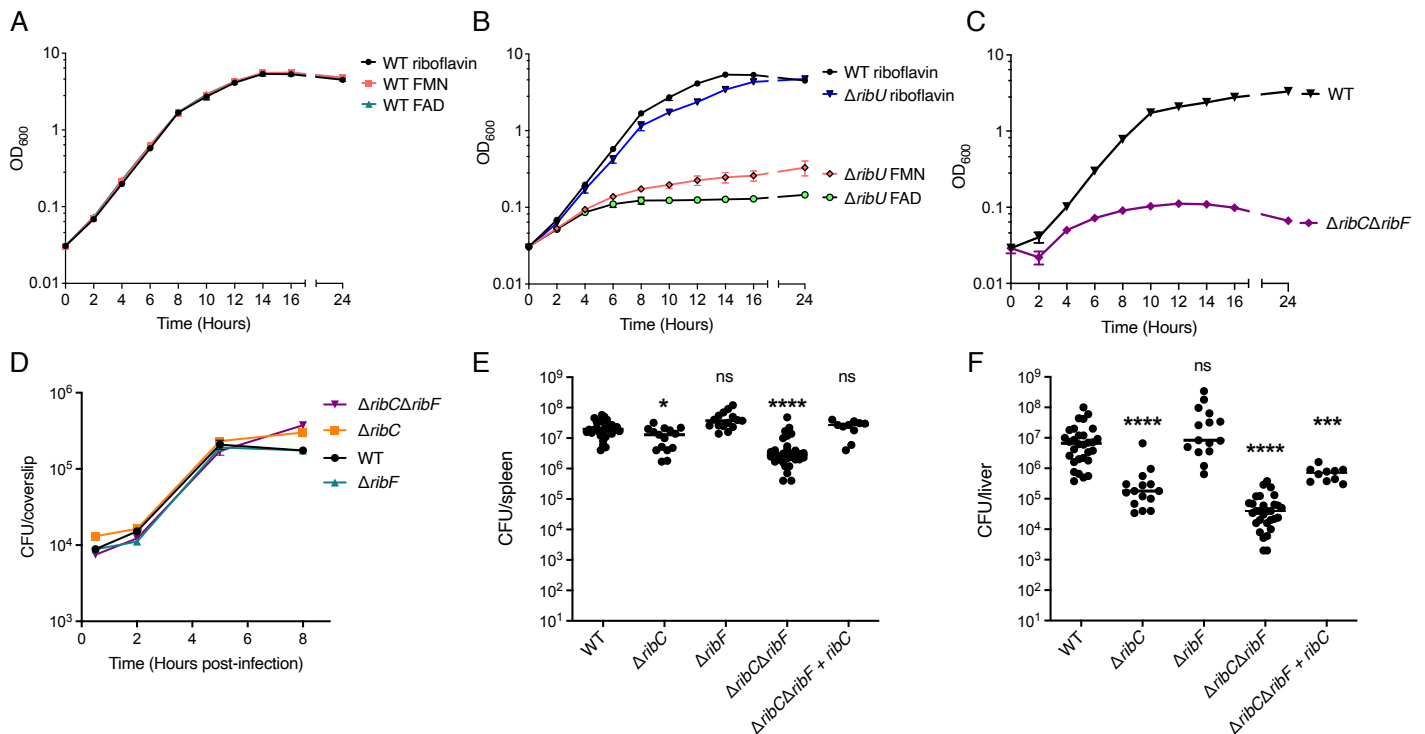


Figure 2.5 *L. monocytogenes* scavenges FMN and FAD from the host cytosol using RibU. (A) Broth growth curve of wild-type *L. monocytogenes* grown in chemically defined synthetic media with riboflavin, FMN, or FAD as the only flavin source. OD₆₀₀ was used to determine cell density.

The data show the means and standard deviations of four independent experiments. (B) Broth growth curve of $\Delta ribU$ mutant *L. monocytogenes* strain grown in chemically defined synthetic media with riboflavin, FMN, or FAD as the sole flavin source. Wild-type *L. monocytogenes* grown in chemically defined media with riboflavin is used as a reference. OD₆₀₀ was used to determine cell density. The data show the means and standard deviations of four independent experiments. (C) Broth growth curve of indicated *L. monocytogenes* strains grown in chemically defined media with riboflavin. OD₆₀₀ was used to determine cell density. The data show the means and standard deviations of two independent experiments. (D) Intracellular growth curves of *L. monocytogenes* strains in murine BMMs. BMMs were infected at an MOI of 0.1 and CFUs were enumerated at the indicated times. The means and standard errors of the mean of two independent experiments are shown. (E-F) Bacterial burdens in CD-1 mice infected intravenously with 1×10^5 CFUs of indicated *L. monocytogenes* strains. 48 h post-infection, the spleens (E) and livers (F) were harvested, homogenized, and plated to determine the CFUs per organ. The data show the combination of at least two independent experiments, WT and $\Delta ribC\Delta ribF$ ($n=30$ mice), $\Delta ribC$ and $\Delta ribF$ ($n=15$ mice), and $\Delta ribC\Delta ribF + ribC$ ($n=10$ mice). The black lines represent the median CFUs for each strain. Statistical significance of logarithmically transformed CFU values was determined using one-way ANOVA and Dunnett's post-test using wild type as the control. ****, $P < 0.0001$; ***, $P < 0.001$; *, $P < 0.01$; ns, not significant $P > 0.05$.

We reasoned that if *L. monocytogenes* imports FMN and FAD from the host cytosol, the $\Delta ribC\Delta ribF$ mutant should not be impaired for intracellular growth. Indeed, these strains replicated intracellularly in BMMs to wild-type *L. monocytogenes* levels (**Fig. 2.5d**). To test if the $\Delta ribC$, $\Delta ribF$, and the $\Delta ribC\Delta ribF$ mutant *L. monocytogenes* strains grew *in vivo*, we performed mouse virulence assays. The $\Delta ribC$, $\Delta ribF$, and $\Delta ribC\Delta ribF$ mutants maintained their virulence and grew to high levels in both the spleens and livers of mice, albeit the $\Delta ribC$ and $\Delta ribC\Delta ribF$ strains had statistically significant 2-log defects in the liver (**Fig. 2.5e,f**). Complementation of the $\Delta ribC\Delta ribF$ strain with the *ribC* gene with its endogenous promoter was able to restore most of the growth in the spleens and livers of infected mice (**Fig. 2.5e,f**). Thus, these results support a model in which *L. monocytogenes* uses RibU to import FMN and FAD from the cytosol of host cells.

2.3.4 The $\Delta ribC\Delta ribF$ mutant cannot grow in blood, gallbladders, or the gastrointestinal tract

The observation that the $\Delta ribC\Delta ribF$ strain replicated similarly to wild-type *L. monocytogenes* in the spleens but not in the livers of mice (**Fig. 2.5e,f**) prompted us to examine if this strain is able to colonize and grow in other sites of infection in mice and use growth as an indicator of flavin availability. Wild-type *L. monocytogenes* can grow extracellularly in the gallbladder, blood, and gastrointestinal (GI) tract of mice (115–118). During infection, *L. monocytogenes* colonizes the lumen of the gallbladder, which is connected to the liver through biliary ducts, and rapidly replicates extracellularly in the bile, establishing this organ as a bacterial reservoir (115, 116). The $\Delta ribC\Delta ribF$ mutant was unable to colonize the gallbladder, while the $\Delta ribC$ and $\Delta ribF$ strains grew to wild-type *L. monocytogenes* levels (**Fig. 2.6a**). Complementation of the $\Delta ribC\Delta ribF$ mutant with a *ribC* gene with its endogenous promoter completely rescued the growth of the $\Delta ribC\Delta ribF$ strain in the gallbladder.

To assess if the $\Delta ribC\Delta ribF$ mutant strain can grow extracellularly in blood, we performed a growth curve in defibrinated sheep's blood and found that the $\Delta ribC\Delta ribF$ mutant did not replicate and observed a 2-3 logs CFU loss by 24 h post-inoculation (**Fig. 2.6b**). Finally, to test if the $\Delta ribC\Delta ribF$ mutant can grow extracellularly in the lumen of the GI tract, mice were pre-treated for 2 days prior to the infection with streptomycin and were infected with 1×10^8 CFU/mouse. Stool pellets were collected daily for 5 days and plated to assess bacterial burden. The $\Delta ribC\Delta ribF$ mutant had a 7-log defect in fecal pellet CFUs compared to wild-type *L. monocytogenes* at 24 h post-infection (**Fig. 2.6c**). No CFUs were recovered from the $\Delta ribC\Delta ribF$ mutant infected mice following day 1 post-infection (**Fig. 2.6c**). Collectively, these observations suggest that the $\Delta ribC\Delta ribF$ strain cannot grow extracellularly in the gallbladder, blood, or GI tract, and that this mutant is restricted to intracellular growth *in vivo*.

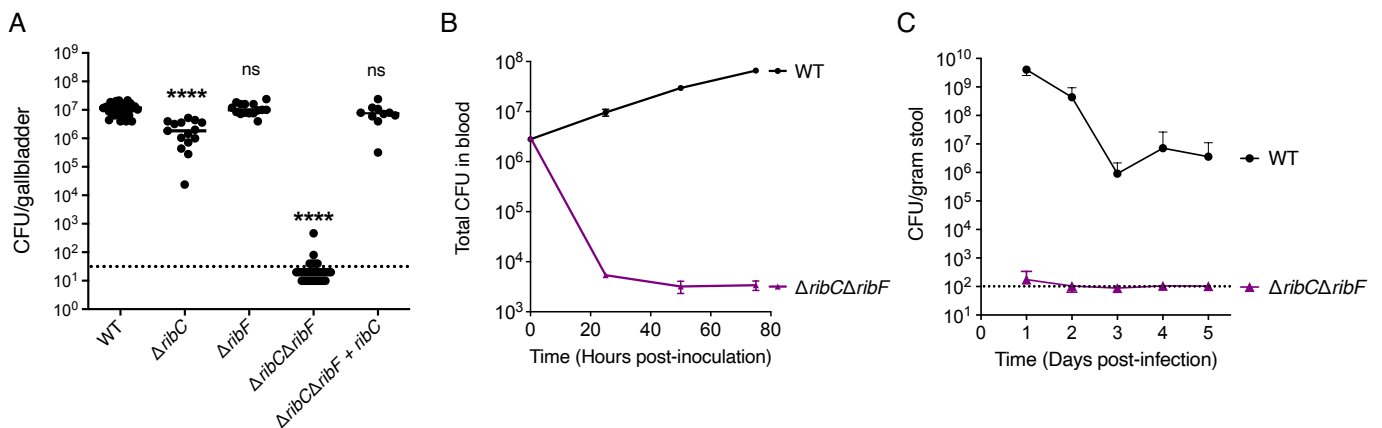


Figure 2.6 An FMN and FAD auxotrophic *L. monocytogenes* strain is restricted to intracellular growth *in vivo*. (A) Bacterial burdens in the gallbladder of CD-1 mice infected intravenously with 1×10^5 CFUs of indicated *L. monocytogenes* strains. 48 h post-infection, the gallbladders were harvested, homogenized, and plated to determine the CFUs per organ. The data show the combination of at least two independent experiments, WT and $\Delta ribC\Delta ribF$ ($n=30$ mice), $\Delta ribC$ and $\Delta ribF$ ($n=15$ mice), and $\Delta ribC\Delta ribF + ribC$ ($n=10$ mice). The black lines represent the median CFUs for each strain. The dashed line represents the limit of detection. Statistical significance of logarithmically transformed CFU values was determined using one-way ANOVA and Dunnett's post-test using wild type as the control. ****, $P < 0.0001$; ns, not significant $P > 0.05$. (B) *In vitro* growth of *L. monocytogenes* strains in defibrinated sheep's blood. Bacterial growth was determined by plating at the indicated times to determine the total CFUs in blood. The means and standard errors of the mean of three independent experiments are shown. (C) Bacterial burdens in the gastrointestinal tract of CD-1 mice infected orally with 1×10^8 CFUs of indicated *L. monocytogenes* strains. Mice were pretreated orally with streptomycin prior to the infection. Stool samples were collected at days 1-5 and plated to determine the CFUs per gram of stool. The data show the means and standard deviations of the mean from a combination of three independent experiments, $n=15$ mice per *L. monocytogenes* strain. The dashed line represents the limit of detection.

2.4 Discussion

The riboflavin derivatives FMN and FAD are redox active cofactors essential to all organisms (1, 4, 103), including pathogens that either synthesize riboflavin or import it from their host (119–121). Little is known about how pathogens that cannot synthesize riboflavin acquire this vitamin during infection. Here we show that the riboflavin auxotrophic, facultative intracellular bacterium *L. monocytogenes* uses the riboflavin transporter, RibU, to acquire FMN and FAD, but not riboflavin, from the cytoplasm of host cells. The finding that *L. monocytogenes* imports FMN and FAD to grow in host cells using RibU is supported by our data showing that a mutant lacking RibU is avirulent *in vivo* (**Fig. 1c,d**) but grew in nutrient-rich media and chemically defined media supplemented with riboflavin, and not with FMN and FAD (**Fig. 3b**). Furthermore, a mutant lacking the enzymes that convert riboflavin to FMN and FAD (*ribC/ribF* double mutant) grew like wild-type *L. monocytogenes* in BMMs (**Fig. 3d**) and *in vivo* in the spleen (**Fig. 3e**). Collectively, these observations led us to conclude that: (1) RibU is a flavin transporter that, in addition to riboflavin, can import FMN and FAD; (2) *L. monocytogenes* might encode another, unknown riboflavin transporter that is unable to import FMN and FAD; and (3) *L. monocytogenes* primarily acquires FMN and FAD *in vivo* to support its intracellular growth.

The reliance of *L. monocytogenes* on host cell FMN and FAD is not surprising given the fact that the concentration of these flavins inside cells far surpasses that of their precursor riboflavin (108–110). To our knowledge, this is the first report that intracellular pathogens can obtain FMN and FAD from the host cell cytoplasm, but we infer that this may be the case for other intracellular pathogens. For example, obligate intracellular pathogens in the *Rickettsia* and *Cryptosporidium* genera do not synthesize riboflavin and lack FMN and FAD synthetases (57, 58). Thus, we speculate that these pathogens must acquire FMN and FAD from the host to satisfy their flavin requirements. Similarly, we hypothesize that riboflavin auxotrophic vacuolar parasites, like members of the Apicomplexa phylum and *Leishmania* species, might rely on FMN and FAD import to grow intracellularly as well. These vacuolar parasites likely employ different mechanisms to scavenge these flavins from the cytosol, as has been shown for other micronutrients (122–124).

The evolutionary path to becoming an obligate intracellular pathogen often results in genome reduction (125–127) involving loss of a pathogen's ability to synthesize its own metabolites and rely on import of nutrients from their hosts. The active cofactors FMN and FAD are highly prevalent in host cells (108–110), which might explain why some intracellular pathogens do not synthesize riboflavin or encode enzymes that convert it to FMN and FAD. In this study, we demonstrate that a *L. monocytogenes* mutant lacking the RibC and RibF enzymes required supplementation of FMN and FAD to grow and was unable to replicate in blood (**Fig. 4b**), the gallbladder (**Fig. 4a**) and GI tract (**Fig. 4c**) of mice, which represent environments where wild-type *L. monocytogenes* grows extracellularly (115–118). In contrast, the *ribC/ribF* double mutant grew intracellularly in macrophages, and the spleen and liver of mice. Thus, we show the apparent conversion of a facultative intracellular pathogen into an obligate intracellular pathogen by eliminating two genes involved in the flavin biosynthesis pathway. This study

provides an example of how pathogens, as an evolutionary adaptation, might lose their biosynthetic capabilities, by discarding genes involved in the production of metabolites prevalent in their hosts, and instead rely on acquisition of nutrients directly from the host, ultimately becoming obligate intracellular pathogens. Our findings may also have practical applications by providing an additional safety measure to *L. monocytogenes* strains used as therapeutic cancer vaccines by preventing extracellular growth and limiting dissemination (128).

Considering that *L. monocytogenes* thrives as a ubiquitous environmental saprophyte and has few nutritional requirements, it is curious that these bacteria lack the capacity to synthesize riboflavin. We hypothesize that the lack of riboflavin biosynthesis may provide *L. monocytogenes* an evolutionary advantage during infection of mammalian hosts, which almost universally have a prevalent population of mucosal-associated invariant T (MAIT) cells (63) that are activated by an intermediate of bacterial riboflavin biosynthesis (37) and kill host cells harboring riboflavin-synthesizing bacteria such as *Francisellae*, *Salmonellae*, and *Legionellae* (89, 96, 97, 129, 130). We are currently testing our hypothesis by examining the pathogenesis of *L. monocytogenes* strains engineered to synthesize riboflavin and the activation status of MAIT cells in infected mice.

2.5 Materials and Methods

Bacterial culture and strains

All strains of *L. monocytogenes* used in this study (Supplementary Table 1) were derived from the wild-type 10403S strain and were cultured in filter-sterilized nutrient-rich Brain Heart Infusion (BHI) media (BD, Sparks, MD, USA) containing 200 µg/mL streptomycin (Sigma-Aldrich, St. Louis, MO, USA). Construction of the $\Delta ribU$ (*Imo1945*), $\Delta ribC$ (*Imo1329*), $\Delta ribF$ (*Imo0728*), and $\Delta ribC\Delta ribF$ strains was done using allelic exchange with the temperature-sensitive plasmid pKSV7, as previously described (131). During the process of generating the $\Delta ribC$, $\Delta ribF$, and double *ribC/ribF* mutant strains, the bacteria were always cultured in BHI media with 2.5 µM FMN (Sigma-Aldrich, St. Louis, MO, USA) and 2.5 µM FAD (Sigma-Aldrich, St. Louis, MO, USA) to circumvent synthetic lethality. For all procedures in which the $\Delta ribC$, $\Delta ribF$, and $\Delta ribC\Delta ribF$ strains were used, the bacteria were always grown in BHI media with 2.5 µM FMN and 2.5 µM FAD.

Generation of the $\Delta ribU$ strain expressing the *ribDEAHT* operon or complementation of the strain expressing *ribU* was done by amplifying the *ribDEAHT* operon with its native promoter from *B. subtilis* and the *ribU* gene with its native promoter from wild-type *L. monocytogenes*, respectively, and cloned into the site-specific pPL2 integrating vector. Similarly, complementation of the $\Delta ribC\Delta ribF$ mutant was done by amplifying the *ribC* gene with its native promoter and cloned into the pPL2 vector and introduced into *L. monocytogenes* by conjugation, as previously described (132).

Broth growth curves were performed with *L. monocytogenes* strains from overnight cultures grown at 37 °C shaking (200 rpm). Nutrient-rich (BHI) and chemically defined synthetic media growth curves were started at an optical density (OD₆₀₀) of 0.03. Chemically defined synthetic media was prepared as previously reported (48). Growth curves were spectrophotometrically measured by optical density at a wavelength of 600 nm (OD₆₀₀).

Tissue culture and growth media

Bone-marrow derived macrophages (BMMs) were prepared by collecting bone marrow from 8-week-old female wild-type (Jackson laboratory) and AIM2 KO (a kind gift from Kate Fitzgerald at the University of Massachusetts Medical School) C57BL/6J mice and differentiated as previously described (133). BMMs were cultured in high glucose Gibco Dulbecco's Modified Eagle's Medium (DMEM) (Thermo Fisher Scientific, Waltham, MA, USA) with 20% fetal bovine serum (FBS) (Avantor-Seradigm, Radnor, PA, USA), 10% M-CSF-producing 3T3 cell supernatant, 1% L-glutamine (Corning, Lowell, MA, USA), 1% sodium pyruvate (Corning, Lowell, MA, USA), 14 mM 2-mercaptoethanol (Gibco Thermo Fisher Scientific, Waltham, MA, USA), or with a modified DMEM recipe described in the experimental procedure.

Intracellular growth curves

Sixteen to eighteen h prior to infection, 3 x 10⁶ BMMs were seeded in 60 mm non-TC treated dishes (MIDSCI, St. Louis, MO, USA) containing 14 12 mm glass coverslips (Thermo Fisher Scientific, Waltham, MA, USA) in each dish. *L. monocytogenes* strains were grown at 30 °C overnight in 14 ml round polypropylene tubes (Thermo Fisher Scientific, Waltham, MA, USA) at a slanted position. The bacteria were washed and diluted in sterile 1X phosphate-buffered saline (PBS) and BMMs were infected at an MOI of 0.25. Half an hour post-infection, the cells were washed twice with 1X PBS. One h post-infection, 50 µg/mL of gentamicin sulfate (Sigma-Aldrich, St. Louis, MO, USA) was added to the cell culture media to kill/prevent bacteria from growing extracellularly. The growth curves then proceeded as previously described (134).

Intracellular growth curves in media lacking riboflavin

To deplete the intracellular flavins in *L. monocytogenes*, bacterial cultures were started 2 days prior to BMM infection in chemically defined media containing 1 µM riboflavin and grown at 37 °C with shaking. The bacteria were washed twice 16-18 h prior to infection, with 1X PBS and then diluted into chemically defined media lacking flavins and grown at 37 °C with shaking.

Macrophages were washed twice, 3 h prior to BMM infection, with 1X PBS and the cell culture media was replaced with DMEM high glucose lacking riboflavin (Millipore Sigma, Burlington, MA, USA), a kind gift from Erin Benanti at Aduro Biotech, with 20% dialyzed FBS- using SnakeSkin dialysis tubing, 3.5K MWCO (Thermo Fisher Scientific, Waltham, MA, USA), and other components as described in the tissue culture and growth media section in methods. The riboflavin-starved *L. monocytogenes* were washed and diluted in sterile 1X PBS and the BMMs were infected at an MOI of 0.25. These growth curves were performed without the addition of

riboflavin, unless otherwise stated in the legend. The growth curve experiments then proceeded as previously described (134).

Cell death (lactate dehydrogenase release) assay

Sixteen to eighteen h before infection, 5×10^5 BMMs/well were seeded in 24-well plates with 100 ng/mL of Pam3CSK4 (InvivoGen, San Diego, CA, USA) in DMEM media. Before infecting the BMMs, the cell culture media was replaced with DMEM media with 5% FBS. *L. monocytogenes* strains were grown overnight, slanted, at 30 °C. For the infection, bacteria were diluted in 1X PBS and BMMs were infected at an MOI of 4. Half an hour post-infection, the BMMs were washed twice with 1X PBS and DMEM media with 5% FBS and 50 µg/mL of gentamicin was added to wells. The experiment was conducted as previously describe (112).

Mouse intravenous infections

Eight-week-old female CD-1 mice (Charles River Laboratories, Wilmington, MA, USA) were infected via the tail vein with 200 µL of PBS containing 1×10^5 logarithmically growing bacteria. The mice were euthanized 48 h post-infection and the spleen, liver, and gallbladder were collected, homogenized, and plated to determine the number of CFU per organ.

Blood growth curve

The growth of *L. monocytogenes* strains in blood was determined using defibrinated sheep's blood (HemoStat Laboratories, Dixon, CA, USA). The bacteria were grown logarithmically for 2.5 h, washed, and resuspended in 3 mL of defibrinated sheep's blood at a concentration of 1×10^6 /mL. Blood cultures were incubated at 37 °C shaking. The growth of *L. monocytogenes* in blood was monitored for 3 days by diluting the blood in 1X PBS and plating to determine the number of CFU in total blood.

Mouse oral infections

Mice were given 5 mg/mL streptomycin sulfate salt (Sigma-Aldrich, St. Louis, MO, USA) in the drinking water, 48 h prior to infection. Mice were transferred to clean cages 18-24 h prior to infection and the food source (mouse colony chow) was removed to start the overnight fast. On the day of the infection, a 3 mm piece of bread was inoculated with 1×10^8 logarithmically growing bacteria in 1X PBS and covered with 3 µL of butter. Each 8-week-old female CD-1 mouse (Charles River Laboratories, Wilmington, MA, USA) was then fed a single piece of infected bread. The streptomycin sulfate water was replaced with standard drinking water and the chow was restored. Fecal samples were collected every day post-infection for 5 days, weighted, vortexed at 4 °C for 10 min, and plated to determine the number of CFU per gram of stool.

Phagosomal escape assay

BMMs were seeded in 24-well plates containing 12 mm glass coverslips (Thermo Fischer Scientific, Waltham, MA, USA) and cultured overnight. BMMs were treated with 250 ng/mL of cytochalasin D (Sigma-Aldrich, St. Louis, MO, USA) 30 min prior to infection (MOI of 15) with *L. monocytogenes* strains grown at 30 °C overnight in a slanted position. At 1 h 15 min post-infection, the BMMs were washed twice with 1X PBS and fixed with 4% paraformaldehyde (Electron Microscopy Sciences, Hatfield, PA, USA) for 15 min. The immunofluorescence staining, microscopy, and image analysis then proceeded as previously described (135). The primary antibodies used were rabbit anti-*Listeria* (BD Difco, Franklin Lakes, NJ, USA; cat. no. 223021) at a 1:1000 dilution, and guinea pig anti-p62 (Fitzgerald, Acton, MA, USA; cat. no. 20R-PP001) at a 1:200 dilution. The secondary antibodies used were Rhodamine Red-X goat anti-rabbit IgG (Invitrogen- Thermo Fisher Scientific, Waltham, MA, USA; cat. no. R6394) at 1:2000 dilution and AlexaFluor-647 goat anti-guinea pig IgG (Invitrogen-Thermo Fisher Scientific, Waltham, MA, USA; cat. no. A21450) at a 1:2000 dilution. At least 100 bacteria per condition were quantified for analysis.

Animal use ethics statement

The mice were maintained by the University of California, Berkeley Office of Laboratory Animal Care personnel according to institutional guidelines. Animal studies were performed in accordance with the guidance and recommendations of the University of California, Berkeley Office of Laboratory Animal Care and the Guide for the Care and Use of Laboratory Animals of the National Institutes of Health. The protocols used in this study were reviewed and approved by the Animal Care and Use Committee at the University of California, Berkeley (AUP-2016-05-8811).

Statistical Analysis

All statistical analyses were performed using GraphPad Prism version 9.2 for MacOS, GraphPad Software, San Diego, CA, USA.

2.6 Supplementary Materials

Table S1. Bacterial strains used in this study

<i>Strains</i>	<i>Strain number</i>	<i>Reference</i>
<i>Listeria monocytogenes</i>		
Wild type	10403S	(136)
$\Delta ribU$	DP-L7376	This study
$\Delta ribU$ + pPL2-pNative <i>ribU</i>	DP-L7377	This study
$\Delta ribU$ + pPL2-pNative <i>ribDEAHT</i>	DP-L7378	This study
Δhly	DP-L2161	(137)
Wild type + pPL2-Holin/Lysin	DP-L5961	(112)
Wild type + pPL2- <i>L.p. flaA</i>	DP-L5964	(113)
$\Delta ribC$	DP-L7379	This study
$\Delta ribF$	DP-L7380	This study
$\Delta ribC/\Delta ribF$	DP-L7381	This study
$\Delta ribC/\Delta ribF$ + pPL2-pNative <i>ribC</i>	DP-L7382	This study
<i>Escherichia coli</i>		
SM10 pPL2-pNative <i>ribU</i>	DP-E7383	This study
SM10 pPL2-pNative <i>ribDEAHT</i>	DP-E7384	This study
SM10 pPL2-pNative <i>ribC</i>	DP-E7385	This study
SM10 pKSV7 <i>ribU</i>	DP-E7204	This study
SM10 pKSV7 <i>ribC</i>	DP-E7386	This study
SM10 pKSV7 <i>ribF</i>	DP-E7387	This study

Chapter 3: Distinct energy-coupling factor transporter subunits enable flavin acquisition and extracytosolic trafficking for extracellular electron transfer in *Listeria monocytogenes*

3.1 Summary of Results

A variety of electron transfer mechanisms link bacterial cytosolic electron pools with functionally diverse redox activities in the cell envelope and extracellular space. In *Listeria monocytogenes*, the ApbE-like enzyme FmnB catalyzes extracytosolic protein flavinylation, covalently linking a flavin cofactor to proteins that transfer electrons to extracellular acceptors. *L. monocytogenes* uses an energy-coupling factor (ECF) transporter complex that contains distinct substrate-binding, transmembrane, ATPase A, and ATPase A' subunits (RibU, EcfT, EcfA, and EcfA') to import environmental flavins, but the basis of extracytosolic flavin trafficking for FmnB flavinylation remains poorly defined. In this study, we show that the proteins EetB and FmnA are related to ECF transporter substrate-binding and transmembrane subunits, respectively, and are essential for exporting flavins from the cytosol for flavinylation. Comparisons of the flavin import versus export capabilities of *L. monocytogenes* strains lacking different ECF transporter subunits demonstrates a strict directionality of substrate-binding subunit transport but partial functional redundancy of transmembrane and ATPase subunits. Based on these results, we propose that ECF transporter complexes with different subunit compositions execute directional flavin import/export through a broadly conserved mechanism. Finally, we present genomic context analyses which show that related ECF exporter genes are distributed across the Firmicutes phylum and frequently co-localize with genes encoding flavinylated extracytosolic proteins. These findings clarify the basis of ECF transporter export and extracytosolic flavin cofactor trafficking in Firmicutes.

3.2 Introduction

Flavins are an important family of redox-active cofactors that catalyze electron transfer in diverse enzymes (138). Flavin mononucleotide (FMN) and flavin adenine dinucleotide (FAD) are synthesized from the precursor riboflavin (also known as vitamin B₂). FMN and FAD are the most common type of protein-bound flavins and are nearly ubiquitous throughout the three domains of life. While the role of flavin-binding proteins (flavoproteins) in cytosolic redox activities is well established, the importance of flavins for extracytosolic activities in prokaryotic biology has become increasingly apparent (8, 35, 62).

In prokaryotes, many extracytosolic flavoproteins are post-translationally linked to their flavin cofactors (flavinylated) through the action of the enzyme ApbE (139). ApbE specifically uses FAD as a substrate, catalyzing a reaction that links the FMN portion of the molecule to a serine/threonine residue in substrate proteins via a phosphodiester bond (**Fig. 3.1a**) (140). Approximately 50% of sequenced bacterial genomes encode proteins flavinylated by ApbE, with ApbE substrates having been implicated in a wide array of redox-dependent activities (62). For example, *Rhodobacter* nitrogen fixation (Rnf) and NADH:quinone oxidoreductase (Nqr) are prominent multi-subunit complexes with ApbE-flavinylated subunits that possess important roles in diverse bacteria and energy metabolisms (141, 142).

Extracellular electron transfer (EET) describes a class of microbial activities that result in the transfer of electrons from the cytosol to the outside of the cell and which often function in anaerobic respiration. We previously found that the foodborne pathogen *Listeria monocytogenes* possesses EET activity that enhances anaerobic growth (143, 144). We further identified an eight-gene cluster responsible for EET (**Fig. 3.1b**) (9). Within this cluster, we found that the gene *fmnB* encoded an ApbE-like protein that flavinylated a second protein from the cluster, PplA, at two sites (9, 60, 145). Homologous genes are present in a number of related Firmicutes and have been implicated in similar EET activities in several bacteria (146–150).

Extracytosolic proteins acquire cofactors through distinct mechanisms. Some proteins are loaded with their cofactors in the cytosol and then transported by the TAT secretion system across the cytoplasmic membrane in a folded state (151). Other proteins are transported across the cytoplasmic membrane in an unfolded state by the Sec secretion system and fold into their active form in the extracytosolic space (151). The latter scenario requires an extracytosolic supply of the cofactor, which can be accomplished by transport from the cytosol. For example, the CcsBA transporter transfers heme across the cytoplasmic membrane and is required for loading heme cofactors into cytochromes (152).

The extracytosolic localization of FmnB and other ApbEs necessitates a source of extracytosolic FAD. We previously proposed that *L. monocytogenes* FAD was supplied by an energy coupling-factor (ECF) transporter that contained FmnA and RibU subunits (9). These functional assignments were made because FmnA and RibU exhibit high sequence homology to characterized flavin transporter subunits and because PplA is unflavinylated in $\Delta fmnA$ and $\Delta ribU$ strains but rescued by the application of exogenous FAD (9, 34, 54).

ECF transporters are a widespread class of bacterial transporters that have been implicated in the import of many metabolites (153). ECF transporters are generally comprised of four protein subunits. This includes a pair of ATPases (ECF-A and ECF-A'), a transmembrane domain (ECF-T), and a substrate-binding subunit (ECF-S). While ECF-S subunits that transport different substrates exhibit highly variable sequences, structural studies have revealed a conserved ECF-S fold. ECF transporters within have previously been identified in bacterial genomes on the basis of: (1) gene colocalization (ECF transporter subunits often cluster together in genomes) and (2) the high sequence homology of ECF-T, ECF-A, and ECF-A' subunits (153).

Here we reevaluate the basis of FAD secretion in *L. monocytogenes*. We show that RibU is dispensable for FAD secretion when the concentration of cytosolic flavins is normalized and identify a second protein in the EET gene cluster, EetB, that serves as the ECF-S for FAD export. We identify homologous genes in many bacterial genomes and find that they often colocalize with *apbE*, suggesting a conserved role in flavinylation. These studies reveal complex basis of ECF transporter function in flavin acquisition and trafficking.

Figure 3.1 ECF transporter subunits and *eetB* are essential for provisioning flavins to the extracytosolic AbpE homolog FmnB in *L. monocytogenes*. (A) Reaction catalyzed by AbpE/FmnB flavin transferases. (B) Genomic organization of *L. monocytogenes* genes addressed in this study. (C) Ferric iron reductase activity of *L. monocytogenes* strains grown in chemically defined media. The dotted lines separate flavin auxotroph (wildtype) strains ($n=4$), flavin auxotroph strains supplemented with extracellular FAD ($n=2$), and flavin prototroph (+*ribDEAHT*) strains ($n=3$). For the non-complemented strains, statistical significance was determined using one-way ANOVA and Dunnett's posttest using wildtype as the control. For the FAD and *ribDEAHT* complemented conditions, statistical significance was determined by performing a *t*-test on the parental non-complemented condition. (D) PplA flavinylation levels in flavin prototroph (+*ribDEAHT*) *L. monocytogenes* strains as assessed by MS. The data show the means and SDs of three independent experiments. Statistical significance was determined using one-way ANOVA and Dunnett's posttest using wildtype as the control. **** $P < 0.0001$; ns, not significant, $P > 0.05$.

3.3.2 FmnA and EetB are required for PplA flavinylation in the absence of exogenous FAD

Having ruled out RibU as a subunit of the FAD exporter, we sought to determine alternative genes essential for FAD secretion. We previously identified *fmnA* as encoding a protein on the EET locus with homology to an ECF-T subunit and found that it was essential for EET activity of cells grown in rich media but that this phenotype could be reversed by the application of exogenous FAD (9). We thus asked how the $\Delta fmnA$ strain responded to engineered flavin prototrophy. In contrast to $\Delta ribU$, we found that expressing *ribDEAHT* had no effect on EET activity and PplA flavinylation of the $\Delta fmnA$ strain (**Fig. 3.1c,d**). This result supported our original interpretation of FmnA representing an ECF-T transporter subunit and suggested that its corresponding ECF-S subunit had been previously overlooked.

We next turned to the question of the identity of the ECF-S that acts with FmnA in FAD export. Since the ECF-S subunit of the FAD exporter should be essential for EET activity, we reasoned the ECF-S gene was likely localized to the EET gene cluster. As *eetA* and *eetB* provided the only genes without an assigned function and encode membrane proteins consistent with a transporter function, we reasoned that they presented the strongest candidates. We generated $\Delta eetA$ and $\Delta eetB$ strains and tested their EET activity. In contrast to the previously described *eetA* transposon mutant, EET activity of the $\Delta eetA$ strain did not differ from wildtype, suggesting that the previously observed phenotype may have been due to a polar effect caused by transposon insertion (9). By contrast, the $\Delta eetB$ strain had negligible EET activity and thus continued to present a promising ECF-S candidate (**Fig. 3.1c**).

We next assessed the flavinylation status of PplA in the *ribDEAHT*-expressing $\Delta eetB$ strain. Proteomic analysis of *L. monocytogenes* cells revealed that PplA was unflavinated in this strain (**Fig. 3.1d**). Consistent with the lack of PplA flavinylation and impaired EET activity resulting from compromised FAD trafficking, supplementing $\Delta eetB$ cells with exogenous FAD partially restored EET activity (**Fig. 3.1c**). Importantly, the lack of PplA flavinylation and EET activity of the $\Delta eetB$ strain was maintained in the *ribDEAHT* flavin prototroph background, ruling out

diminished cytosolic flavin concentrations as the source of the $\Delta eetB$ phenotype (Fig. 3.1c). These findings demonstrate a role for EetB in FAD export.

3.3.3 EetB is an FAD-binding protein that resembles characterized ECF-S subunits

As our genetic studies support the conclusion that *eetB* is essential for FAD secretion, we questioned whether EetB was the FAD-exporting ECF-S. Since experimentally characterized ECF-S subunits with distinct substrate specificities possess low sequence homology but similar tertiary structures, we used the structure modeling software AlphaFold to interrogate structural attributes of EetB (155–157). A predicted AlphaFold model of EetB revealed striking structural similarity to experimentally characterized ECF-Ss, including RibU, bolstering the case for the protein possessing an ECF-S functionality (Fig. 3.2a).

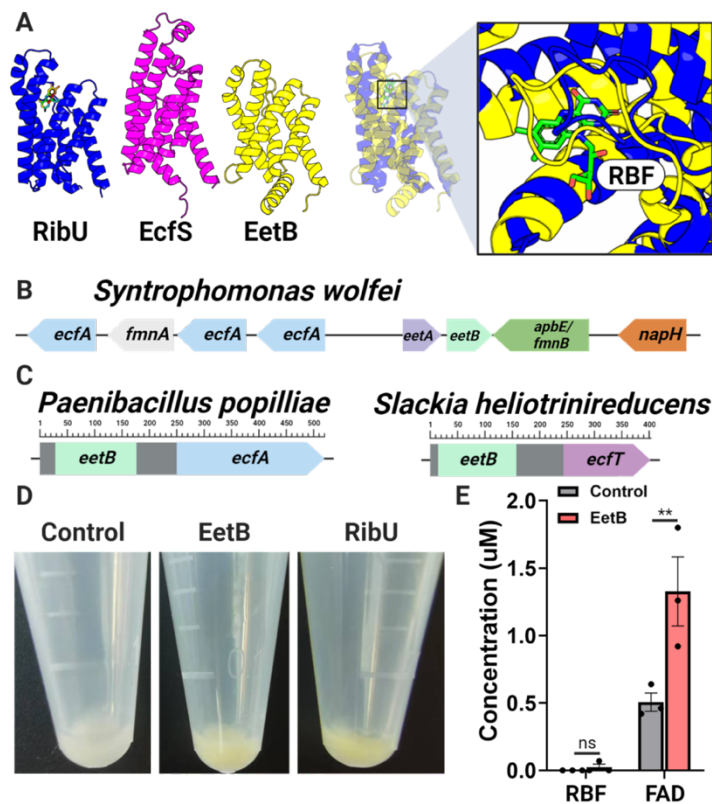


Figure 3.2 EetB resembles ECF substrate-binding proteins and binds FAD. (A) Comparison of AlphaFold model of EetB to crystal structures of ECF riboflavin and pantothenate substrate-binding subunits, RibU (PDB code 5KBW) and EcfS (PDB code 4RFS), respectively. Riboflavin (RBF) is represented as a stick in the RibU structure. (B) A representative bacterial gene cluster in which *eetB* neighbors genes with ECF-T, ECF-A, and ECF-A' domains. (C) Domain architecture of representative bacterial proteins (NCBI accessions WP_006284433.1 and WP_012799238.1) that contain *eetB* and ECF domains. (D) Induced *E. coli* cell pellets containing *ribU*, *eetB*, and plasmid control overexpression vectors. (E) Riboflavin (RBF) and FAD pulled down from *E. coli* cells containing *eetB* and plasmid control overexpression vectors. The means and SEMs of three

independent experiments are shown. Statistical significance was determined by performing a *t*-test comparing plasmid control and *eetB* overexpression vectors. **P < 0.01; ns, not significant, P > 0.05.

Genes encoding subunits of characterized ECF transporters are often co-transcribed from an operon. We thus reasoned that the genomic context of *eetB* genes could provide additional evidence of ECF functionality. Indeed, we identified *eetB* genes in several bacterial genomes that colocalized with genes encoding ECF-T and ECF-A/ECF-A' subunits (**Fig. 3.2b**). Following a similar logic regarding the relationship of functionally related proteins, protein subunits that form a multi-protein complex in one organism are often contained on a single polypeptide chain within other organisms (158). The observation of multiple genes from different bacterial genomes that encode proteins with EetB and ECF-T domains (*e.g.*, NCBI accessions WP_021725833.1, MBE6480012.1, and MBQ3267887.1) or EetB and Ecf-A domains (*e.g.*, NCBI accessions WP_006284433.1, WP_111154897.1, and WP_143797423.1) thus provides additional support for the attributed role of EetB as an ECF-S (**Fig. 3.2c**).

To address whether EetB might be a flavin-transporting ECF-S similar to RibU, we expressed RibU and EetB in *E. coli*. We observed that both proteins localized to the insoluble fraction of the resulting cell lysates and presented a yellowish hue, consistent with an association with flavins (which are naturally colored yellow) (**Fig. 3.2d**). To address the hypothesized flavin-binding activity of EetB, we measured flavin levels in the insoluble fraction of EetB-overexpressing *E. coli* cells and found that EetB pulled down FAD (**Fig. 3.2e**). Collectively, these analyses demonstrate that EetB is an FAD-binding protein that possesses an ECF-S-like structure consistent with a transport function.

3.3.4 ECF ATPases are required for PplA flavinylation in the absence of exogenous FAD

Previous ECF transporter characterization has focused on small molecule import. As the putative EetB-FmnA complex is the first transporter identified with apparent export activity, we sought to clarify its mechanism of action. ECF importers typically require two ATPase subunits (ECF-A and ECF-A') for transporter function. As some bacteria use the same ATPase subunits to engage multiple ECF transport systems, we reasoned that the ATPases that function in the RibU ECF transporter flavin import system might also participate in FAD secretion (159, 160). To test this hypothesis, we generated an $\Delta ecfA/ecfA'$ strain that lacked both of the previously characterized RibU ATPases (151). Consistent with EcfA/EcfA' being essential for FAD export, the $\Delta ecfA/ecfA'$ strain was deficient for EET activity, PplA flavinylation, and resembled $\Delta fmnA$ and $\Delta eetB$ strains in its response to RibDEAHT expression and exogenous FAD application (**Fig. 3.1c**). These findings thus provide evidence that the EcfA/EcfA' provide dual functions in flavin import and export.

3.3.5 Structural models illuminate ECF transporters with distinct subunit compositions

Previous studies suggest that RibU, EcfT, EcfA, and EcfA' form an ECF transporter responsible for riboflavin, FMN, and FAD uptake in *L. monocytogenes* (51, 54, 154). By contrast, the phenotypes for *L. monocytogenes* $\Delta eetB$, $\Delta fmnA$, $\Delta ecfA/ecfA'$ strains identified in our studies suggest that FAD export occurs through an ECF transporter with EetB, FmnA, EcfA, and EcfA' subunits (Fig. 3.1c). To further address the feasibility of the distinct implied modes of flavin transport, we used the AlphaFold-multimer software to model putative RibU/EcfT/EcfA/EcfA' and EetB/FmnA/EcfA/EcfA' complex structures. Both resulting transporter structures exhibit striking similarity to a previously determined crystal structure of the folate ECF transporter (Fig. 3.3a). These structural models are thus broadly consistent with the idea that ECF transporters with distinct subunit compositions could be responsible for the observed phenotypes.

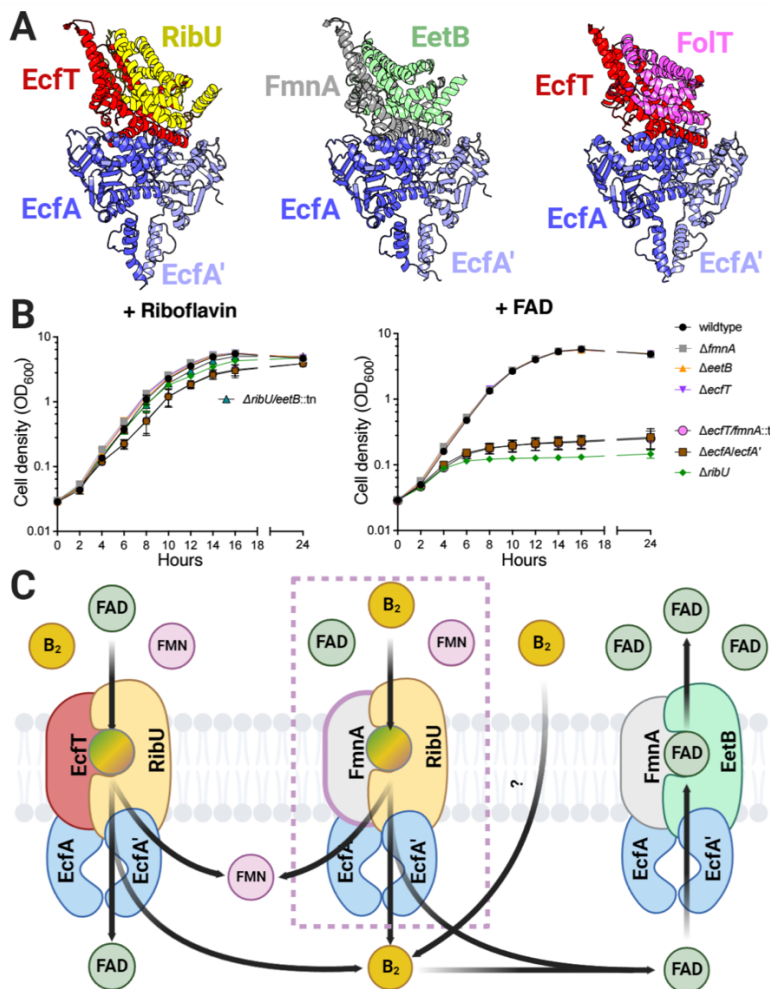


Figure 3.3 ECF transporter subunits are partially functionally redundant for flavin import and export in *L. monocytogenes*. (A) Comparison of AlphaFold-multimer RibU-EcfT-EcfA-EcfA' and EetB-FmnA-EcfA-EcfA' complex models to a crystal structure of the Folt-EcfT-EcfA-EcfA' folate ECF transporter (PDB code 4HUQ). (B) Growth curves of indicated *L. monocytogenes* strains

grown in chemically defined media supplemented with riboflavin as the sole flavin source. Means and SDs from three independent experiments are shown. (C) Growth curves of indicated *L. monocytogenes* strains grown in chemically defined media supplemented with FAD as the sole flavin source. Means and SDs from three independent experiments are shown. (D) Model of ECF complexes that function in *L. monocytogenes* flavin import and export supported observed phenotypes.

3.3.6 EcfT and FmnA ECF-T subunits are functionally redundant in flavin import

We next sought to address how the direction of transport (import vs. export) could be achieved through related ECF transporters. *L. monocytogenes* is a flavin auxotroph and we previously found that *ribU* was essential for growth in conditions where FMN or FAD are the sole available flavin (154). In contrast to these flavin nucleotides, the $\Delta ribU$ strain lacked a phenotype in the presence of riboflavin (154). While it thus seemed plausible that EetB could contribute to riboflavin uptake, we found that a $\Delta ribU/eetB::tn$ strain grew similarly to wildtype *L. monocytogenes* in chemically defined media that contained riboflavin as the sole flavin (**Fig. 3.3b**). These results suggest that EetB does not substitute for the RibU ECF-S in flavin uptake, and that riboflavin can be imported through a presently unknown alternative mechanism.

We next asked about the functional redundancy of ECF-T subunits. While the observation that FmnA is essential for PplA flavinylation suggests that EcfT cannot substitute in FAD export, we wondered if the converse was true (i.e., whether FmnA could facilitate flavin import in the absence of EcfT). Since RibU was essential for growth when FAD was the sole flavin present, we tested ECF-T mutants in this condition (154). Growth of the $\Delta ecfT$ and $\Delta fmnA$ strains resembled wildtype *L. monocytogenes* in conditions with riboflavin or FAD (**Fig. 3.3b**). By contrast, the $\Delta ecfT/fmnA::tn$ strain failed to grow in the presence of FAD, similar to the $\Delta ribU$ and $\Delta ecfA/ecfA'$ strains (**Fig. 3.3b**). These results suggest that either EcfT or FmnA provides a functionally viable ECF-T for RibU-mediated flavin import and underscore the flexible ECF-T subunit usage for flavin import (**Fig. 3.3c**).

3.3.7 Gene colocalization suggests a conserved role for EetB in ApbE-associated flavin trafficking

Having established EetB-FmnA function in FAD export, we next sought to address whether this transporter might be important for FAD trafficking in other microbes. We reasoned that the unique substrate-binding subunit provided the clearest marker of likely FAD export activity and thus searched for *eetB* homologs (Pfam accession PF07456) within a collection of 31,910 genomes representative of the genetic diversity of the prokaryotes (161, 162). We identified 4,214 bacterial genomes that encode an *eetB* homolog. Taxonomic analyses revealed that *eetB* homologs are most abundant in Firmicutes, but also present in a subset of genomes from other phyla (**Fig. 3.4a**).

To clarify the role of EetB in diverse microbes, we next applied a guilt-by-association-based analysis. Our approach took advantage of the frequent colocalization of genes with related

functions on prokaryotic genomes and was previously employed to differentiate distinct subtypes of ApbE flavinylation based on colocalization with *apbE*. Inspecting the genes that colocalized with *eetB* subunit genes led to several insights, which are elaborated below.

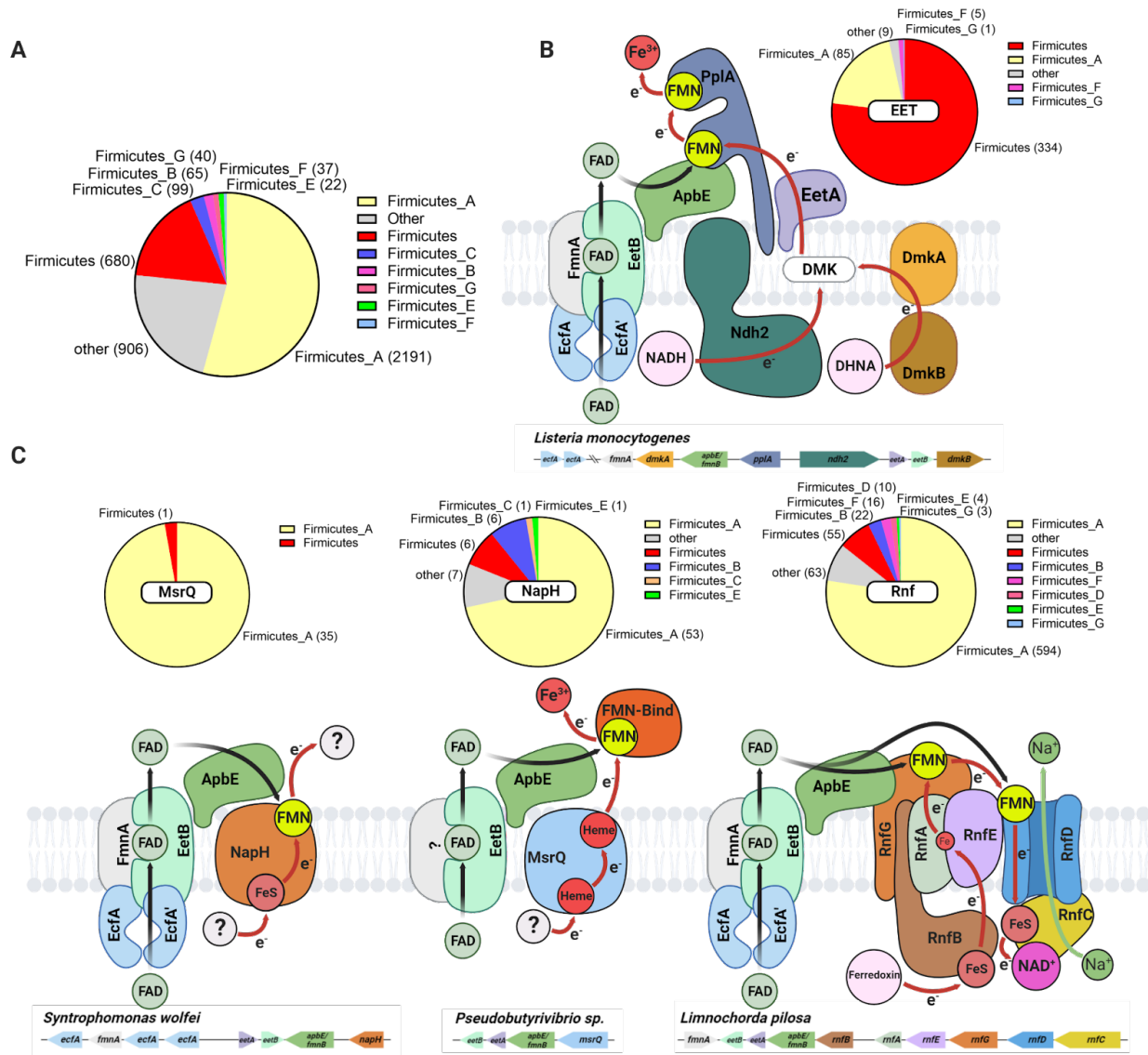


Figure 3.4 *eetB* genes frequently colocalize with ApbE-associated extracytosolic flavinylation system genes in bacterial genomes. (A) Pie chart showing the number of GTDB reference genomes/phylum that encode an *eetB* homolog. (B) Proposed basis of flavin export for *L. monocytogenes* flavinylation and EET activity. Pie chart shows the number of GTDB reference genomes that contain a gene cluster with both EET and *eetB* genes. (C) Proposed models of flavin export in previously identified flavinylation-associated MsrQ-like, NapH, and Rnf electron transfer systems (62). Pie charts show the number of GTDB reference genomes that contain a system gene cluster with an *eetB* homolog.

Supporting the proposed relationship of EetB with other ECF transporter subunits, we found that *eetB* colocalized with ECF-T subunit genes in 291 genomes and ECF-A/ECF-A' subunits in 796 genomes, often with ECF subunit genes arranged in an apparent operon. Additionally, *eetB* colocalized with *eetA* in 3,328 genomes. While the *L. monocytogenes* Δ *eetA* strain lacked an EET phenotype, this conserved synteny suggests a functional link between EetA and EetB. Further supporting this functional association, we identified genes encoding a single polypeptide chain with both EetA and EetB domains in 14 genomes.

We also found that *eetB* colocalizes with *apbE* on 2,169 genomes. ApbEs have been shown to function in multiple extracytosolic redox activities and we recently proposed operational definitions that enable the identification of gene clusters encoding 10 types of ApbE flavinylated systems with different mechanisms of membrane electron transfer or substrate specificity (8). We applied these definitions to determine which types of ApbE flavinylated systems colocalize with *eetB* and found that *eetB* most commonly colocalizes with Rnf and EET systems, but also some MsrQ-like and NapH-like systems (**Fig. 3.4b,c**). The association with Rnf was particularly pronounced in the class Clostridia, with *eetB* colocalized with Rnf genes in 572 genomes. These results thus suggest that ECF exporters traffic FAD to a functionally diverse subset of bacterial ApbE subunits.

3.4 Discussion

The studies presented here establish the basis of FAD trafficking in *L. monocytogenes* and, notably, provide the most extensive evidence of the role of ECF-like transporters in small molecule export. Strikingly, our comparison of strains deficient in various ECF components supports the existence of distinct import and export transporters that share subunits (ECF-AA') and exhibit partial functional redundancies (import ECF-Ts). These findings thus suggest a complex basis of bidirectional flavin transport across the *L. monocytogenes* cytoplasmic membrane (**Fig. 3.3d**).

While little is known about the mechanism of ECF export, previous research has generated considerable evidence about the basis of ECF import. These studies reveal that ECF-S remains monomeric in the absence of substrate, likely adopting an 'outward' facing orientation that enables substrate binding from the extracytosolic space (54, 163, 164). Once substrate is bound, ECF-S undergoes a 'toppling' conformational change to an 'inward' orientation where it engages the ECF-T, ECF-A, ECF-A' complex in a manner that facilitates substrate release into the cytosol. ATP hydrolysis in the ECF complex then causes release of apo ECF-S, which reverts to its monomeric 'outward' orientation (**Fig. 3.5a**) (54, 164). Considering the similarity of subunits, the proposed mechanism of ECF import has implications for how EetB might function in FAD export. Simply reversing the relationship between ECF-S with the rest of the ECF transporter complex could reverse the direction of transport (**Fig. 3.5b**). While additional studies will be necessary to definitively address transport mechanisms, ECF export may differ from ECF import in inverting the ECF complex's unliganded versus substrate-bound ECF-S affinity and the kinetics of ATP hydrolysis/ECF-S release.

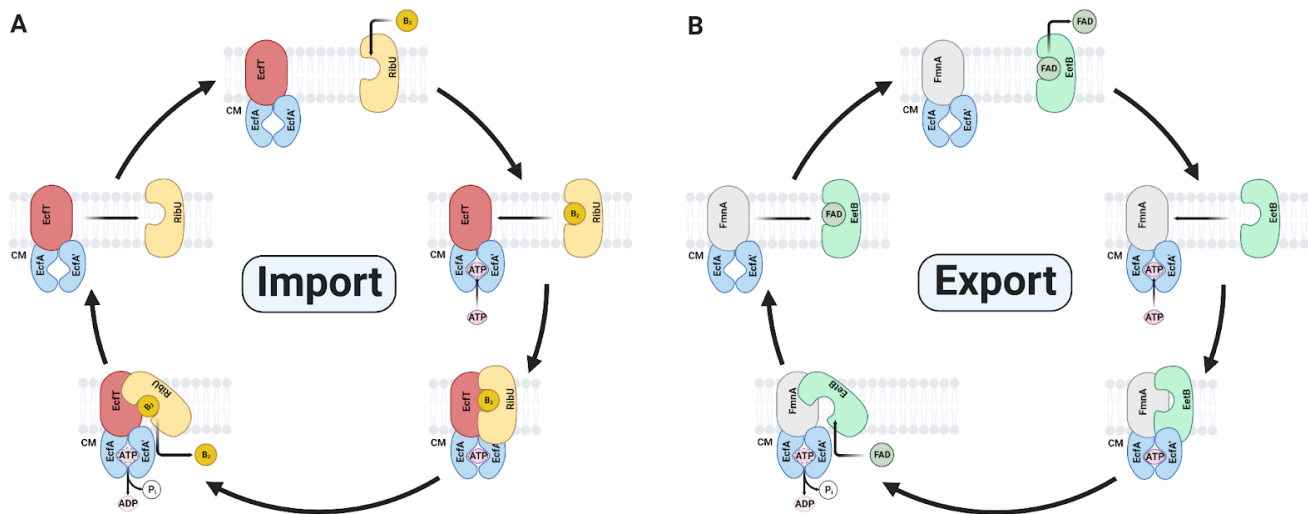


Figure 3.5 Proposed basis of bidirectional ECF transport. (A) Summary of previously proposed models of ECF import. (B) Speculative model of ECF export illustrating how directionality of transport could be achieved through a broadly conserved mechanism.

An interesting aspect of *eetB* and other flavin exporter genes identified in our bioinformatic analyses regards their frequent colocalization with an *apbE* gene. This distinguishes the ECF transporter from a previously identified flavin exporter that similarly traffics flavins in some Gram-negative bacteria (8, 35). The *eetB-apbE* association suggests that EetB may be adapted for efficient flavin delivery to ApbE. Indeed, a regulatory mechanism that enabled targeted delivery to ApbE might explain why, despite several efforts, we were unable to detect differences in the level of extracellular flavins within *eetB*-deficient strains. Flavin delivery to ApbE may thus provide an attractive model for future investigations into the mechanism of targeted extracytosolic cofactor delivery in bacteria.

3.5 Materials and Methods

Bacterial strains and culture

All strains of *L. monocytogenes* used in this study (**Table S1**) were derived from the wildtype 10403S strain and cultured in a previously described chemically defined synthetic media containing 200 $\mu\text{g}/\text{mL}$ of streptomycin (48, 136). Deletion of genes was done using allelic exchange with the temperature-sensitive plasmid pKSV7, as previously described (131). Generation of the strains expressing the *ribDEAHT* operon from the constitutive promoter pHyper (pHyper *ribDEAHT* construct) was done by amplifying the *ribDEAHT* operon from *B. subtilis* and cloning it into the site-specific pPL2 integrating vector. The plasmids were then introduced into *L. monocytogenes* by conjugation, as previously described (132). Broth growth curves were performed with *L. monocytogenes* strains from overnight cultures grown in chemically defined synthetic media at 37 °C with shaking (200 rpm). Growth was measured by

optical density at a wavelength of 600 nm (OD_{600}) and the growth curves were started at an OD_{600} of 0.03.

Ferric iron reductase activity assays

Strains were grown to mid-log phase ($OD_{600} = \sim 0.4-0.6$) in chemically defined synthetic media, or chemically defined synthetic media supplemented with 0.5 mM FAD, washed twice, then normalized to an OD_{600} of 0.5. One mL of the washed bacteria was then resuspended in 4 mM Ferrozine in chemically defined synthetic media. To conduct the assay, 100 μ L of resuspended bacteria were mixed with 100 μ L of 100 mM ferric ammonium citrate, in chemically defined synthetic media, and transferred into a 96-well plate format in triplicate. Measurements were done using a plate reader with the temperature set at 37 °C and absorbance was read at 560 nm every 30 seconds for 1.5 hours. Maximal rates (typically over 2 min) were calculated and reported as the percent ferric iron reductase activity of wildtype.

Recombinant *ribU* and *eetB* expression and FAD pulldown

L. monocytogenes 10403S *eetB* and *ribU* genes were cloned into the pMCSG53 vector. Resulting constructs were transformed into *E. coli* BL21 cells. Overnight cultures of *E. coli* BL21 containing pMCSG53::*empty*, pMCSG53::*eetB*, and pMCSG53::*ribU* were diluted in 5 mL of Luria-Bertani broth (LB) with a final OD_{600} of 0.05. When cell growth reached log phase, FAD was added to a final concentration of 1 μ M and protein expression was induced with isopropyl β -D-1-thiogalactopyranoside (IPTG) at a final concentration of 1 mM. Induced cultures were grown overnight at 30°C. Cultures were normalized to an OD_{600} of 1.0 and then 1 mL of cells was collected by centrifugation at 22,100 x g for 1 min. Cell pellets were washed twice with 1 mL of diH₂O and resuspended in 190 μ L of diH₂O to remove free FAD. To facilitate the release of protein-bound FAD, cell suspensions were incubated at 100°C for 20 minutes and centrifuged at 22,100 x g for 1 minute. Supernatants were collected for the analysis of flavin content.

Liquid chromatography-mass spectrometry for the detection of flavins

Samples were incubated at -80 °C for at least one hour or up to overnight. Extraction solvent (4 volumes of 100% methanol spiked with internal standards and stored at -80 °C) was added to the liquid sample (1 volume) in a microcentrifuge tube. Tubes were then centrifuged at -10 °C, 20,000 x g for 15 min, and supernatant was used for subsequent metabolomic analysis. Samples were dried down completely using a Genevac EZ-2 Elite. Samples were resuspended in 50 μ L of 50:50 water:methanol and added to an Eppendorf thermomixer® at 4 °C, 1000 rpm for 15 min to resuspend analytes. Samples were then centrifuged at 4 °C, 20,000 x g for 15 min to remove insoluble debris, and 40 μ L of supernatant was transferred to a 96 deep-well plate (Agilent 5065-4402). Samples were analyzed on an Agilent 1290 infinity II liquid chromatography system coupled to an Agilent 6470 triple quadrupole mass spectrometer, operating in positive mode, equipped with an Agilent Jet Stream Electrospray Ionization source (LC-ESI-QQQ). Each sample (2 μ L) was injected into an Acquity UPLC HSS PFP column, 1.8 μ m, 2.1 x 100 mm (Waters; 186005967), equipped with an Acquity UPLC HSS PFP VanGuard Pre- column, 100Å, 1.8 μ m, 2.1

mm X 5 mm (Waters; 186005974), at 45 °C. Mobile phase A was 0.35% formic acid in water and mobile phase B was 0.35% formic acid in 95:5 acetonitrile:water. The flow rate was set to 0.5 mL/min starting at 0% B held constant for 3 min, then linearly increased to 50% over 5 min, then linearly increased to 95% B over 1 min, and held at 100% B for the next 3 min. Mobile phase B was then brought back down to 0% over 0.5 min and held at 0% for re-equilibration for 2.5 min. The QQQ electrospray conditions were set with capillary voltage at 4 kV, nozzle voltage at 500 V, and Dynamic MRM was used with a cycle time of 500 ms. Transitions were monitored in positive mode for two analytes, riboflavin and flavin adenine dinucleotide (FAD). The transitions for riboflavin and FAD were 377.1 m/z to 243 m/z and 786.1 m/z to 348 m/z, respectively. Authentic standards were purchased for riboflavin (Supelco; riboflavin B2) and FAD (Sigma-Aldrich; flavin adenine dinucleotide disodium salt hydrate) to make 1 mg/mL-stock solutions in methanol. These solutions were used to prepare a 10-point calibration curve, ranging from 3.1 nM to 0.2 mM for riboflavin and 3.9 nM to 1 mM for FAD. Data analysis was performed using MassHunter Quant software (version B.10, Agilent Technologies) and confirmed by comparison with standards. Normalized peak areas were calculated by dividing raw peak areas of the targeted analytes by averaged raw peak areas of two internal standards (melatonin and kynurenic acid).

Transporter structural models

The AlphaFold model of EetB (accession AF-Q927J9-F1) was downloaded from the Uniprot database (165). RibU-EcfT-EcfA-EcfA' and EetB-FmnA-EcfA-EcfA' complex models were generated with AlphaFold-multimer software using default settings in the ColabFold platform (166, 167).

Liquid chromatography-mass spectrometry analysis of trypsin-digested proteins

Samples of trypsin-digested proteins were analyzed using a Synapt G2-Si ion mobility mass spectrometer that was equipped with a nanoelectrospray ionization source (Waters, Milford, MA). The mass spectrometer was connected in line with an Acquity M-class ultra-performance liquid chromatography system that was equipped with trapping (Symmetry C18, inner diameter: 180 µm, length: 20 mm, particle size: 5 µm) and analytical (HSS T3, inner diameter: 75 µm, length: 250 mm, particle size: 1.8 µm) columns (Waters). Data-independent, ion mobility-enabled, high-definition mass spectra and tandem mass spectra were acquired in the positive ion mode (168–171). Data acquisition was controlled using MassLynx software (version 4.1) and tryptic peptide identification and relative quantification using a label-free approach were performed using Progenesis QI for Proteomics software (version 4.0, Waters) (172–174). Data were searched against the *Listeria monocytogenes* serotype 1/2a (strain 10403S) protein database to identify tryptic peptides, with carbamidomethylcysteine as a fixed post-translational modification and methionine sulfoxide and threonine flavinylation as variable post-translational modifications (175). Calculation of the percentage of flavinylation for each bacterial strain was performed by dividing the abundance of a residue/peptide bearing a flavinylation modification by the total abundance and multiplying by 100.

Genome collection for analysis of *eetB* gene clusters

The 30,238 bacterial and 1672 archaeal genomes from the GTDB (release 05-RS95 of July 17, 2020) were downloaded with the taxonomy and predicted protein sequences (161, 162).

Functional annotation of *eetB* gene clusters

Protein sequences were functionally annotated based on the accession of their best Hmmssearch match, version 3.3 (E-value cut-off 0.001) (176) against the KOfam database (downloaded on February 18, 2020) (177). Domains were predicted using the same Hmmssearch procedure against the Pfam database, version 33.0 (178). SIGNALP, version 5.0, was run to predict the putative cellular localization of the proteins using the parameters -org arch in archaeal genomes and -org gram+ in bacterial genomes (179). Prediction of transmembrane helices in proteins was performed using TMHMM, version 2.0 (default parameters) (180).

Detection of *eetB* gene clusters and association with flavinylated systems

The five genes downstream and upstream of an *eetB* (Pfam accession PF07456) encoding genes were first collected. The *eetB* gene clusters were then assigned to flavinylated systems based on the presence of previously reported key genes (62).

3.6 Supplemental Figures

Table S1. Bacterial strains used in this study

<i>Strains</i>	<i>Strain number</i>	<i>Reference</i>
<i>Listeria monocytogenes</i>		
Wildtype	10403S	(136)
$\Delta ribU$	DP-L7376	(154)
$\Delta eetA$	DP-L7197	This study
$\Delta eetB$	DP-L7198	This study
$\Delta fmnA$	DP-L7194	This study
$\Delta fmnB$	DP-L7195	(144)
$\Delta ecfA/ ecfA'$	DP-L7486	This study
$\Delta ecfT$	DP-L7487	This study
$\Delta ecfT/ fmnA::tn$	DP-L7488	This study
$\Delta ribU/ eetB::tn$	DP-L7489	This study
Wild type + pPL2-pHyper <i>ribDEAHT</i>	DP-L7490	This study
$\Delta ribU$ + pPL2-pHyper <i>ribDEAHT</i>	DP-L7491	This study
$\Delta eetA$ + pPL2-pHyper <i>ribDEAHT</i>	DP-L7492	This study
$\Delta eetB$ + pPL2-pHyper <i>ribDEAHT</i>	DP-L7493	This study
$\Delta fmnA$ + pPL2-pHyper <i>ribDEAHT</i>	DP-L7494	This study
$\Delta fmnB$ + pPL2-pHyper <i>ribDEAHT</i>	DP-L7495	This study
$\Delta ecfA/ ecfA'$ + pPL2-pHyper <i>ribDEAHT</i>	DP-L7496	This study
$\Delta ecfT$ + pPL2-pHyper <i>ribDEAHT</i>	DP-L7497	This study
<i>Escherichia coli</i>		
SM10 + pPL2-pHyper <i>ribDEAHT</i>	DP-E7498	This study
SM10 + pKSV7-oriT <i>eetA</i>	DP-E7499	This study
SM10 + pKSV7-oriT <i>eetB</i>	DP-E7500	This study
SM10 + pKSV7-oriT <i>fmnA</i>	DP-E7501	This study
SM10 + pKSV7-oriT <i>ecfA/ecfA'</i>	DP-E7502	This study
SM10 + pKSV7-oriT <i>ecfT</i>	DP-E7503	This study
Rosetta + pMCSG53 <i>ribU</i>	SL-457	This study
Rosetta + pMCSG53 <i>eetB</i>	SL-458	This study

Chapter 4: MAIT cell avoidance is a determinant of *Listeria monocytogenes* pathogenesis

4.1 Summary of Results

Listeria monocytogenes is a facultative, intracellular pathogen that causes the foodborne illness listeriosis, which affects immunocompromised individuals such as pregnant women, neonates, and the elderly. Unlike most bacteria, *L. monocytogenes* lacks the riboflavin biosynthetic genes and acquires its flavins using the flavin transporter RibU. Flavins are essential cofactors used in many redox reactions and are indispensable for bacterial growth and *L. monocytogenes* pathogenesis. Thus, it is intriguing that *L. monocytogenes* cannot synthesize riboflavin *de novo*. We speculated that lacking the riboflavin biosynthetic pathway allows *L. monocytogenes* to avoid recognition by mucosal-associated invariant T (MAIT) cells. MAIT cells are innate-like T cells that can account for up to 10% and 40% of T cells in human peripheral blood and livers, respectively. The MAIT cell T cell receptor recognizes microbially derived vitamin B precursors, including the riboflavin intermediate 5-OP-RU, bound to the non-classical MHC-related protein 1 (MR1) presented on the surface of infected cells. Upon recognition of MR1:5-OP-RU complexes, MAIT cells produce inflammatory cytokines and can kill infected cells using the cytolytic mediators granzyme and perforin. *L. monocytogenes* are riboflavin auxotrophs and thus do not stimulate MAIT cells. To assess the hypothesis that *L. monocytogenes* avoid MAIT cell responses by lacking the ability to synthesize riboflavin, we engineered *L. monocytogenes* to express the riboflavin biosynthetic genes from *Bacillus subtilis*. Riboflavin-producing *L. monocytogenes* were 100-fold attenuated in the spleens and livers of infected mice, which was not observed in mice lacking MAIT cells. Additionally, MAIT cells accumulated four days post-infection in the spleens and livers of mice infected with riboflavin-producing *L. monocytogenes* strains. To test if MAIT cells restrict riboflavin-producing *L. monocytogenes* by directly killing infected cells, we infected mice lacking perforin. Indeed, no virulence defect was observed in perforin KO mice suggesting that direct killing of infected cells is the primary mechanism employed by MAIT cells to restrict growth of riboflavin-producing *L. monocytogenes*. These results suggest that *L. monocytogenes* avoid MAIT cell responses by importing cytosolic flavins instead of synthesizing riboflavin *de novo*.

4.2 Introduction

Mucosal-associated invariant T (MAIT) cells are highly abundant innate-like T cells that recognize microbial-derived riboflavin precursors presented by host cells infected with riboflavin-producing microorganisms (37, 76, 96). MAIT cells were initially discovered in the 1990s and described as unconventional T cells with memory/effector-like phenotype present in mucosal tissues that express an invariant T cell receptor- α (TCR- α) chain highly conserved in mammals, including humans (67). These innate-like lymphocytes are activated upon antigen presentation by the major histocompatibility complex (MHC) class I-related protein 1 (MR1). MR1 is a non-classical MHC class I molecule that also has an unusually high degree of sequence conservation in mammals- 90% between mice and humans- and is required for the thymic development of MAIT cells (75, 181–183). In humans, MAIT cells account for up to 10% and 40% of all T cells in the blood and liver, respectively. In contrast, in laboratory mice, MAIT cells are rare and account for only 0.6% of all T cells in the liver (63). Although it was assumed that MAIT

cells must play important biological roles due to their high frequency and conservation, for more than a decade, attempts at elucidating their immunological function and antigen specificity were largely unsuccessful (69, 184). The lack of mouse models harboring higher frequencies of MAIT cells and tools to specifically identify them made it difficult for the field to progress (184, 185). In 2012, the discovery that, unlike conventional MHC molecules that display short peptides to T cells, MR1 covalently binds and presents microbially derived vitamin B metabolites to MAIT cells, propelled the development of tools and interest in MAIT cells (37).

One of the best characterized and most potent MAIT cell activators is 5-OP-RU (5-(2-oxopropylideneamino)-6-D-ribitylaminouracil) (76, 79, 186). This antigen arises from the non-enzymatic condensation of 5-A-RU (5-amino-6-D-ribitylaminouracil), an intermediate of the riboflavin biosynthesis pathway, and methylglyoxal, a highly reactive compound generated as a byproduct of metabolism (78, 79). MR1 is present in all nucleated cells and resides in the endoplasmic reticulum (ER) in an unfolded state (80, 81). During infection with riboflavin-synthesizing microorganisms, 5-OP-RU localizes to the ER and covalently binds MR1 by forming a Schiff base (79). This reaction causes a conformational change that triggers MR1 to properly fold with its ligand and exit the ER to be presented at the cell surface (187). Due to their effector/memory-like phenotype, upon recognition of the MR1:5-OP-RU complex and costimulatory signals, MAIT cells rapidly activate, expand, and display effector functions (64). Activated MAIT cells are capable of recognition and direct killing of infected host cells, by delivery of cytolytic effectors like granzymes and perforin, as well as activation of other immune cells by secreting proinflammatory cytokines interferon- γ (IFN- γ), tumor necrosis factor- α (TNF- α) and IL-17 (85, 88, 188, 189). TCR-independent activation of MAIT cells can also occur in viral and bacterial infections and is mediated by proinflammatory cytokines IL-7, IL-12, IL-15, IL-18, and type-I IFNs (86, 190). In this context, cytokine secretion by MAIT cells contributes to the inflammatory state used to restrict pathogens (86, 191). Not surprisingly, MAIT cells display potent antimicrobial responses, especially to some riboflavin-producing intracellular pathogens (87, 88, 192). Pulmonary infection of mice lacking B cells and conventional $\alpha\beta$ T cells with *Legionella longbeacheae* and *Francisella tularensis* demonstrated that MAIT cells were sufficient to protect from lethal doses of these intracellular pathogens (96, 97). However, the roles played by MAIT cells in response to *Mycobacterium tuberculosis* (*Mtb*), a leading cause of death worldwide, are far from being elucidated. For example, even though MAIT cells get activated and respond to *Mtb*, a slow-growing riboflavin prototrophic bacterium, they do not contribute to the restriction of *Mtb* growth in the initial phases of the infection (98).

We recently discovered that the facultative intracellular pathogen *Listeria monocytogenes* imports the riboflavin-derived cofactors flavin mononucleotide (FMN) and flavin adenine dinucleotide (FAD) directly from the host cell cytosol using the riboflavin transporter, RibU (154). *L. monocytogenes* is a riboflavin auxotrophic bacterium that is found ubiquitously in the environment but can become an intracellular pathogen of mammals including humans if ingested with *Listeria*-contaminated food (39). This pathogen primarily affects immunocompromised individuals like the elderly and pregnant women and has a high mortality rate (20-30% of cases) (193). The intracellular life cycle of *L. monocytogenes* begins when it is internalized via receptor-mediated internalization or phagocytosed by professional phagocytes

in the intestine. Upon internalization, *L. monocytogenes* escapes from phagosomes into the cytosol and activates its virulence program, including the actin nucleating-inducing protein ActA (194). This major virulence factor allows *L. monocytogenes* to move around the cell using actin polymerization and spread from cell to cell (195). Interestingly, *L. monocytogenes* can synthesize most of its metabolites (50), but, unlike most bacteria, it lacks the capacity for *de novo* riboflavin synthesis (29, 196). The riboflavin-derived FMN and FAD cofactors are essential for all organisms and are employed in a myriad of redox-dependent reactions (1, 4). Surprisingly, even though *L. monocytogenes* do not synthesize riboflavin, they have a flavin-centric lifestyle. During infection, import of FMN and FAD from the cytosol of host cells is essential for intracellular growth and pathogenesis (154). Furthermore, export of flavins is indispensable for extracellular electron transfer, a flavin-dependent process that provides *L. monocytogenes* a growth advantage in the gastrointestinal lumen of mice (9, 197). Additionally, this electron transfer mechanism is partially responsible for maintaining redox homeostasis intracellularly and preventing cytosolic bacteriolysis (144). Hence, if flavins are essential for *L. monocytogenes* physiology, metabolism, and pathogenesis, why does it lack the capacity to synthesize riboflavin *de novo*? We speculated that lacking the riboflavin biosynthetic pathway allows *L. monocytogenes* to avoid detection by MAIT cells. Thus, to test this hypothesis, we engineered *L. monocytogenes* to produce riboflavin and evaluated the role of MAIT cells during infection. We found that MAIT cells proliferated to high numbers in infected tissues and restricted the growth of riboflavin-producing *L. monocytogenes* in a murine model of infection. These results suggest that *L. monocytogenes* avoid MAT cell responses by importing flavins from the host instead of synthesizing riboflavin *de novo*.

4.3 Results

4.3.1 *L. monocytogenes* expressing *ribDEAHT* produce riboflavin and have no detectable virulence defects in host cells

We previously found that *L. monocytogenes* rely significantly on flavins for their physiology, metabolism, and pathogenesis and that import of flavins is the only mechanism used to satisfy their flavin requirements (9, 144, 154, 197). Indeed, a *L. monocytogenes* strain lacking the flavin importer RibU is avirulent in mice (154). Since intracellular riboflavin-producing bacteria are restricted by MAIT cells (96, 97), we speculated that by lacking the riboflavin biosynthetic pathway, *L. monocytogenes* might be avoiding MAIT cell activation and responses. To test if this is the case, we engineered *L. monocytogenes* to synthesize riboflavin by introducing the five-gene riboflavin biosynthetic operon *ribDEAHT* from the closely related Gram-positive bacterium *Bacillus subtilis* onto the *L. monocytogenes* chromosome. Two strains were constructed, one containing a constitutively active promoter driving expression of *ribDEAHT* (pHyper *ribDEAHT*), which continuously produced riboflavin, and another that regulated riboflavin production (**Fig. 4.1a**). The second strain (Δ *ribU* pNative *ribDEAHT*) contained the native promoter from the *B. subtilis* *ribDEAHT* operon which contains an FMN riboswitch capable of regulating *ribDEAHT* expression in response to the concentration of flavins in the bacterial cytosol. During growth in high flavin concentrations, FMN binds the riboswitch and blocks translation. Since *L.*

monocytogenes uses RibU to import flavins from the host cell cytosol, which could shut off *ribDEAHT* expression through the native promoter, we constructed this strain in a RibU-minus background. Therefore $\Delta ribU$ pNative *ribDEAHT* strain was unable to import flavins from the host, and forced to synthesize riboflavin to grow (154).

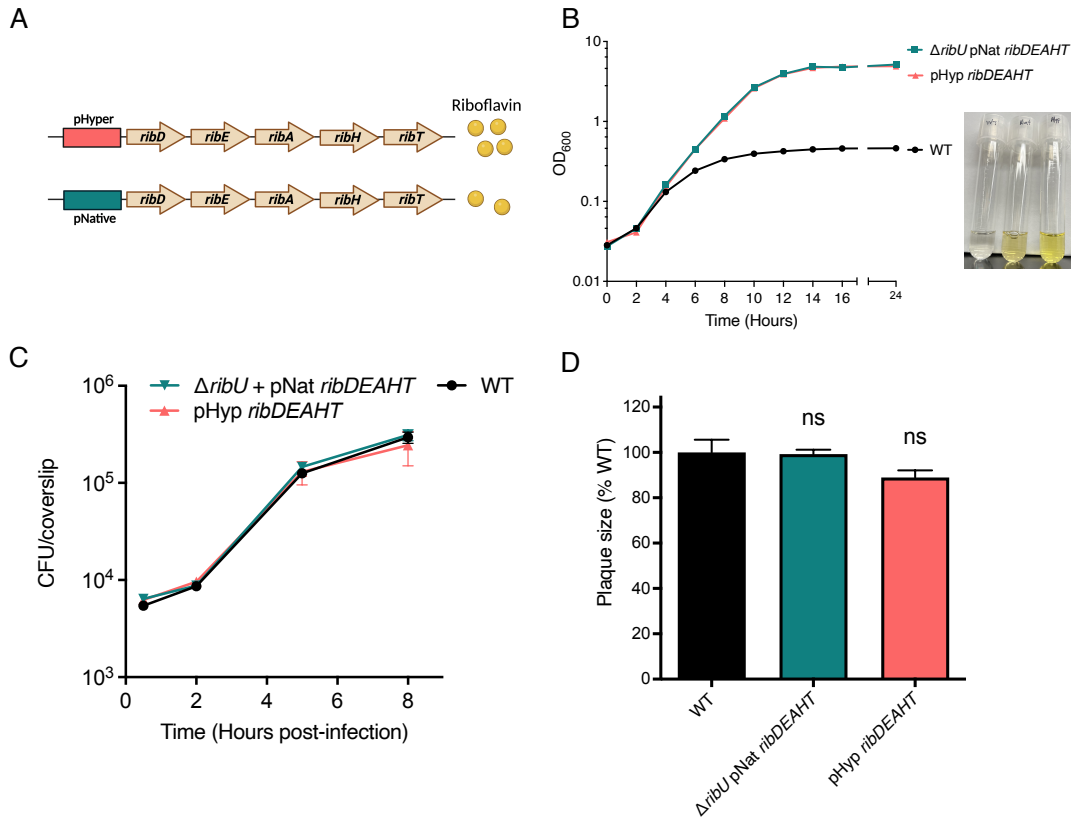


Figure 4.1 *L. monocytogenes* expressing *ribDEAHT* produce riboflavin and have no detectable virulence defects *in vitro* in broth and host cells. (A) Representation of the *ribDEAHT* operon used for construction of the riboflavin-producing *L. monocytogenes* strains. Top: The pHyper promoter (pHyper) leads to the constitutive expression of the *ribDEAHT* genes, and thus unregulated production of riboflavin. Bottom: The Native promoter (pNative) from the *B. subtilis* *ribDEAHT* operon. It contains an FMN riboswitch that, when flavins are high in the bacterial cytosol, blocks translation of the *ribDEAHT* operon, and thus regulates riboflavin production. (B) Broth growth curve of *L. monocytogenes* strains grown in chemically defined media lacking flavins. To determine cell density, the OD₆₀₀ was measured at the time points indicated. The data show the means and standard deviations from three independent experiments. The image to the left shows the media supernatant of wild type (left), $\Delta ribU$ pNat *ribDEAHT* (center), and pHyp *ribDEAHT* (right) after 24 h of growth at 37 °C shaking. The change in color from colorless to bright yellow, the natural color of flavins, is indicative of riboflavin production. (C) Intracellular growth curves of *L. monocytogenes* strains in murine bone marrow-derived macrophages (BMMs). BMMs were infected at a multiplicity of infection (MOI) of 0.1, and CFUs were enumerated at the indicated times. (D) Plaque formation of *L. monocytogenes* strains in monolayers of murine L2 fibroblast cells. The mean plaque size of each strain is shown

as a percentage relative to the wild-type plaque size. Error bars represent standard deviations of the mean plaque size from three independent experiments. Statistical analysis was performed using one-way ANOVA and Dunnett's post-test comparing wild type to all the other strains. ns, no significant difference ($P > 0.05$).

To confirm that these strains produced riboflavin *de novo*, we performed growth curves in chemically defined synthetic media lacking flavins. Unlike wild type, the pHyper and pNative *ribDEAHT* strains grew in the absence of exogenous flavins (**Fig. 4.1b**). Furthermore, *ribDEAHT* expression caused the culture media to change from translucent to bright yellow, the natural color of flavins, although differences in color intensity were observed (**Fig. 4.1b**). pHyper *ribDEAHT* expression correlated with higher color intensity (**Fig. 4.1b**). Thus, we concluded that the pHyper and pNative *ribDEAHT* strains can produce riboflavin *de novo* and that expression from the constitutive promoter (Hyper) leads to more riboflavin production.

To test if the riboflavin-producing *L. monocytogenes* strains had growth or virulence defects outside the context of MAIT cells, we decided to characterize their growth *in vitro* in cells. The riboflavin-producing strains grew intracellularly in bone marrow-derived macrophages and no differences were detected when comparing them with wild-type *L. monocytogenes* (**Fig. 4.1c**). Furthermore, we evaluated their capacity to grow and perform cell-to-cell spread in fibroblasts using a plaque assay. Plaque formation requires *L. monocytogenes* to infect a monolayer of cells, escape from phagosomes, grow intracellularly, and spread from cell to cell over a period of days. The riboflavin-producing *L. monocytogenes* strains formed plaques equal in size to wild type (**Fig. 4.1d**). These results show that the riboflavin-producing strains behave like wild-type *L. monocytogenes* in host cells and have no detectable growth or virulence defects *in vitro*.

4.3.2 Riboflavin-producing *L. monocytogenes* are attenuated in mice

After confirming that *de novo* riboflavin production did not affect *L. monocytogenes* intracellular growth, we evaluated their growth in a murine model of infection. At 2d post-infection, the pNative *ribDEAHT* strain had a 1-log virulence defect in the spleens and livers of mice, while the pHyper *ribDEAHT* strain had a 1-log defect in the livers, but no defect in the spleens, compared to wild-type *L. monocytogenes* (**Fig. 4.2**). However, at 4d post-infection, both riboflavin-producing strains had a 2- to 3-log virulence defect in these organs (**Fig. 4.2**). By 7d post-infection, no colony-forming (CFU) units could be recovered from the spleens of mice infected with the riboflavin-producing strains, while a 1- to 2-log attenuation was observed in the livers (**Fig. 4.2**). The virulence defect of the riboflavin-producing strains observed *in vivo* suggests that *de novo* riboflavin synthesis is detrimental to *L. monocytogenes* virulence, which led us to hypothesize that this attenuation might be mediated by MAIT cells.

4.3.3 MAIT cells accumulate in response to riboflavin-producing *L. monocytogenes* infection and lead to their attenuation *in vivo*

To test if MAIT cells contribute to the attenuation of the riboflavin-producing strains, we infected MR1 knockout (KO) mice, which lack MAIT cells, and MR1 heterozygous (MR1 Het) littermate controls. Since the highest attenuation was observed at 4d post-infection, we focused on this time point. Strikingly, there was no difference in bacterial CFUs in the livers or spleens of MR1 KO mice between the riboflavin-producing strains and wild-type *L. monocytogenes* (Fig. 4.3a), while a 1- to 2-log attenuation was observed in MR1 Het littermate controls (Fig. 4.3b). MAIT cells accumulate in the lungs of mice infected with *L. longbeachae* (97) and in the lungs, spleen, liver, and kidney of *F. tularensis* (96, 198), but fail to do so during *M. tuberculosis* infection (100, 199), thus we wondered how MAIT cells would respond to the riboflavin-producing *L. monocytogenes* strains. In naïve and wild-type *L. monocytogenes* infected murine spleens, MAIT cells (identified as CD3⁺CD4⁻CD8⁻ (DN), MR1:5-OP-RU tetramer⁺ T cells) composed 0.6% of DN T cells, while the frequency of MAIT cells in mice infected with riboflavin-producing *L. monocytogenes* was approximately 2.6%, an almost 5-fold increase in MAIT cells (Fig. 4.3c). Based on these results, we concluded that MAIT cells respond specifically to riboflavin-producing *L. monocytogenes* by accumulating in infected tissues and are very likely contributing to the attenuation observed in wild-type mice.

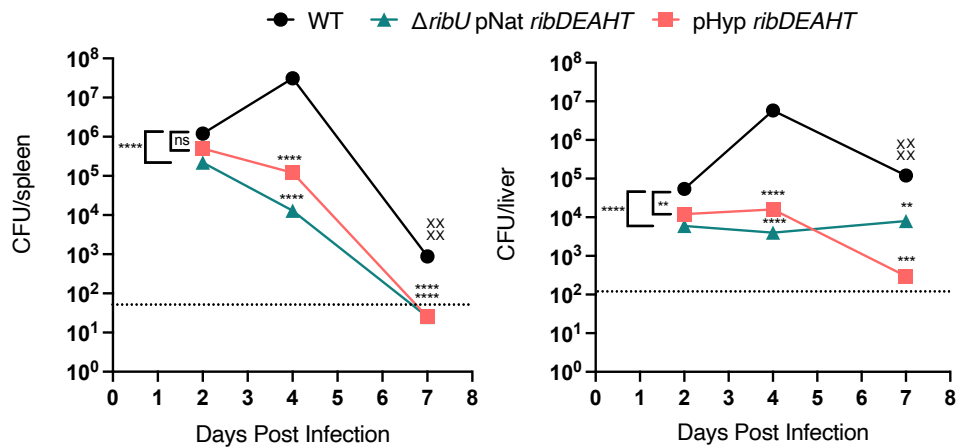


Figure 4.2 Riboflavin-producing *L. monocytogenes* strains are attenuated in mice. Bacterial burdens in C57BL/6 mice infected intravenously with 1×10^3 CFUs of indicated *L. monocytogenes* strains. Mice were sacrificed at 2, 4, and 7 d post-infection and the spleens (left) and livers (right) were harvested, homogenized, and plated to determine the CFUs per organ. The data show the median value from a combination of at least three independent experiments. The “X” denotes mice that succumbed to the infection and no CFUs were collected. The dashed line represents the limit of detection. Statistical significance of logarithmically transformed CFU values was determined using one-way ANOVA and Dunnett’s posttest using WT as the control for each individual time point. ****P < 0.0001; ***P < 0.001; **P < 0.01; ns, not significant, P > 0.05

4.3.4 High-dose infection with riboflavin-producing *L. monocytogenes* strains in an ActA-minus background leads to substantial and sustained accumulation of MAIT cells in infected tissues

Although we observed a 5-fold increase of MAIT cells in tissues infected with riboflavin-producing *L. monocytogenes*, we wondered if we could enhance this response by infecting mice with more bacteria. However, since the strains used in the previous experiments were in the wild-type *L. monocytogenes* background, and the 50% lethal dose (LD₅₀) in mice is approximately 5-fold higher than the administered dose, infecting with higher doses would result in the death of the mice. Thus, we decided to introduce the pNative and pHyper *ribDEAHT* operon constructs into the ActA-minus *L. monocytogenes* background ($\Delta actA \Delta ribU$ pNative and pHyper *ribDEAHT*). ActA-minus *L. monocytogenes* cannot spread from cell to cell and thus is highly attenuated in mice (approximately 1000-fold compared to wild-type in BALB/C) (195), which allowed us to infect with substantially more bacteria without killing the mice. First, we performed a virulence experiment by infecting mice with a higher dose than the one previously administered (1×10^7 CFU/mouse, instead of 1×10^3 CFU/mouse) of the strains in the ActA-minus background to confirm that the attenuation observed with the riboflavin-producing strains in the wild-type background was reproducible. Indeed, at 4d post-infection, the ActA-minus riboflavin-producing strains were 2-logs attenuated in the spleens and livers (**Fig. 4.4a**), as previously observed with the strains in the wild-type *L. monocytogenes* background (**Fig. 4.2**). Strikingly, we observed that the frequency of MAIT cells (CD3⁺TCR- β ⁺MR1:5-OP-RU tetramer⁺ T cells) in the mice infected with the ActA-minus pHyper *ribDEAHT* strain represented as high as 30% of $\alpha\beta$ -T cells in the livers of infected mice (**Fig. 4.4b**). The median frequencies of MAIT cells in the spleens and livers of mice infected with the ActA-minus pHyper *ribDEAHT* strain were 15% and 20% of all $\alpha\beta$ T cells, respectively (**Fig. 4.4c**). In contrast, the frequencies of MAIT cells in the spleens and livers of mice infected with the $\Delta actA$ *L. monocytogenes* control were between 0.5% and 1% of all T cells, which were the same as in naïve mice (**Fig. 4.4c**).

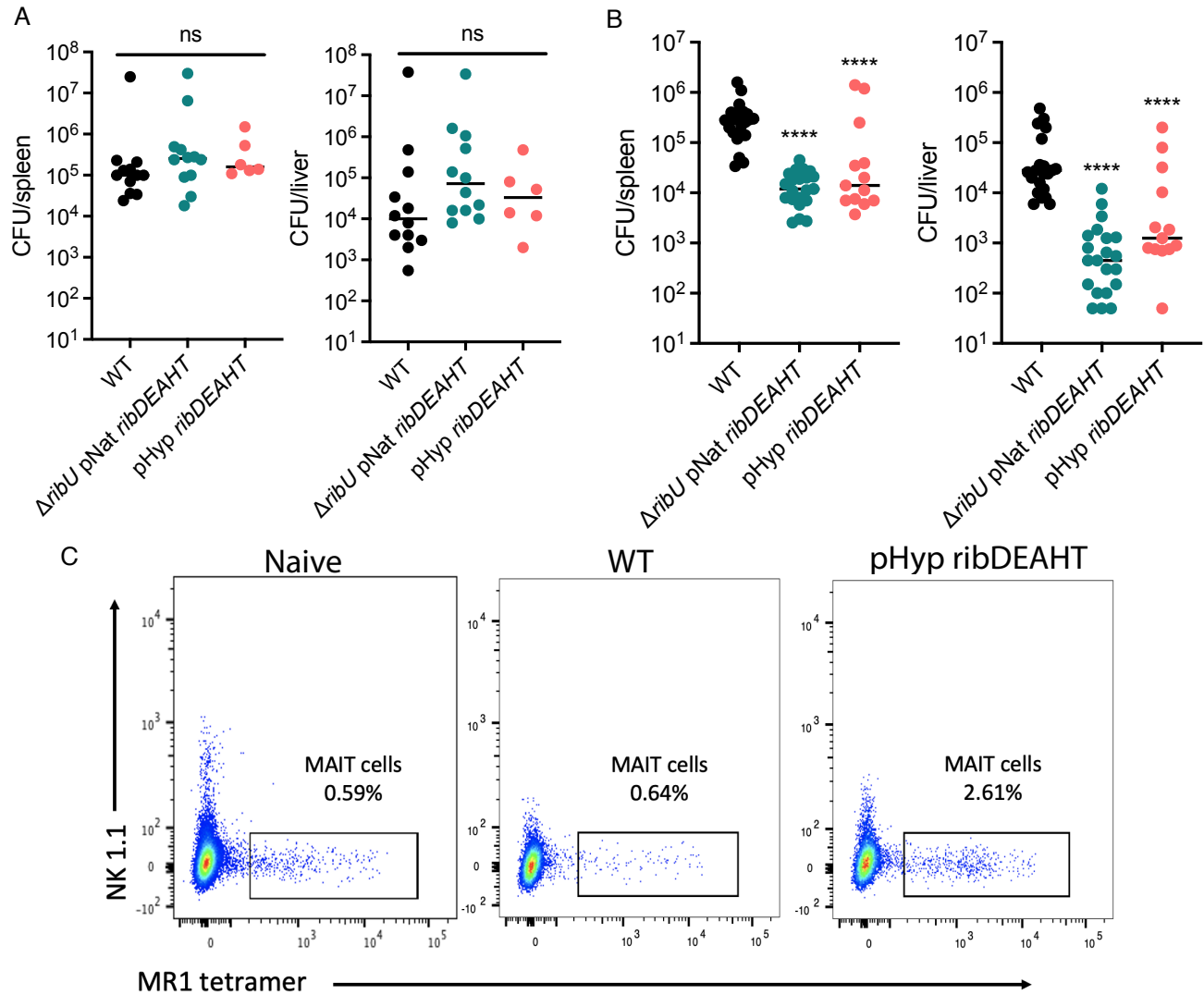


Figure 4.3 MAIT cells respond and mediate growth restriction of the riboflavin-producing *L. monocytogenes*. (A and B) Bacterial burdens in (A) MR1 KO C57BL/6 mice, which lack MAIT cells, and (B) MR1 Het C57BL/6 littermate controls infected intravenously with 1×10^3 CFUs of indicated *L. monocytogenes* strains. At 4 d post-infection, the spleens (left) and livers (right) were harvested, homogenized, and plated to determine the CFUs per organ. For (A): the data show the combination of at least two independent experiments: WT ($n = 12$ mice), Δ ribU pNat ribDEAHT ($n = 12$ mice), and pHyp ribDEAHT ($n = 6$ mice). For (B): the data show the combination of at least three independent experiments: WT ($n = 22$ mice), Δ ribU pNat ribDEAHT ($n = 20$ mice), and pHyp ribDEAHT ($n = 13$ mice). Statistical significance of logarithmically transformed CFU values was determined using one-way ANOVA and Dunnett's posttest using WT as the control for each individual time point. **** $P < 0.0001$; ns, not significant, $P > 0.05$. (C) Representative flow cytometry plots showing the frequency of splenic MAIT cells in naïve, wild type, or pHyper ribDEAHT 4 d post-infection of C57BL/6 mice. Infection dose was 1×10^4 CFU/mouse. MAIT cell percentages of live, CD45 positive, CD4/CD8 double negative, MR1:5-OP-RU tetramer-positive T cells are shown.

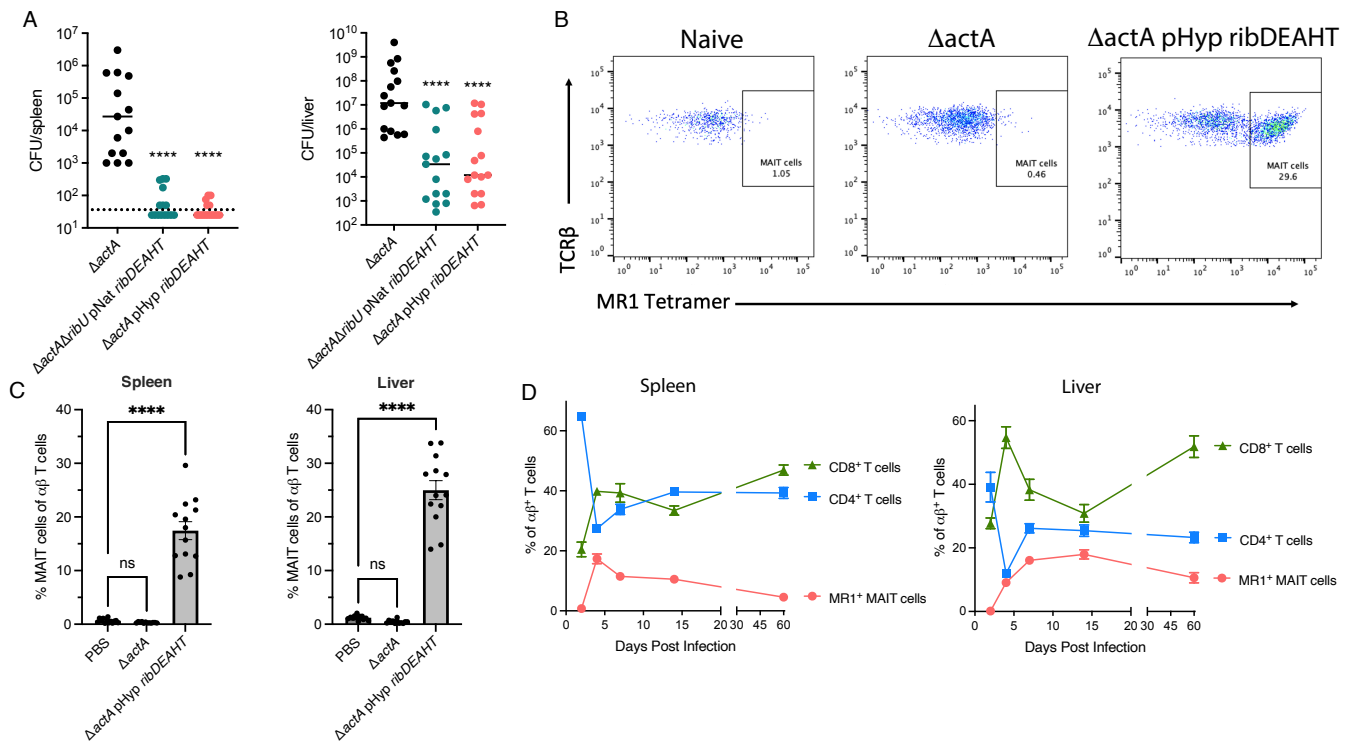


Figure 4.4 Infection with attenuated riboflavin-producing *L. monocytogenes* strains in ActA-minus backgrounds leads to substantial and sustained accumulation of MAIT cells in infected tissues. (A) Bacterial burdens in C57BL/6 mice infected intravenously with 1×10^7 CFUs of indicated *L. monocytogenes* strains. At 4 d post-infection, the spleens (left) and livers (right) were harvested, homogenized, and plated to determine the CFUs per organ. The data show the combination of three independent experiments: $\Delta actA$, $\Delta actA\Delta ribU$ pNat *ribDEAHT*, and $\Delta actA$ pHyp *ribDEAHT* ($n = 15$ mice). The black lines represent the median CFUs for each strain. The dashed line represents the limit of detection. Statistical significance of logarithmically transformed CFU values was determined using one-way ANOVA and Dunnett's posttest using WT as the control. **** $P < 0.0001$. (B and C) (B) Representative flow cytometry plots from liver MAIT cells and (C) summarized data from spleens and livers showing the frequency of MAIT cells in naive, $\Delta actA$, or $\Delta actA$ pHyper *ribDEAHT* 4 d post-infection of C57BL/6 mice. Infection dose was 1×10^7 CFU/mouse. MAIT cell percentages of live, CD45 positive, TCR β positive, MR1:5-OP-RU tetramer positive T cells are shown. In (C), the means and SEMs of three independent experiments are shown: naive ($n = 14$ mice), $\Delta actA$ ($n = 10$ mice), and $\Delta actA$ pHyp *ribDEAHT* ($n = 13$ mice). Statistical significance was determined using one-way ANOVA and Dunnett's posttest using (PBS) naive mice as the control. **** $P < 0.0001$; ns, not significant, $P > 0.05$. (D) MAIT cell kinetic experiments showing the frequencies of MAIT cells, CD4 $^+$ T cells, and CD8 $^+$ T cells at 2, 4, 7, 14, and 60 d post-infection in mice infected with 1×10^7 CFU/mouse of $\Delta actA$ pHyper *ribDEAHT*. Percentages of cells gated as live, CD45 positive, TCR β positive, and then as MR1:5-OP-RU tetramer-positive CD4 $^-$ /CD8 $^-$ negative cells (MAIT cells), CD4 $^+$ /CD8 $^-$ (CD4 $^+$ T cells), and CD4 $^-$ /CD8 $^+$ (CD8 $^+$ T cells), are shown. PBS; Phosphate buffer saline.

Subsequent to infection, MAIT cells can remain in tissues long after the infection has subsided (97), thus we wondered if that would be the case after infection with *L. monocytogenes* producing riboflavin. We infected mice with ActA-minus pHyper *ribDEAHT* and collected the spleens and livers at 2, 4, 7, 14, and 60d post-infection. From less than 1% of all $\alpha\beta$ T cells at 2d post-infection, MAIT cell frequencies peaked at 20% in the spleens on day 4 post-infection, and in the livers on day 14 post-infection (**Fig. 4.4d**). At 60d post-infection, MAIT cells comprised an average of 5% and 10% of all $\alpha\beta$ T cells in the spleens and livers, respectively (**Fig. 4.4d**). CD8+ T cell frequencies started approximately at 20% in both organs and peaked 4d post-infection at 40% in the spleens and 60% in the livers (**Fig. 4.4d**). In contrast, at day 2 post-infection, CD4+ T cells were at their highest frequencies at 60% in the spleens and 40% in the livers of $\alpha\beta$ T cells (**Fig. 4.4d**). By day 4 post-infection, their frequencies were as low as 25% and 10% in the spleens and livers, respectively (**Fig. 4.4d**). At 60d post-infection, CD4+ T cells ended with lower frequencies in both organs than their initial frequencies at the beginning of the experiments (**Fig. 4.4d**). These MAIT cell kinetic experiments showed that the frequencies of MAIT cells peaked at 4d post-infection in the spleen and 14 days in the liver and were maintained for 60d in these organs at higher frequencies than the frequencies of MAIT cells in naïve mice (**Fig. 4.4c**) and 2d infected mice (**Fig. 4.4d**). These data suggest that MAIT cells strongly respond to attenuated riboflavin-producing *L. monocytogenes* strains by accumulating in high frequencies in infected organs and that they can remain in tissues at frequencies higher than those found in naïve mice.

4.3.5 Perforin is required for MAIT cells to restrict riboflavin-producing *L. monocytogenes* in mice

Our data show that MAIT cells specifically restrict riboflavin-producing *L. monocytogenes* (**Fig. 4.2** and **Fig. 4.3a**), and we wondered which mechanism(s) are involved. MAIT cells have two primary effector functions that mediate control of pathogens; production of cytokines which will activate bystander cells, or direct killing of infected cells using the cytolytic effectors granzyme B and perforin (63, 130). Since *L. monocytogenes* is an intracellular pathogen, we hypothesized that direct killing of infected cells would be the response employed by MAIT cells to restrict riboflavin-producing *L. monocytogenes*. We infected mice lacking perforin (perforin KO), which should prevent all cytotoxic cells including MAIT cells from directly killing infected cells, and observed that the riboflavin-producing *L. monocytogenes* had no virulence defect compared to wild-type *L. monocytogenes* (**Fig. 4.5a**). To confirm that MAIT cells are still responding and accumulating in infected tissues, and not that the response at d4 post-infection is different in perforin KO mice, we infected these mice with the ActA-minus riboflavin-producing *L. monocytogenes* strains and determined the frequencies of MAIT cells in organs. The frequencies of MAIT cells in perforin KO mice were 15% and 20% of all $\alpha\beta$ -T cells in the spleens and livers, respectively (**Fig. 4.5b**), similar to the frequencies observed in wild-type infected mice (**Fig. 4.3c**). These results suggested that the primary mechanism used by MAIT cells to restrict riboflavin-producing *L. monocytogenes* is direct killing of infected cells.

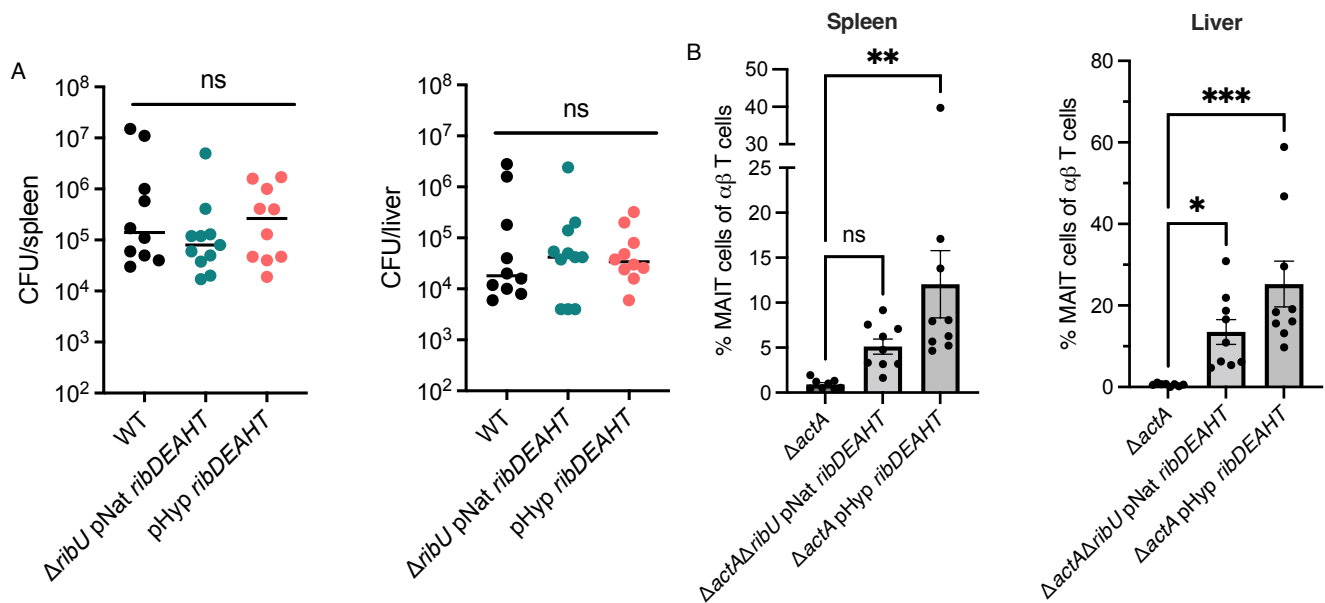


Figure 4.5 Perforin-minus MAIT cells restrict riboflavin-producing *L. monocytogenes*. Bacterial burdens in perforin KO C57BL/6 mice, which lack the cytolytic effector perforin, infected intravenously with 1×10^3 CFUs of indicated *L. monocytogenes* strains. At 4d post-infection, the spleens (left) and livers (right) were harvested, homogenized, and plated to determine the CFUs per organ. The data show the combination of two independent experiments: WT ($n = 20$ mice), $\Delta ribU$ pNat ribDEAHT ($n = 11$ mice), and pHyper ribDEAHT ($n = 10$ mice). Statistical significance of logarithmically transformed CFU values was determined using one-way ANOVA and Dunnett's posttest using WT as the control. ns, not significant, $P > 0.05$. (B) Summarized data showing the frequency of MAIT cells in the spleens and livers of naïve, $\Delta actA$, or $\Delta actA$ pHyper ribDEAHT at 4 d post-infection in perforin KO C57BL/6 mice. Infection dose was 1×10^7 CFU/mouse. MAIT cell percentages of live, CD45 positive, TCR β positive, MR1:5-OP-RU tetramer positive T cells are shown. The means and SEMs of two independent experiments are shown: $\Delta actA$ ($n = 8$ mice), $\Delta actA \Delta ribU$ pNat ribDEAHT ($n = 9$ mice), and $\Delta actA$ pHyper ribDEAHT ($n = 9$ mice). Statistical significance was determined using one-way ANOVA and Dunnett's posttest using $\Delta actA$ mice as the control. *** $P < 0.001$; ** $P < 0.01$; * $P < 0.05$; ns, not significant, $P > 0.05$.

4.4 Discussion

L. monocytogenes is a facultative intracellular pathogen that, unlike most bacteria, lacks the riboflavin biosynthetic genes (196). However, like all organisms, they rely significantly on flavins for metabolism, physiology, and pathogenesis (9, 197) and must therefore obtain flavins from the host. In a previous study, we showed that *L. monocytogenes* uses the flavin transporter RibU to import FMN and FAD from the cytosol of infected host cells (154). Not surprisingly, RibU-minus mutants are avirulent. In this study, we asked if the lack of riboflavin synthesis provides an advantage to *L. monocytogenes* during infection by allowing them to avoid activation of MAIT cells. MAIT cells are conserved and abundant innate-like T cells that can

exhibit potent antimicrobial responses against certain riboflavin-producing microorganisms (95). Thus, we speculated that, although *L. monocytogenes* requires flavins, it would be detrimental to synthesize riboflavin during infection because it would lead to activation of MAIT cells and their potent antimicrobial responses. Thus, to investigate if *L. monocytogenes* is avoiding MAIT cell responses by lacking the capacity to synthesize riboflavin *de novo*, we constructed strains of *L. monocytogenes* that express the *B. subtilis* riboflavin biosynthetic genes and compared their virulence in wild-type mice and MR1-minus mice that lack MAIT cells. The results of this study show that *L. monocytogenes* strains that produce riboflavin cause the expansion and accumulation of MAIT cells in the liver and spleen (Fig. 4.3c, Fig. 4.4c, and Fig. 4.5b), and strikingly restrict the growth of riboflavin-producing *L. monocytogenes* in wild-type mice (Fig. 4.2). In contrast, the virulence of riboflavin-producing *L. monocytogenes* was not affected in perforin-minus mice suggesting that the mechanism by which MAIT cells provide protection is by killing infected cells. Collectively, these observations suggest that *L. monocytogenes* avoids MAIT cell detection by importing flavins from the host instead of synthesizing riboflavin *de novo* (Fig. 4.6).

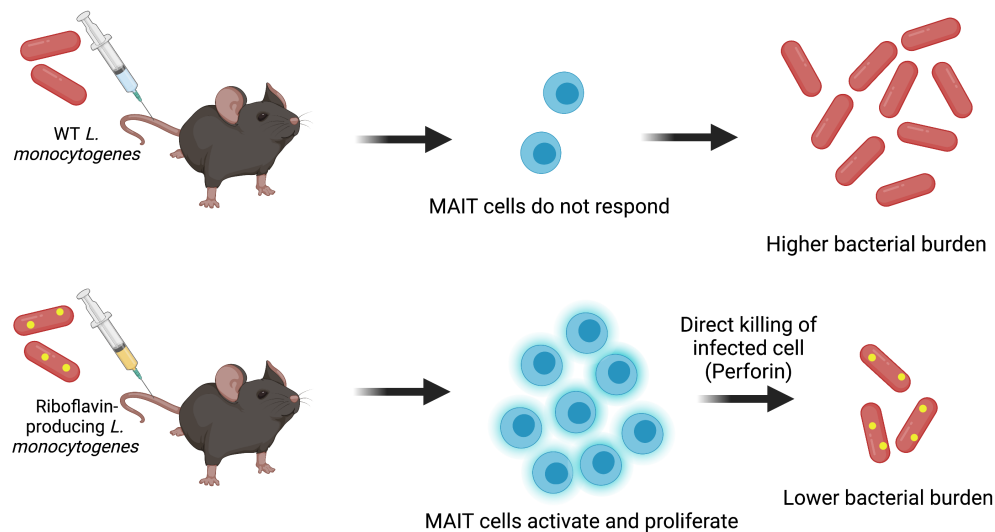


Figure 4.6 Summary model: *L. monocytogenes* avoid MAIT cell detection by importing flavins from the host instead of synthesizing riboflavin *de novo*. Top, wild-type *L. monocytogenes* do not produce riboflavin or the precursor for the MAIT cell activating ligand 5-OP-RU. MAIT cells are unable to detect wild-type *L. monocytogenes* and thus, do not respond by proliferating or killing wild-type *L. monocytogenes*. To satisfy their flavin requirements, *L. monocytogenes* encodes the transporter RibU, which bypasses the need for *de novo* riboflavin production and imports flavins from the host. Bottom, riboflavin-producing *L. monocytogenes* generate the precursor of the MAIT cell ligand (yellow circles) and thus are recognized by MAIT cells during infection. MAIT cells respond by activating, proliferating, and potentially directly killing cells infected with riboflavin-producing *L. monocytogenes*.

MAIT cells respond and restrict the growth of some riboflavin-producing intracellular pathogens *in vivo*, including *L. longbeachae* and *F. tularensis*, but not all, i.e., *M. tuberculosis* (96, 97, 198, 199). This study shows that in wild-type C57BL/6 mice, which have very low numbers of MAIT cells compared to humans (63), riboflavin-producing *L. monocytogenes* strains are highly attenuated (**Fig. 4.2**). The growth restriction of the riboflavin-producing *L. monocytogenes* strains suggests that MAIT cell responses against these strains are similar to those observed against *L. longbeachae* and *F. tularensis*, and not *M. tuberculosis* (96, 97, 198, 199). We found that MAIT cells substantially accumulate in the spleens and livers infected with riboflavin-producing *L. monocytogenes* (**Fig. 4.4c**), which is similar to what occurs in the lungs infected with *L. longbeachae* and, as well as the lung, liver, spleen, kidney, and blood infected with *F. tularensis* (96, 97, 198), unlike the response to *M. tuberculosis* where expansion does not occur (100, 199). These previous studies performed with *L. longbeachae* and *F. tularensis*, shed light on MAIT cell responses in tissues and highlighted the proliferation potential of MAIT cells. Infection with the riboflavin-producing *L. monocytogenes* generated a significant accumulation of MAIT cells in the spleen (up to 15% of $\alpha\beta$ T cells) and the liver (up to 30% of $\alpha\beta$ -T cells) of wild-type mice (**Fig. 4.4c**). These results expand our understanding of MAIT cell responses and proliferation potential, especially to pathogens that infect the spleen and the liver. Our results also suggest that the main mechanism used by MAIT cells to restrict growth of riboflavin-producing *L. monocytogenes* is direct killing of infected cells using perforin (**Fig. 4.5a**). We performed these experiments using perforin-minus mice, which should prevent the cytotoxic potential of MAIT cells, and found that the riboflavin-producing *L. monocytogenes* strains had no defects in growth or virulence compared to wild-type *L. monocytogenes* (**Fig. 4.2**). In contrast, perforin does not appear to play a role in restriction of growth during *L. longbeachae* infection (97). During *L. longbeachae* lung infection, cytokine secretion, specifically IFN- γ production, was the main effector response that controlled the burden of this pathogen (97). We did not assess the contribution of cytokines to the restriction of riboflavin-producing *L. monocytogenes*, and thus cannot rule out that this response might also play a role. Interestingly, we also observed that MAIT cells activated with attenuated riboflavin-producing *L. monocytogenes* strains persisted in the spleens and livers and mostly mimic the kinetics of CD8⁺ T cells (**Fig. 4.4d**). Similarly, MAIT cells were retained in the lungs of mice long after *L. longbeachae* infection at frequencies higher than the frequencies before infection (97). These results confirm that MAIT cells can be retained in tissues after resolution of the infection and might have the potential to be restimulated, which has interesting therapeutic potential.

Since most bacteria can synthesize riboflavin (29), including pathogens, it is reasonable to suggest that *L. monocytogenes* lost the capacity to synthesize riboflavin to avoid MAIT cell responses. Indeed, *Listeria grayi*, one of the most distantly related non-pathogenic *Listeria* species, contains all the genes necessary for riboflavin production (200). Also, interestingly, the RibU transporter in the non-pathogenic bacterium *Lactococcus lactis* cannot import FAD (34). Thus, by adapting RibU to import FMN and FAD, the flavins available during intracellular growth, *L. monocytogenes* might have had less of an evolutionary barrier to shed the riboflavin biosynthetic pathway, which would allow them to avoid MAIT cell activation (154). This hypothesis is supported by the fact that MAIT cells are present in many mammalian hosts (182) and localize to most tissues including the intestine, spleen, and liver, which *L. monocytogenes*

colonizes (192). The other possibility would be that *L. monocytogenes* never possessed the riboflavin biosynthetic genes and transport was the only mechanism employed to acquire flavins. Since *L. monocytogenes* have a flavin-centric lifestyle and can occupy very diverse environments (like intracellularly in host cells or free-living in soil), it is not unreasonable to hypothesize that previously they could have synthesized their own flavins but disposed of that ability due to evolutionary pressure exerted by MAIT cells.

4.5 Materials and Methods

Bacterial strains and culture

All strains of *L. monocytogenes* used in this study (Table S1) were derived from the wildtype 10403S strain and were cultured in filter-sterilized nutrient-rich brain heart infusion (BHI) media (BD) containing 200 µg/mL streptomycin (Sigma-Aldrich). The strains expressing the *ribDEAHT* operon from the constitutive promoter pHyper (pHyper *ribDEAHT* construct) or the pNative promoter (pNative *ribDEAHT*) were done by amplifying the *ribDEAHT* operon (for pNative with its native promoter) from *B. subtilis* and cloning it into the site-specific pPL2 integrating vector. The plasmids were then introduced into *L. monocytogenes* by conjugation, as previously described (132). Broth growth curves were performed with *L. monocytogenes* strains from overnight cultures grown in chemically defined synthetic media with 1 µM riboflavin at 37 °C with shaking (200 rpm) and the experiment was done in chemically defined synthetic media lacking flavins. Growth was measured by optical density at a wavelength of 600 nm (OD₆₀₀) and the growth curves were started at an OD₆₀₀ of 0.03.

Intracellular macrophage growth curves

L. monocytogenes strains were grown overnight slanted at 30°C and were diluted in sterile PBS. A total of 3×10^6 BMMs from C57BL/6 mice were seeded in 60 mm non-TC treated dishes containing 14 12 mm glass coverslips in each dish and infected at an MOI of 0.25 as previously described (134).

Plaque assays

L. monocytogenes strains were grown overnight slanted at 30°C and were diluted in sterile phosphate-buffered saline (PBS). Six-well plates containing 1.2×10^6 mouse L2 fibroblast cells per well were infected with the *L. monocytogenes* strains at a multiplicity of infection (MOI) of approximately 0.1. At 1-hour post-infection, the L2 cells were washed with PBS and overlaid with Dulbecco's Modified Eagle Medium (DMEM) containing 0.7% agarose and gentamicin (10 µg/mL) to kill extracellular bacteria, and then plates were incubated at 37°C with 5% CO₂. At 72-hour post-infection, L2 cells were overlaid with a staining mixture containing DMEM, 0.7% agarose, neutral red (Sigma), and gentamicin (10 µg/mL), and plaques were scanned and analyzed using ImageJ, as previously described (201).

Mouse Intravenous Infections

Eight to twelve-wk-old C57BL/6 mice (Jackson labs), Perforin KO (Jackson labs), MR1 KO mice (a kind gift from Dr. Siobhan Cowley at U.S. Food and Drug Administration Division of Bacterial, Parasitic & Allergenic Products), and MR1 heterozygous mice (bred inhouse) were infected via the tail vein with 200 μ L of PBS containing 1×10^3 or 1×10^7 logarithmically growing bacteria, as specified. The mice were euthanized, and the spleens and livers were collected, homogenized, and plated to determine the number of CFU per organ.

Flow cytometry

Eight to twelve-wk-old C57BL/6 mice (Jackson labs) were infected via the tail vein with 200 μ L of PBS containing 1×10^4 or 1×10^7 logarithmically growing bacteria, as specified. The mice were euthanized, and the spleens and livers were collected, processed, and resuspended as single cells. Two million cells were resuspended for flow cytometry analysis. Surface staining was performed at RT with the following antibodies: Live/Dead (AmCyan), CD45 (BUV 395), CD8 (BUV737), CD4 (BV 785), CD3 (FITC), Thy1.2 (APC-Cy7), TCR β (PerCPCy5.5), MR1:5-OP-RU (PE), and NK1.1 (BV650). Cells were fixed with 1% paraformaldehyde prior to analysis on LSR Fortessa or Celeste (BD Biosciences) flow cytometers. Flow cytometric data analysis was performed with FlowJo10 software (Ashland, OR).

Chapter 5: Conclusions and Future Directions

Conclusions

Every organism on the planet requires flavins to live since these molecules function as cofactors for a multitude of proteins involved in essential biological processes (4). Flavins participate in the metabolism of amino acids, fatty lipids, and other vitamins, as well as generation of energy (10, 15, 17, 20). As protein cofactors, their main function is the exchange of electrons during reduction-oxidation reactions (4). Flavin mononucleotide (FMN) and flavin adenine dinucleotide (FAD) serve as the biologically active cofactors and are synthesized from riboflavin (26). Plants, fungi, most bacteria and archaea satisfy their flavin requirements by synthesizing riboflavin *de novo*, while animals and a minority of bacterial species obtain riboflavin from the environment (29, 30). This study set out to elucidate the basis of flavin acquisition, metabolism, and their role in pathogenesis using the riboflavin auxotrophic, intracellular pathogen *L. monocytogenes*.

Flavin acquisition during *L. monocytogenes* intracellular growth

Prior to this study, it was known that *L. monocytogenes* lack the riboflavin biosynthetic genes and that they encode a putative energy-coupling factor (ECF) transporter RibU (51). *L. monocytogenes* RibU binds riboflavin *in vitro* and heterologous expression in a riboflavin auxotrophic *B. subtilis* strain promoted growth at lower riboflavin concentrations (51, 54). In another study, we identified a mutant with a transposon insertion in the *ribU* gene that lacked extracellular electron transfer activity but had no apparent growth defects in rich media (9). Since RibU was the only annotated transporter for riboflavin and no growth phenotype was observed during *in vitro* growth in rich media, we wondered how *L. monocytogenes* acquires riboflavin while growing intracellularly, an environment that is predicted to lack riboflavin. Strikingly, we discovered that RibU is essential for virulence and intracellular growth and that instead of importing riboflavin, it scavenges FMN and FAD directly from the host cell cytosol. We showed this by generating a strain ($\Delta ribC\Delta ribF$) that could not convert riboflavin to FMN and FAD. The $\Delta ribC\Delta ribF$ mutant strain grew in peripheral organs of mice infected intravenously, in contrast with the RibU-minus mutant which was avirulent. Furthermore, we showed that the $\Delta ribC\Delta ribF$ mutant was restricted to intracellular growth since we did not detect bacteria growing at sites where *L. monocytogenes* is known to colonize extracellularly like the gallbladders, gastrointestinal tract, or blood. Since the $\Delta ribC$ single mutant, which requires FMN, grew extracellularly in gallbladders while the $\Delta ribC\Delta ribF$, which requires both FMN and FAD, did not, we speculate that *L. monocytogenes* grows on riboflavin and/or FMN extracellularly *in vivo* and that FAD is not available at concentrations that support growth.

Flavin export for extracellular flavinylation is mediated by a novel ECF exporter in *L. monocytogenes*

Extracellular electron transfer (EET) mechanisms are involved in the transfer of electrons from the bacterial cytosol across the membrane for functionally diverse redox systems outside the cell (8, 9, 60). Recently, bioinformatic analyses revealed that approximately 50% of sequenced bacterial genomes contain extracellular flavinylated proteins that are predicted to be modified

by ApbE, an FMN transferase (62). How flavins are provided to extracytosolic FmnB was unknown. *L. monocytogenes* possesses a flavin-dependent EET system that uses flavinylated proteins and secreted flavins to transfer the cytosolic electrons to extracellular electron acceptors (9). Previously, based on assays of EET activity, we hypothesized that RibU formed a transporter involved in exporting FAD together with FmnA (9). Extracellular FAD serves as the substrate for FmnB-dependent flavinylation of the lipoproteins PplA and FrdA. However, using a RibU-minus, riboflavin-prototrophic *L. monocytogenes* strain, we found that RibU was not involved in EET activity and that the lack of activity previously observed was likely due to low concentration of cytosolic flavins. We discovered that the uncharacterized proteins EetB, which is a homolog of RibU, and FmnA, a transmembrane structural protein, are involved in FAD export. EetB and FmnA form a novel ECF exporter capable of secreting flavins. This constitutes the first example of an ECF transporter with export function that is also present in other firmicutes and suggests it provides flavins for extracytosolic redox-dependent processes.

L. monocytogenes* avoids MAIT cell responses by importing flavins instead of producing riboflavin *de novo

Since *L. monocytogenes* depends on flavins for its metabolism, physiology, and pathogenesis it is curious that they lack the riboflavin biosynthesis pathway (196). Interestingly, mucosal-associated invariant T (MAIT) cells, an evolutionary conserved and abundant innate-like T cell subset, is activated upon recognition of riboflavin-producing organisms during infection and respond by secreting inflammatory cytokines and killing cells harboring these organisms (86). We speculated that by lacking the riboflavin biosynthetic genes, *L. monocytogenes* avoids MAIT cell responses. Indeed, we found that *L. monocytogenes* strains producing riboflavin are highly attenuated *in vivo*. Furthermore, using attenuated riboflavin-producing strains, we found that MAIT cells can substantially accumulate in infected organs, and can expand to as many as 30% of all $\alpha\beta$ T cells. The frequencies of MAIT cells remained high in infected organs for at least 60 days, and the kinetics resembled those of conventional T cells. Even though MAIT cell frequencies contracted over time, they remained elevated long after the infection had been resolved. Finally, our findings also suggest that the mechanism used by MAIT cells to restrict riboflavin-producing *L. monocytogenes* is direct killing of infected cells mediated by perforin. These results suggest that *L. monocytogenes* is avoiding MAIT cell responses by importing flavins directly from the host cytosol instead of performing riboflavin biosynthesis.

Future directions

This dissertation addressed how *L. monocytogenes* acquire flavins during infection, how and which proteins are involved in flavin import and export, and provided an explanation as to why *L. monocytogenes* may lack the capacity to make riboflavin. Even though we clarified and provided answers, our findings generated more questions that should be addressed in the future.

First, how do RibU mutants of *L. monocytogenes* acquire riboflavin to grow *in vitro*? Does *L. monocytogenes* encode another transporter that is able to import riboflavin, but not FMN or FAD? Or, does riboflavin diffuse through the membrane? We hypothesize that *L. monocytogenes* encodes another transporter that imports riboflavin since the riboflavin auxotrophic *B. subtilis* strain requires more than 10-times more riboflavin to form colonies (51). Also, as noted in chapter two, why do RibU-minus *L. monocytogenes* lyse in host cells? Is riboflavin starvation causing bacteriolysis intentionally, to provide nutrients to neighboring cells, or is it due to inhibition of metabolic or physiological processes? If the latter is the answer, which essential flavoprotein(s) are contributing to bacteriolysis? We speculate that the reason the RibU-minus *L. monocytogenes* lyses is because of inhibition due to riboflavin starvation. For example, the flavoprotein MurB is an essential protein involved in the biosynthesis of peptidoglycan. If MurB function is impaired, loss of peptidoglycan homeostasis can lead to dividing bacteria lysing since they cannot septate properly or recycle damaged peptidoglycan after cell division. Another question is, why is the $\Delta ribC\Delta ribF$ strain attenuated in the liver but not the spleen? Are the flavin requirements or concentrations different in the liver vs. the spleen? We hypothesize that the concentrations are different in the spleen vs. the liver because of differences in the infected host cells. In the liver, *L. monocytogenes* mainly grows in hepatocytes while in the spleen they infect macrophages. Hepatocytes and macrophages are quite different so it is not unreasonable to suspect that they might have different concentrations of flavins.

Second, can EetB export only FAD, or FMN and riboflavin as well? Like in the case of RibU, EetB might be able to bind all three flavins, and mediate their export. We also wonder, why we failed to detect secreted FAD in the media, as it has been described with *Shewanella oneidensis* (35)? We hypothesize that FAD export in *L. monocytogenes* is not a random process, but rather that exported FAD is selectively delivered to FmnB for subsequent flavinylation of lipoprotein substrates. Additionally, does *L. monocytogenes* possess a flavin-degrading enzyme like UshA from *S. oneidensis*? This could be another reason why we failed to detect FAD in supernatants. In addition, we observed that EetA colocalizes with EetB in many bacterial genomes and sometimes are fused as one protein. Thus, what is EetA's function? Could EetA be mediating the interaction of the EetB exporter complex with FmnB for targeted delivery of FAD? Another question that should be addressed is, what mechanism is the ECF transporter using to export flavins? Evidence suggests that both EcfA ATPases are required for export, thus, is energy also required for this process?

Third, since *L. monocytogenes* infect different cells in the spleen and the liver, does it make a difference which cell/signals are activating MAIT cells during riboflavin-producing *L. monocytogenes*? Are there different cytokines in the liver vs spleen that could lead to different MAIT cell effector responses? It would be ideal to compare the transcriptomic profiles of splenic vs. liver cells, including MAIT cells, during infection. This would allow us to examine which cytokines are produced in the tissues as well as the entire activation/effector state of MAIT cells. We observed differences in MAIT cell kinetics in the spleen vs. the liver. In the liver, the response was slower, but MAIT cells persisted at higher frequencies over time. In contrast, in the spleen, the response was more rapid and MAIT cells reached their highest frequency

earlier, but MAIT cells contracted more rapidly. Why are the kinetics between the spleen and the liver different? One possible explanation is that MAIT cells are following the kinetics of the attenuated riboflavin-producing *L. monocytogenes* strains in the tissues. Attenuated riboflavin-producing *L. monocytogenes* are cleared faster from the spleen but persist in the liver for longer. Thus, MAIT cell activation and accumulation might be following these patterns. Our experiments with perforin KO mice suggested that MAIT cells kill infected cells directly, thus destroying the replicative niche of riboflavin-producing *L. monocytogenes*, and that this process is mediated by perforin. However, since all cytotoxic cells in the perforin KO mice lack this effector, we cannot rule out that perforin from CD8⁺ T cells or natural killer cells might be contributing to the attenuation observed with riboflavin-producing *L. monocytogenes*. An important question from the bacterial side is, how are the MAIT cell activating ligands generated and how do they get out of the bacteria? Are the bacteria lysing in the cytosol and releasing the riboflavin precursor? Or, are the bacteria actively secreting these metabolites? If the latter is true, are these metabolites toxic to bacteria, and is that the reason they are secreted? In addition, what is the source of methylglyoxal that is necessary to form the MAIT cell ligand; is it bacterial or host-derived? And finally, how does the MAIT cell activating ligand localize to the endoplasmic reticulum (ER) where it binds MR1? Is there an ER transporter for these pathogen-associated molecular pattern that imports the ligands, or do they diffuse into the ER?

Many of these important and exciting questions can be explored with the strains described in this dissertation, in combination with other mutations and tools available to study *L. monocytogenes*. For example, we can use riboflavin-producing mutants unable to escape from phagosomes (LLO-minus) to ask if MR1 presentation still occurs. We can also use the $\Delta ribC\Delta ribF$ mutant to test if in specific sites *in vivo* (like the brain) are sites for extracellular growth and an important aspect of *L. monocytogenes* pathogenesis. Furthermore, the $\Delta ribC\Delta ribF$ is a great strain because it can only grow intracellularly and thus could serve as a safer strain for vaccine vector platforms.

Chapter 6: References

1. S. O. Mansoorabadi, C. J. Thibodeaux, H. W. Liu, The diverse roles of flavin coenzymes - Nature's most versatile thespians. *J. Org. Chem.* **72**, 6329–6342 (2007).
2. A. Niemz, J. Imbriglio, V. M. Rotello, Model systems for flavoenzyme activity: One- and two-electron reduction of flavins in aprotic hydrophobic environments. *J. Am. Chem. Soc.* **119**, 887–892 (1997).
3. A. M. Edwards, Structure and general properties of flavins. *Methods Mol. Biol.* **1146**, 3–13 (2014).
4. V. Massey, The chemical and biological versatility of riboflavin. *Biochem. Soc. Trans.* **28**, 283–296 (2000).
5. S. Engst, P. Vock, M. Wang, J.-J. P. Kim, S. Ghisla, Mechanism of Activation of Acyl-CoA Substrates by Medium Chain Acyl-CoA Dehydrogenase: Interaction of the Thioester Carbonyl with the Flavin Adenine Dinucleotide Ribityl Side Chain (1999) <https://doi.org/10.1021/bi9815041>.
6. W. Zhang, *et al.*, Redox induced changes in flavin structure and the roles of the flavin N(5) and ribityl 2'-OH in regulating PutA-membrane binding. *Biochemistry* **46**, 483–491 (2007).
7. L. De Colibus, A. Mattevi, New frontiers in structural flavoenzymology. *Curr. Opin. Struct. Biol.* **16**, 722–728 (2006).
8. E. D. Kees, *et al.*, Secreted Flavin Cofactors for Anaerobic Respiration of Fumarate and Urocanate by *Shewanella oneidensis*: Cost and Role. *Appl. Environ. Microbiol.* **85**, 1–12 (2019).
9. S. H. Light, *et al.*, A flavin-based extracellular electron transfer mechanism in diverse Gram-positive bacteria. *Nature* **562**, 140–144 (2018).
10. A. Okamoto, *et al.*, Cell-secreted Flavins Bound to Membrane Cytochromes Dictate Electron Transfer Reactions to Surfaces with Diverse Charge and pH. *Sci. Reports* **4**, 1–8 (2014).
11. N. Q. K. Le, B. P. Nguyen, Prediction of FMN Binding Sites in Electron Transport Chains Based on 2-D CNN and PSSM Profiles. *IEEE/ACM Trans. Comput. Biol. Bioinforma.* **18**, 2189–2197 (2021).
12. K. M. Manoj, Aerobic Respiration: Criticism of the Proton-centric Explanation Involving Rotary Adenosine Triphosphate Synthesis, Chemiosmosis Principle, Proton Pumps and Electron Transport Chain. <https://doi.org/10.1177/1178626418818442> **11**, 117862641881844 (2018).
13. T. V. Nguyen, *et al.*, Identification of isobutyryl-CoA dehydrogenase and its deficiency in humans. *Mol. Genet. Metab.* **77**, 68–79 (2002).
14. A. Besrat, C. E. Polan, L. M. Henderson, Mammalian metabolism of glutaric acid. *J. Biol. Chem.* **244**, 1461–1467 (1969).
15. M. Kilstrup, K. Hammer, P. Ruhdal Jensen, J. Martinussen, Nucleotide metabolism and its control in lactic acid bacteria. *FEMS Microbiol. Rev.* **29**, 555–590 (2005).
16. S. Graziani, *et al.*, Functional analysis of FAD-dependent thymidylate synthase ThyX from *Paramecium bursaria* Chlorella virus-1. *J. Biol. Chem.* **279**, 54340–54347 (2004).
17. R. Eggers, *et al.*, The scope of flavin-dependent reactions and processes in the model plant *Arabidopsis thaliana*. *Phytochemistry* **189** (2021).
18. J. T. Pinto, A. J. L. Cooper, From Cholesterologenesis to Steroidogenesis: Role of Riboflavin

- and Flavoenzymes in the Biosynthesis of Vitamin D. *Adv. Nutr.* **5**, 144–163 (2014).
19. H. Nakagawa, A. Asano, R. Sato, Ascorbate-synthesizing System in Rat Liver Microsomes A Peptide-bound Flavin as the Prosthetic Group of L-Gulonolactone Oxidase. *J. Biochem* **77**, 221–232 (1975).
 20. K. Kiuchi, M. Nishikimi, K. Yagi, L-gulonolactone oxidase activity and vitamin C status in riboflavin-deficient rats. *Biochim. Biophys. Acta - Gen. Subj.* **630**, 330–337 (1980).
 21. A. Panday, M. K. Sahoo, D. Osorio, S. Batra, NADPH oxidases: an overview from structure to innate immunity-associated pathologies. *Cell. Mol. Immunol.* **2014** *121* **12**, 5–23 (2014).
 22. D. L. Coppock, C. Thorpe, Multidomain Flavin-Dependent Sulfhydryl Oxidases. *Antioxid Redox Signal* **8**, 300–311 (2006).
 23. I. M. Y. Cheung, C. N. J. Mcghee, T. Sherwin, Beneficial effect of the antioxidant riboflavin on gene expression of extracellular matrix elements, antioxidants and oxidases in keratoconic stromal cells. *Clin. Exp. Optom.* **97**, 349–355 (2014).
 24. A. V. Peraza, *et al.*, Riboflavin and pyridoxine restore dopamine levels and reduce oxidative stress in brain of rats. *BMC Neurosci.* **19** (2018).
 25. T. A. Giancaspero, *et al.*, Remaining challenges in cellular flavin cofactor homeostasis and flavoprotein biogenesis. *Front. Chem.* **3**, 30 (2015).
 26. C. A. Abbas, A. A. Sibirny, Genetic Control of Biosynthesis and Transport of Riboflavin and Flavin Nucleotides and Construction of Robust Biotechnological Producers. **75** (2011).
 27. M. Fischer, A. Bacher, Biosynthesis of vitamin B2 in plants. *Physiol. Plant.* **126**, 304–318 (2006).
 28. M. Fischer, A. Bacher, Biosynthesis of Vitamin B2 and Flavocoenzymes in Plants. *Adv. Bot. Res.* **58**, 93–152 (2011).
 29. V. A. García-Angulo, Overlapping riboflavin supply pathways in bacteria. *Crit. Rev. Microbiol.* **43**, 196–209 (2017).
 30. M. Barile, T. A. Giancaspero, P. Leone, M. Galluccio, C. Indiveri, Riboflavin transport and metabolism in humans. *J. Inherit. Metab. Dis.* **39**, 545–557 (2016).
 31. H. J. Powers, Riboflavin (vitamin B-2) and health. *Am. J. Clin. Nutr.* **77**, 1352–1360 (2003).
 32. A. Gutiérrez-Preciado, *et al.*, Extensive Identification of Bacterial Riboflavin Transporters and Their Distribution across Bacterial Species. *PLoS One* **10**, e0126124 (2015).
 33. C. Vogl, *et al.*, Characterization of Riboflavin (Vitamin B2) Transport Proteins from *Bacillus subtilis* and *Corynebacterium glutamicum*. *J. Bacteriol.* **189**, 7367–7375 (2007).
 34. R. H. Duurkens, M. B. Tol, E. R. Geertsma, H. P. Permentier, D. J. Slotboom, Flavin binding to the high affinity riboflavin transporter RibU. *J. Biol. Chem.* **282**, 10380–10386 (2007).
 35. N. J. Kotloski, J. A. Gralnick, Flavin electron shuttles dominate extracellular electron transfer by *Shewanella oneidensis*. *MBio* **4**, 10–13 (2013).
 36. M. J. Mcanulty, T. K. Wood, YeeO from *Escherichia coli* exports flavins. *Bioengineered* **5**, 386–392 (2014).
 37. L. Kjer-Nielsen, *et al.*, MR1 presents microbial vitamin B metabolites to MAIT cells. *Nature* (2012) <https://doi.org/10.1038/nature11605>.
 38. S. B. G. Eckle, *et al.*, Recognition of Vitamin B Precursors and Byproducts by Mucosal Associated Invariant T Cells. *J. Biol. Chem.* **290**, 30204–30211 (2015).
 39. N. E. Freitag, G. C. Port, M. D. Miner, *Listeria monocytogenes* — from saprophyte to

- intracellular pathogen. *Nat. Rev. Microbiol.* 2009 79 **7**, 623–628 (2009).
40. Z. Wang, X. Tao, S. Liu, Y. Zhao, X. Yang, An Update Review on Listeria Infection in Pregnancy (2021) <https://doi.org/10.2147/IDR.S313675>.
 41. L. Radoshevich, P. Cossart, Listeria monocytogenes: towards a complete picture of its physiology and pathogenesis. *Nat. Rev. Microbiol.* **16**, 32–46 (2017).
 42. R. Henry, *et al.*, Cytolysin-dependent delay of vacuole maturation in macrophages infected with Listeria monocytogenes. *Cell. Microbiol.* **8**, 107–119 (2006).
 43. J. L. Portman, S. B. Dubensky, B. N. Peterson, A. T. Whiteley, D. A. Portnoy, Activation of the Listeria monocytogenes Virulence Program by a Reducing Environment. *MBio* **8**, e01595-17 (2017).
 44. B. N. Nguyen, D. A. Portnoy, An Inducible Cre-lox System to Analyze the Role of LLO in Listeria monocytogenes Pathogenesis. *Toxins* 2020, Vol. 12, Page 38 **12**, 38 (2020).
 45. M. Hamon, H. Bierne, P. Cossart, Listeria monocytogenes: a multifaceted model. *Nat. Rev. Microbiol.* **4**, 423–434 (2006).
 46. L. A. Zenewicz, H. Shen, Innate and adaptive immune responses to Listeria monocytogenes: a short overview. *Microbes Infect.* **9**, 1208–15 (2007).
 47. S. C. Corr, L. A. J. O’Neill, Listeria monocytogenes infection in the face of innate immunity. *Cell. Microbiol.* **11**, 703–709 (2009).
 48. A. T. Whiteley, *et al.*, c-di-AMP modulates Listeria monocytogenes central metabolism to regulate growth, antibiotic resistance and osmoregulation. *Mol. Microbiol.* **104**, 212–233 (2017).
 49. J.-D. Sauer, A. A. Herskovits, M. X. D. O’Riordan, Metabolism of the Gram-Positive Bacterial Pathogen Listeria monocytogenes. *Microbiol. Spectr.* **7** (2019).
 50. A. T. Whiteley, A. J. Pollock, D. A. Portnoy, The PAMP c-di-AMP Is Essential for Listeria monocytogenes Growth in Rich but Not Minimal Media due to a Toxic Increase in (p)ppGpp. *Cell Host Microbe* **17**, 788–798 (2015).
 51. A. Matern, D. Pedrolli, S. Großhennig, J. Johansson, M. Mack, Uptake and metabolism of antibiotics roseoflavin and 8-demethyl-8-aminoriboflavin in riboflavin-auxotrophic Listeria monocytogenes. *J. Bacteriol.* **198**, 3233–3243 (2016).
 52. M. Mansjö, J. Johansson, The riboflavin analog roseoflavin targets an FMN-riboswitch and blocks Listeria monocytogenes growth, but also stimulates virulence gene-expression and infection. *RNA Biol.* **8**, 674–80 (2011).
 53. J. Ter Beek, R. H. Duurkens, G. B. Erkens, D. J. Slotboom, Quaternary Structure and Functional Unit of Energy Coupling Factor (ECF)-type Transporters. *J. Biol. Chem.* **286**, 5471–5475 (2011).
 54. N. K. Karpowich, J. M. Song, N. Cocco, D.-N. Wang, ATP binding drives substrate capture in an ECF transporter by a release-and-catch mechanism. *Nat. Struct. Mol. Biol.* **22**, 565–571 (2015).
 55. T. Eitinger, D. A. Rodionov, M. Grote, E. Schneider, Canonical and ECF-type ATP-binding cassette importers in prokaryotes: diversity in modular organization and cellular functions. *FEMS Microbiol. Rev.* **35**, 3–67 (2011).
 56. M. Sebastián, S. Arilla-Luna, J. Bellalou, I. Yruela, M. Medina, The Biosynthesis of Flavin Cofactors in Listeria monocytogenes. *J. Mol. Biol.* **431**, 2762–2776 (2019).
 57. T. P. Driscoll, *et al.*, Wholly rickettsia! Reconstructed metabolic profile of the

- quintessential bacterial parasite of eukaryotic cells. *MBio* **8** (2017).
58. Z. Xu, Y. Guo, D. M. Roellig, Y. Feng, L. Xiao, Comparative analysis reveals conservation in genome organization among intestinal *Cryptosporidium* species and sequence divergence in potential secreted pathogenesis determinants among major human-infecting species. *BMC Genomics* **20**, 406 (2019).
 59. A. Bateman, *et al.*, UniProt: the universal protein knowledgebase in 2021. *Nucleic Acids Res.* **49**, D480–D489 (2021).
 60. S. H. Light, *et al.*, Extracellular electron transfer powers flavinylated extracellular reductases in Gram-positive bacteria. *Proc. Natl. Acad. Sci. U. S. A.* **116**, 26892–26899 (2019).
 61. D. Min, *et al.*, Enhancing Extracellular Electron Transfer of *Shewanella oneidensis* MR-1 through Coupling Improved Flavin Synthesis and Metal-Reducing Conduit for Pollutant Degradation. *Environ. Sci. Technol.* **51**, 5082–5089 (2017).
 62. R. Méheust, S. Huang, R. Rivera-Lugo, J. F. Banfield, S. H. Light, Post-translational flavinylation is associated with diverse extracytosolic redox functionalities throughout bacterial life. *Elife* **10**, 1–22 (2021).
 63. A. Kurioka, L. J. Walker, P. Klenerman, C. B. Willberg, MAIT cells: new guardians of the liver. *Clin. Transl. Immunol.* **5**, e98 (2016).
 64. M. Dusseaux, *et al.*, Human MAIT cells are xenobiotic-resistant, tissue-targeted, CD161hi IL-17-secreting T cells. *Blood* **117**, 1250–1259 (2011).
 65. N. A. Gherardin, *et al.*, Human blood MAIT cell subsets defined using MR1 tetramers. *Immunol. Cell Biol.* **96** (2018).
 66. L. Le Bourhis, *et al.*, Antimicrobial activity of mucosal-associated invariant T cells. *Nat. Immunol.* **11**, 701–708 (2010).
 67. F. Tilloy, *et al.*, An invariant T cell receptor α chain defines a novel TAP-independent major histocompatibility complex class Ib-restricted α/β T cell subpopulation in mammals. *J. Exp. Med.* **189** (1999).
 68. E. Treiner, *et al.*, Mucosal-associated invariant T (MAIT) cells: an evolutionarily conserved T cell subset. *Microbes Infect.* **7**, 552–559 (2005).
 69. M. C. Gold, *et al.*, Human Mucosal Associated Invariant T Cells Detect Bacterially Infected Cells. *PLoS Biol.* **8**, e1000407 (2010).
 70. O. Rouxel, *et al.*, Cytotoxic and regulatory roles of mucosal-associated invariant T cells in type 1 diabetes. *Nat. Immunol.* **18** (2017).
 71. B. Ruf, *et al.*, Activating mucosal-associated invariant t cells induces a broad antitumor response. *Cancer Immunol. Res.* **9** (2021).
 72. A. Chiba, G. Murayama, S. Miyake, Mucosal-associated invariant T cells in autoimmune diseases. *Front. Immunol.* **9** (2018).
 73. S. Porcelli, C. E. Yockey, M. B. Brenner, S. P. Balk, Analysis of T cell antigen receptor (TCR) expression by human peripheral blood CD4-8- α/β T cells demonstrates preferential use of several V beta genes and an invariant TCR alpha chain. *J. Exp. Med.* **178**, 1–16 (1993).
 74. K. Hashimoto, M. Hirai, Y. Kurosawa, A gene outside the human MHC related to classical HLA class I genes. *Science (80-.)*. **269** (1995).
 75. E. Treiner, *et al.*, Selection of evolutionarily conserved mucosal-associated invariant T

- cells by MR1. *Nature* **422**, 164–169 (2003).
76. A. J. Corbett, *et al.*, T-cell activation by transitory neo-antigens derived from distinct microbial pathways. *Nature* **509**, 361–365 (2014).
 77. C. Soudais, *et al.*, In Vitro and In Vivo Analysis of the Gram-Negative Bacteria–Derived Riboflavin Precursor Derivatives Activating Mouse MAIT Cells. *J. Immunol.* **194**, 4641–4649 (2015).
 78. I. Allaman, M. Bélanger, P. J. Magistretti, Methylglyoxal, the dark side of glycolysis. *Front. Neurosci.* **9** (2015).
 79. K. Li, *et al.*, Synthesis, stabilization, and characterization of the MR1 ligand precursor 5-amino-6-D-ribitylaminoouracil (5-A-RU). *PLoS One* **13**, e0191837 (2018).
 80. H. E. G. McWilliam, *et al.*, The intracellular pathway for the presentation of Vitamin B-related antigens by the antigen-presenting molecule MR1. *Nat. Immunol.* **17**, 531–537 (2016).
 81. H. E. G. McWilliam, *et al.*, Endoplasmic reticulum chaperones stabilize ligand-receptive MR1 molecules for efficient presentation of metabolite antigens. *Proc. Natl. Acad. Sci. U. S. A.* **117** (2020).
 82. R. Lamichhane, J. E. Ussher, Expression and trafficking of MR1. *Immunology* **151**, 270–279 (2017).
 83. H. E. G. McWilliam, J. A. Villadangos, How MR1 Presents a Pathogen Metabolic Signature to Mucosal-Associated Invariant T (MAIT) Cells MR1 Presents Derivatives of a Vitamin Building-Block Metabolite Conserved in Microbes. *Trends Immunol.* **38**, 679–689 (2017).
 84. S. Huang, *et al.*, MR1 uses an endocytic pathway to activate mucosal-associated invariant T cells. *J. Exp. Med.* **205**, 1201–11 (2008).
 85. R. Lamichhane, *et al.*, TCR- or Cytokine-Activated CD8+ Mucosal-Associated Invariant T Cells Are Rapid Polyfunctional Effectors That Can Coordinate Immune Responses. *Cell Rep.* **28**, 3061-3076.e5 (2019).
 86. T. S. C. Hinks, X. W. Zhang, MAIT Cell Activation and Functions. *Front. Immunol.* **11**, 1014 (2020).
 87. L. Le Bourhis, *et al.*, MAIT Cells Detect and Efficiently Lyse Bacterially-Infected Epithelial Cells. *PLoS Pathog.* **9**, e1003681 (2013).
 88. A. Kurioka, *et al.*, MAIT cells are licensed through granzyme exchange to kill bacterially sensitized targets. *Mucosal Immunol.* **8**, 429–440 (2015).
 89. L. J. Howson, *et al.*, MAIT cell clonal expansion and TCR repertoire shaping in human volunteers challenged with Salmonella Paratyphi A. *Nat. Commun.* **9**, 253 (2018).
 90. M. Ioannidis, V. Cerundolo, M. Salio, The Immune Modulating Properties of Mucosal-Associated Invariant T Cells. *Front. Immunol.* **11**, 1556 (2020).
 91. B. Van Wilgenburg, *et al.*, MAIT cells are activated during human viral infections. *Nat. Commun.* **7** (2016).
 92. B. van Wilgenburg, *et al.*, MAIT cells contribute to protection against lethal influenza infection in vivo. *Nat. Commun.* **9** (2018).
 93. L. Loh, *et al.*, Human mucosal-associated invariant T cells contribute to antiviral influenza immunity via IL-18-dependent activation. *Proc. Natl. Acad. Sci. U. S. A.* **113** (2016).
 94. C. Phetsouphanh, *et al.*, Human MAIT cells respond to and suppress HIV-1. *Elife* **10** (2021).

95. E. W. Meermeier, M. J. Harriff, E. Karamooz, D. M. Lewinsohn, MAIT cells and microbial immunity. *Immunol. Cell Biol.* **96**, 607–617 (2018).
96. A. Meierovics, W.-J. C. Yankelevich, S. C. Cowley, MAIT cells are critical for optimal mucosal immune responses during in vivo pulmonary bacterial infection. *Proc. Natl. Acad. Sci. U. S. A.* **110**, E3119-28 (2013).
97. H. Wang, *et al.*, MAIT cells protect against pulmonary *Legionella longbeachae* infection. *Nat. Commun.* **2018 91 9**, 1–15 (2018).
98. M. N. T. Souter, J. McCluskey, A. J. Corbett, When it's good to have MAITs. *Immunol. Cell Biol.* **98** (2020).
99. C. Malka-Ruimy, *et al.*, Mucosal-Associated Invariant T Cell Levels Are Reduced in the Peripheral Blood and Lungs of Children With Active Pulmonary Tuberculosis. *Front. Immunol.* **10**, 206 (2019).
100. S. Sakai, *et al.*, MAIT cell-directed therapy of *Mycobacterium tuberculosis* infection. *Mucosal Immunol.* **2020 141 14**, 199–208 (2020).
101. C. K. Vorkas, *et al.*, Efficient 5-OP-RU-Induced Enrichment of Mucosa-Associated Invariant T Cells in the Murine Lung Does Not Enhance Control of Aerosol *Mycobacterium tuberculosis* Infection. *Infect. Immun.* **89** (2020).
102. W. J. Chua, *et al.*, Polyclonal mucosa-associated invariant T cells have unique innate functions in bacterial infection. *Infect. Immun.* **80** (2012).
103. S. Ghisla, D. E. Edmondson, Flavin Coenzymes. *eLS* (2014) <https://doi.org/10.1002/9780470015902.A0000654.PUB3>.
104. I. A. Rodionova, *et al.*, A novel bifunctional transcriptional regulator of riboflavin metabolism in Archaea. *Nucleic Acids Res.* **45**, 3785–3799 (2017).
105. A. Yonezawa, K. I. Inui, Novel riboflavin transporter family RFVT/SLC52: Identification, nomenclature, functional characterization and genetic diseases of RFVT/SLC52. *Mol. Aspects Med.* **34**, 693–701 (2013).
106. D. E. Balcazar, *et al.*, The superfamily keeps growing: Identification in trypanosomatids of RibJ, the first riboflavin transporter family in protists. *PLoS Negl. Trop. Dis.* **11**, e0005513 (2017).
107. R. K. Deka, C. A. Brautigam, B. A. Bidy, W. Z. Liu, M. V Norgard, Evidence for an ABC-Type Riboflavin Transporter System in Pathogenic Spirochetes. *MBio* **4**, e00615-12 (2013).
108. T. Y. Aw, D. P. Jones, D. B. McCormick, Uptake of Riboflavin by Isolated Rat Liver Cells. *J. Nutr.* **113**, 1249–1254 (1983).
109. S. Hustad, *et al.*, Riboflavin, Flavin Mononucleotide, and Flavin Adenine Dinucleotide in Human Plasma and Erythrocytes at Baseline and after Low-Dose Riboflavin Supplementation. *Clin. Chem.* **48**, 1571–1577 (2002).
110. A. T. Vasilaki, *et al.*, Relation between riboflavin, flavin mononucleotide and flavin adenine dinucleotide concentrations in plasma and red cells in patients with critical illness. *Clin. Chim. Acta* **411**, 1750–1755 (2010).
111. A. G. Vitreschak, D. A. Rodionov, A. A. Mironov, M. S. Gelfand, Regulation of riboflavin biosynthesis and transport genes in bacteria by transcriptional and translational attenuation. *Nucleic Acids Res.* **30**, 3141–51 (2002).
112. J. D. Sauer, *et al.*, *Listeria monocytogenes* Triggers AIM2-Mediated Pyroptosis upon

- Infrequent Bacteriolysis in the Macrophage Cytosol. *Cell Host Microbe* **7**, 412–419 (2010).
113. J.-D. Sauer, *et al.*, *Listeria monocytogenes* engineered to activate the Nlr4 inflammasome are severely attenuated and are poor inducers of protective immunity. *Proc. Natl. Acad. Sci.* **108**, 12419–12424 (2011).
 114. G. Gastaldi, *et al.*, Riboflavin Phosphorylation Is the Crucial Event in Riboflavin Transport by Isolated Rat Enterocytes. *J. Nutr.* **130**, 2556–2561 (2000).
 115. T. Zhang, *et al.*, Deciphering the landscape of host barriers to *Listeria monocytogenes* infection. *Proc. Natl. Acad. Sci.* **114**, 6334–6339 (2017).
 116. A. Louie, T. Zhang, S. Becattini, M. K. Waldor, D. A. Portnoy, A multiorgan trafficking circuit provides purifying selection of *Listeria monocytogenes* virulence genes. *MBio* **10**, e02948-19 (2019).
 117. H. Mehmood, A. D. J. K. Marwat, N. A. J. Khan, Invasive *Listeria monocytogenes* Gastroenteritis Leading to Stupor, Bacteremia, Fever, and Diarrhea: A Rare Life-Threatening Condition: <https://doi.org/10.1177/2324709617707978> **5**, 1–3 (2017).
 118. T. P. Burke, *et al.*, *Listeria monocytogenes* is resistant to lysozyme through the regulation, not the acquisition, of cell wall-modifying enzymes. *J. Bacteriol.* **196**, 3756–3767 (2014).
 119. H. Wang, *et al.*, Dual-Targeting Small-Molecule Inhibitors of the *Staphylococcus aureus* FMN Riboswitch Disrupt Riboflavin Homeostasis in an Infectious Setting. *Cell Chem. Biol.* **24**, 576-588.e6 (2017).
 120. A. Fuentes Flores, I. Sepúlveda Cisternas, J. I. Vásquez Solís de Ovando, A. Torres, V. A. García-Angulo, Contribution of riboflavin supply pathways to *Vibrio cholerae* in different environments. *Gut Pathog.* 2017 **91** **9**, 1–9 (2017).
 121. H. R. Bonomi, *et al.*, An Atypical Riboflavin Pathway Is Essential for *Brucella abortus* Virulence. *PLoS One* **5**, e9435 (2010).
 122. A. Krishnan, J. Kloehn, M. Lunghi, D. Soldati-Favre, Vitamin and cofactor acquisition in apicomplexans: Synthesis versus salvage. *J. Biol. Chem.* **295**, 701–714 (2020).
 123. A. Valigurová, I. Florent, Nutrient Acquisition and Attachment Strategies in Basal Lineages: A Tough Nut to Crack in the Evolutionary Puzzle of Apicomplexa. *Microorg.* 2021, Vol. 9, Page 1430 **9**, 1430 (2021).
 124. D. A. Gold, *et al.*, The *Toxoplasma* Dense Granule Proteins GRA17 and GRA23 Mediate the Movement of Small Molecules between the Host and the Parasitophorous Vacuole. *Cell Host Microbe* **17**, 642–652 (2015).
 125. K. R. Sakharkar, P. K. Dhar, V. T. K. Chow, Genome reduction in prokaryotic obligatory intracellular parasites of humans: a comparative analysis. *Int. J. Syst. Evol. Microbiol.* **54**, 1937–1941 (2004).
 126. A. N. Khachane, K. N. Timmis, V. A. P. Martins dos Santos, Dynamics of Reductive Genome Evolution in Mitochondria and Obligate Intracellular Microbes. *Mol. Biol. Evol.* **24**, 449–456 (2007).
 127. V. Merhej, M. Royer-Carenzi, P. Pontarotti, D. Raoult, Massive comparative genomic analysis reveals convergent evolution of specialized bacteria. *Biol. Direct* 2009 **41** **4**, 1–25 (2009).
 128. J. C. Flickinger, U. Rodeck, A. E. Snook, *Listeria monocytogenes* as a Vector for Cancer Immunotherapy: Current Understanding and Progress. *Vaccines* 2018, Vol. 6, Page 48 **6**,

- 48 (2018).
129. T. Hinks, *et al.*, MAIT cells protect against fatal intracellular pulmonary legionella infection via IFN- γ . *Eur. Respir. J.* **50**, PA4122 (2017).
 130. J. E. Ussher, P. Klenerman, C. B. Willberg, Mucosal-Associated Invariant T-Cells: New Players in Anti-Bacterial Immunity. *Front. Immunol.*, 450 (2014).
 131. A. Camilli, L. L. G. Tilney, D. A. Portnoy, Dual roles of plcA in *Listeria monocytogenes* pathogenesis. *Mol. Microbiol.* **8**, 143–157 (1993).
 132. P. Lauer, M. Y. N. Chow, M. J. Loessner, D. A. Portnoy, R. Calendar, Construction, characterization, and use of two *Listeria monocytogenes* site-specific phage integration vectors. *J. Bacteriol.* **184**, 4177–4186 (2002).
 133. B. N. Nguyen, *et al.*, TLR2 and endosomal TLR-mediated secretion of IL-10 and immune suppression in response to phagosome-confined *Listeria monocytogenes*. *PLOS Pathog.* **16**, e1008622 (2020).
 134. D. A. Portnoy, P. Suzanne Jacks, D. J. Hinrichs, Role of hemolysin for the intracellular growth of *Listeria monocytogenes*. *J. Exp. Med.* **167**, 1459 (1988).
 135. M. I. Cheng, C. Chen, P. Engström, D. A. Portnoy, G. Mitchell, Actin-based motility allows *Listeria monocytogenes* to avoid autophagy in the macrophage cytosol. *Cell. Microbiol.* **20**, e12854 (2018).
 136. C. Bécavin, *et al.*, Comparison of Widely Used *Listeria monocytogenes* Strains EGD, 10403S, and EGD-e Highlights Genomic Differences Underlying Variations in Pathogenicity. *MBio* **5** (2014).
 137. S. Jones, D. A. Portnoy, Characterization of *Listeria monocytogenes* Pathogenesis in a Strain Expressing Perfringolysin O in Place of Listeriolysin O. *Infect. Immun.*, 5608–5613 (1994).
 138. M. W. Fraaije, A. Mattevi, Flavoenzymes: Diverse catalysts with recurrent features. *Trends Biochem. Sci.* **25**, 126–132 (2000).
 139. Y. V. Bertsova, *et al.*, Alternative pyrimidine biosynthesis protein ApbE is a flavin transferase catalyzing covalent attachment of FMN to a threonine residue in bacterial flavoproteins. *J. Biol. Chem.* **288**, 14276–14286 (2013).
 140. A. V. Bogachev, A. A. Baykov, Y. V. Bertsova, Flavin transferase: the maturation factor of flavin-containing oxidoreductases. *Biochem. Soc. Trans.* **46**, 1161–1169 (2018).
 141. W. Zhou, *et al.*, Sequencing and Preliminary Characterization of the Na⁺-Translocating NADH:Ubiquinone Oxidoreductase from *Vibrio harveyi*. *Biochemistry* **38**, 16246–16252 (1999).
 142. J. Backiel, D. V. Zagorevski, Z. Wang, M. J. Nilges, B. Barquera, Covalent Binding of Flavins to RnfG and RnfD in the Rnf Complex from *Vibrio cholerae*. *Biochemistry* **47**, 11273–11284 (2008).
 143. Z. Zeng, *et al.*, Bacterial Microcompartments Coupled with Extracellular Electron Transfer Drive the Anaerobic Utilization of Ethanolamine in *Listeria monocytogenes*. *mSystems* **6** (2021).
 144. R. Rivera-Lugo, *et al.*, *Listeria monocytogenes* requires cellular respiration for NAD⁺ regeneration and pathogenesis. *Elife* **11**, 2013–2015 (2022).
 145. B. Xayarath, F. Alonzo, N. E. Freitag, D. Portnoy, J. Wehland, Identification of a Peptide-Pheromone that Enhances *Listeria monocytogenes* Escape from Host Cell Vacuoles. *PLoS*

- Pathog.* **11**, e1004707 (2015).
146. D. Keogh, *et al.*, Extracellular Electron Transfer Powers *Enterococcus faecalis* Biofilm Metabolism. *MBio* **9**, 1–16 (2018).
 147. G. Pankratova, D. Leech, L. Gorton, L. Hederstedt, Extracellular Electron Transfer by the Gram-Positive Bacterium *Enterococcus faecalis*. *Biochemistry* **57**, 4597–4603 (2018).
 148. L. Hederstedt, L. Gorton, G. Pankratova, Two Routes for Extracellular Electron Transfer in *Enterococcus faecalis*. *J. Bacteriol.* **202** (2020).
 149. S. Tejedor-Sanz, *et al.*, Extracellular electron transfer increases fermentation in lactic acid bacteria via a hybrid metabolism. *Elife* **11**, 1–29 (2022).
 150. J. G. Tolar, S. Li, C. M. Ajo-Franklin, The differing roles of flavins and quinones in extracellular electron transfer in *Lactiplantibacillus plantarum*. *bioRxiv*, 1–21 (2022).
 151. E. R. Green, J. Meccas, “Bacterial Secretion Systems: An Overview” in *Virulence Mechanisms of Bacterial Pathogens*, (ASM Press, 2016), pp. 213–239.
 152. E. R. Frawley, R. G. Kranz, CcsBA is a cytochrome c synthetase that also functions in heme transport. *Proc. Natl. Acad. Sci.* **106**, 10201–10206 (2009).
 153. D. A. Rodionov, *et al.*, A novel class of modular transporters for vitamins in prokaryotes. 42–51 (2009).
 154. R. Rivera-Lugo, S. H. Light, N. E. Garelis, D. A. Portnoy, RibU is an essential determinant of *Listeria* pathogenesis that mediates acquisition of FMN and FAD during intracellular growth. *Proc. Natl. Acad. Sci.* **119**, 1–8 (2022).
 155. M. Zhang, *et al.*, Structure of a pantothenate transporter and implications for ECF module sharing and energy coupling of group II ECF transporters. *Proc. Natl. Acad. Sci. U. S. A.* **111**, 18560–18565 (2014).
 156. N. K. Karpowich, J. Song, D. N. Wang, An Aromatic Cap Seals the Substrate Binding Site in an ECF-Type S Subunit for Riboflavin. *J. Mol. Biol.* **428**, 3118–3130 (2016).
 157. R. P. A. Berntsson, *et al.*, Structural divergence of paralogous S components from ECF-type ABC transporters. *Proc. Natl. Acad. Sci.* **109**, 13990–13995 (2012).
 158. A. J. Enright, I. Iliopoulos, N. C. Kyrpides, C. A. Ouzounis, Protein interaction maps for complete genomes based on gene fusion events. *Nature* **402**, 86–90 (1999).
 159. G. B. Erkens, *et al.*, The structural basis of modularity in ECF-type ABC transporters. *Nat. Struct. Mol. Biol.* **18**, 755–760 (2011).
 160. I. Setyawati, *et al.*, In vitro reconstitution of dynamically interacting integral membrane subunits of energy-coupling factor transporters. *Elife* **9**, 1–21 (2020).
 161. D. H. Parks, *et al.*, A standardized bacterial taxonomy based on genome phylogeny substantially revises the tree of life. *Nat. Biotechnol.* **36**, 996 (2018).
 162. D. H. Parks, *et al.*, A complete domain-to-species taxonomy for Bacteria and Archaea. *Nat. Biotechnol.* **38**, 1079–1086 (2020).
 163. L. J. Y. M. Swier, A. Guskov, D. J. Slotboom, Structural insight in the toppling mechanism of an energy-coupling factor transporter. *Nat. Commun.* **7**, 11072 (2016).
 164. C. Thangaratnarajah, J. Rheinberger, C. Paulino, D. J. Slotboom, Insights into the bilayer-mediated toppling mechanism of a folate-specific ECF transporter by cryo-EM. *Proc. Natl. Acad. Sci. U. S. A.* **118**, 1–9 (2021).
 165. J. Jumper, *et al.*, Highly accurate protein structure prediction with AlphaFold. *Nature* **596**, 583–589 (2021).

166. R. Evans, *et al.*, Protein complex prediction with AlphaFold-Multimer. *bioRxiv*, 2021.10.04.463034 (2022).
167. M. Mirdita, *et al.*, ColabFold: making protein folding accessible to all. *Nat. Methods* **19**, 679–682 (2022).
168. R. S. Plumb, *et al.*, UPLC/MS(E); a new approach for generating molecular fragment information for biomarker structure elucidation. *Rapid Commun. Mass Spectrom.* **20**, 1989–94 (2006).
169. P. V Shliaha, N. J. Bond, L. Gatto, K. S. Lilley, Effects of traveling wave ion mobility separation on data independent acquisition in proteomics studies. *J. Proteome Res.* **12**, 2323–39 (2013).
170. U. Distler, *et al.*, Drift time-specific collision energies enable deep-coverage data-independent acquisition proteomics. *Nat. Methods* **11**, 167–70 (2014).
171. D. Helm, *et al.*, Ion mobility tandem mass spectrometry enhances performance of bottom-up proteomics. *Mol. Cell. Proteomics* **13**, 3709–15 (2014).
172. K. A. Neilson, *et al.*, Less label, more free: approaches in label-free quantitative mass spectrometry. *Proteomics* **11**, 535–53 (2011).
173. S. Nahnsen, C. Bielow, K. Reinert, O. Kohlbacher, Tools for label-free peptide quantification. *Mol. Cell. Proteomics* **12**, 549–56 (2013).
174. U. Distler, J. Kuharev, P. Navarro, S. Tenzer, Label-free quantification in ion mobility-enhanced data-independent acquisition proteomics. *Nat. Protoc.* **11**, 795–812 (2016).
175. UniProt Consortium, UniProt: the universal protein knowledgebase in 2021. *Nucleic Acids Res.* **49**, D480–D489 (2021).
176. S. R. Eddy, Profile hidden Markov models. *Bioinformatics* (1998) <https://doi.org/10.1093/bioinformatics/14.9.755>.
177. T. Aramaki, *et al.*, KofamKOALA: KEGG Ortholog assignment based on profile HMM and adaptive score threshold. *Bioinformatics* **36**, 2251–2252 (2020).
178. J. Mistry, *et al.*, Pfam: The protein families database in 2021. *Nucleic Acids Res.* **49**, D412–D419 (2021).
179. J. J. Almagro Armenteros, *et al.*, SignalP 5.0 improves signal peptide predictions using deep neural networks. *Nat. Biotechnol.* (2019) <https://doi.org/10.1038/s41587-019-0036-z>.
180. A. Krogh, B. Larsson, G. von Heijne, E. L. Sonnhammer, Predicting transmembrane protein topology with a hidden Markov model: application to complete genomes. *J. Mol. Biol.* **305**, 567–80 (2001).
181. P. Riegert, V. Wanner, S. Bahram, Genomics, isoforms, expression, and phylogeny of the MHC class I-related MR1 gene. *J. Immunol.* **161** (1998).
182. S. Huang, *et al.*, MR1 antigen presentation to mucosal-associated invariant T cells was highly conserved in evolution. *Proc. Natl. Acad. Sci. U. S. A.* **106**, 8290–8295 (2009).
183. N. Seach, *et al.*, Double Positive Thymocytes Select Mucosal-Associated Invariant T Cells. *J. Immunol.* **191**, 6002–6009 (2013).
184. I. Kawachi, J. Maldonado, C. Strader, S. Gilfillan, MR1-Restricted V 19i Mucosal-Associated Invariant T Cells Are Innate T Cells in the Gut Lamina Propria That Provide a Rapid and Diverse Cytokine Response. *J. Immunol.* **176**, 1618–1627 (2006).
185. Z. Chen, *et al.*, Characterization and Purification of Mouse Mucosal-Associated Invariant

- T (MAIT) Cells. *Curr. Protoc. Immunol.* **127** (2019).
186. T. Matsuoka, *et al.*, The effects of 5-OP-RU stereochemistry on its stability and MAIT-MR1 axis. *ChemBioChem* **22**, 672–678 (2021).
 187. E. Karamooz, M. J. Harriff, D. M. Lewinsohn, MR1-dependent antigen presentation. *Semin. Cell Dev. Biol.* **84** (2018).
 188. A. J. R. Cooper, J. Clegg, F. C. Cassidy, A. E. Hogan, R. M. McLoughlin, Human MAIT Cells Respond to *Staphylococcus aureus* with Enhanced Anti-Bacterial Activity. *Microorganisms* **10** (2022).
 189. T. Parrot, *et al.*, MAIT cell activation and dynamics associated with COVID-19 disease severity. *Sci. Immunol.* **5** (2020).
 190. J. E. Ussher, *et al.*, CD161⁺CD8⁺ T cells, including the MAIT cell subset, are specifically activated by IL-12+IL-18 in a TCR-independent manner. *Eur. J. Immunol.* **44**, 195–203 (2014).
 191. J. E. Ussher, C. B. Willberg, P. Klenerman, MAIT cells and viruses. *Immunol. Cell Biol.* **96**, 630–641 (2018).
 192. I. Nel, L. Bertrand, A. Toubal, A. Lehen, MAIT cells, guardians of skin and mucosa? *Mucosal Immunol.* **2021 144 14**, 803–814 (2021).
 193. M. H. Choi, *et al.*, Increasing incidence of listeriosis and infection-Associated clinical outcomes. *Ann. Lab. Med.* **38** (2018).
 194. D. A. Portnoy, V. Auerbuch, I. J. Glomski, The cell biology of *Listeria monocytogenes* infection: the intersection of bacterial pathogenesis and cell-mediated immunity. *J. Cell Biol.* **158**, 409–14 (2002).
 195. R. A. Brundage, G. A. Smith, A. Camilli, J. A. Theriot, D. A. Portnoy, Expression and phosphorylation of the *Listeria monocytogenes* actA protein in mammalian cells. *Proc. Natl. Acad. Sci. U. S. A.* **90**, 11890–11894 (1993).
 196. H. J. WELSHIMER, VITAMIN REQUIREMENTS OF *LISTERIA MONOCYTOGENES*. *J. Bacteriol.* **85**, 1156–1159 (1963).
 197. R. Rivera-Lugo, *et al.*, Distinct energy-coupling factor transporter subunits enable flavin acquisition and extracytosolic trafficking for extracellular electron transfer in *Listeria monocytogenes*. *bioRxiv*, 2022.11.04.515267 (2022).
 198. Z. Zhao, *et al.*, *Francisella tularensis* induces Th1 like MAIT cells conferring protection against systemic and local infection. *Nat. Commun.* **12** (2021).
 199. A. N. Bucsan, *et al.*, Mucosal-activated invariant T cells do not exhibit significant lung recruitment and proliferation profiles in macaques in response to infection with *Mycobacterium tuberculosis* CDC1551. *Tuberculosis* **116** (2019).
 200. M. Chiara, *et al.*, Comparative Genomics of *Listeria* Sensu Lato: Genus-Wide Differences in Evolutionary Dynamics and the Progressive Gain of Complex, Potentially Pathogenicity-Related Traits through Lateral Gene Transfer. *Genome Biol. Evol.* **7**, 2154–2172 (2015).
 201. A. N. Sun, A. Camilli, D. A. Portnoy, Isolation of *Listeria monocytogenes* small-plaque mutants defective for intracellular growth and cell-to-cell spread. *Infect. Immun.* **58** (1990).